KONINKLIJK NEDERLANDS METEOROLOGISCH INSTITUUT

MEDEDELINGEN EN VERHANDELINGEN

No. 99

H. TIMMERMAN

METEOROLOGICAL EFFECTS ON TIDAL HEIGHTS IN THE NORTH SEA

1977

Prijs f 45,—

STAATSDRUKKERIJ / 'S-GRAVENHAGE

METEOROLOGICAL EFFECTS ON TIDAL HEIGHTS IN THE NORTH SEA

KONINKLIJK NEDERLANDS METEOROLOGISCH INSTITUUT

MEDEDELINGEN EN VERHANDELINGEN

No. 99

H. TIMMERMAN

METEOROLOGICAL EFFECTS ON TIDAL HEIGHTS IN THE NORTH SEA

1977

STAATSDRUKKERIJ/'S-GRAVENHAGE

PUBLIKATIENUMMER: K.N.M.I. 102-99

U.D.C.: 551.556.8:
551.466.7

Contents

1 Introduction

1.0 The low situation of important parts of the Netherlands causes a permanent threat of the sea. Often high water-levels resulted in disasters. These high levels coincided with severe gales, so even in early days the term 'storm surge' did belong to common language. Well-known surges are those of 18 November 1421 (10000 persons perished and 72 villages swept away by the sea), 1 November 1570, 25 December 1717, 14 November 1775, 4 February 1825, 13 January 1916. After the last mentioned flood a 'warning service for storm surges' was established in the Netherlands. The organization of this service was extended and improved after the devastating storm surge of 1 February 1953. Today, for a number of stations along the Netherlands coast the deviation of the water-level is computed at the KNMI (Royal Netherlands Meteorological Institute) on a routine basis. If an excess of critical levels, fixed in advance, is to be expected, a close co-operation between KNMI and Rijkswaterstaat starts. In addition, extra information on water-levels is provided, according to international agreements between countries around the North Sea. It is the responsibility of Rijkswaterstaat, in close contact with local inspections of dikes, to decide which kind of precautionary measures for the protection of the dikes has to be taken in relation to the predicted meteorological effects on the water-levels and the observed water-levels along the Netherlands coast.

It is self-evident that in connection with the Warning Service for storm surges many investigations were carried out in order to give the relationship between wind and water-levels a quantitative basis. Gradually the insight in the effect of the wind on the transport of water was growing, leading to a more accurate forecast of storm surges. This increasing knowledge was also useful with respect to the forecast of small deviations of the water-levels, of importance with a view to inshore activities, to drill activities over sea or with respect to the navigation of supertankers over the shallow waters of the southern part of the North Sea. Furthermore it can be of use for the knowledge of currents, which is indispensable for the transport of pollutants.

1.1 The variation in the height of the sea-level is caused not only by the wind but also by forces related to atmospheric pressure gradients in a more direct sense and by astronomical forces. Although the effects of the three forces on the North Sea are comparable, the order of magnitude of the three forces is different. Acting on one cubic metre water the tide-generating force is about 10^{-3}N, while in a well-developed depression the pressure gradient force is about $5 * 10^{-3}$ N. In order to compare the force related to the wind, which acts as a wind stress on the sea surface, the wind stress has to be divided by the depth of the basin. Taking a depth of 50 m, representative of the North Sea, the order of magnitude of the force related to the wind, again in well-developed depressions, appears to be about $5 * 10^{-2}$ N. This gives a ratio of 1 : 5 : 50. As already remarked the effects of these forces are more comparable. The amplitude of the tidal wave in the North Sea is in many places 1-2 m, while the amplitude of the wave related to the wind is sometimes 2-3 m. The order of magnitude of the wave connected with the pressure gradient appears to be about $\frac{1}{2}$ m. This fact can be clarified in a qualitative way. It is well known that the astronomical forces affect the whole earth, solid as well as liquid. As a consequence, the solid earth shows a deformation with an amplitude of 1-2 dm, and the liquid earth a deformation of 5-7 dm. The latter wave is generated for an important part over the extensive masses of water in the southern hemisphere. This wave, which enters the northern hemisphere, for instance via the Atlantic Ocean, is modified by the topography of the earth, such as the smaller depth and the shape of the North Sea. The final result in the North Sea is a fluctuation of the sea-level with an amplitude of 1-2 m in many places. It is an indirect effect of the astronomical force on the North Sea; the direct one is negligible, because there is not a sufficient amount of water in the North Sea. Contrary to the astronomical force the wind is of importance only in the presence of storm depressions. Besides it acts only along the surface layers of the sea. Especially in connection with the funnel-shaped North Sea northwesterly gales may give rise to long waves with amplitudes of 2-3 m. It is purely accidental that in the North Sea the effect of the astronomical force and the effect of the wind are of the same order of magnitude. The atmospheric pressure gradient force acts upon the whole water column, from surface to bottom, as does the astronomical force. But it is only of importance near storm depressions, as is the case with the wind-effect. A sufficient depth of water is necessary, in agreement with the astronomical force. These water depths are not available in the North Sea. However, they can be found just outside the continental shelf, where a sharp increase of the depth from 100 m to about 3000 m occurs. Now this amount of ocean water just outside the continental shelf seems to be sufficient to create under certain conditions a considerable wave, which enters the North Sea in the same way as the tidal wave does, causing deviations of the water-level of about $\frac{1}{2}$ m.

Generally the effect of these forces may be considered as separate phenomena. However, under certain conditions, mainly if the depth of the sea is less than 30 m, there is an interaction between the effect of the forces, which is not altogether negligible.

1.2 The investigation of the influence of meteorological forces on the sea has statistical as well as physical aspects. In the Netherlands the investigation was at first mainly statistical but during the last decades the physical aspects have become more important. The work by the Government Committee for the 'Rotterdamse Waterweg' [1920] and that of Schalkwijk [1947] showed a mainly statistical approach. Its results were used to compute the deviation of water-levels in Hook of Holland (respectively before and after World War II) until the storm surge of 1953. The method of Weenink [1958] had a more physical and dynamical basis, because it made use of a solution of the hydrodynamical equations. It was used in the operational service for the computation of the deviations of the water-levels at Flushing, Hook of Holland, Den Helder, Harlingen and Delfzijl, during the period 1954-1971. These three investigations are briefly reviewed in Chapter 3.

The present method for the computation of the deviation of water-levels is related to a solution of the hydrodynamical equations as well. It is discussed thoroughly with several applications in Chapters 5, 6, 8 and 9. Chapter 2 gives a number of definitions. In Chapter 4 problems related to the wind stress are treated. In Chapter 7 the automation of the computation of water-levels is discussed. Finally, Chapter 10 deals with surges generated by two severe storms displaced in such a way that the conditions for the southern part of the North Sea were as unfavourable as could be. How realistic such a displacement is, remains to be questioned.

2 Some definitions

In this publication a number of concepts is used, such as meteorological effect, wind-effect, airpressure-effect, set-up, surge, negative surge, internal surge, external surge.

The definitions read as follows:

meteorological effect	= effect on the sea, especially on the water-level, due to meteorological phenomena.
wind-effect	= effect on the sea, especially on the water-level, due to the wind.
airpressure-effect	= effect on the sea, especially on the water-level, due to atmospheric pressure.
set-up	= difference between the observed tidal height and the tidal height predicted on an astronomical basis.
surge	= a situation with a considerable set-up
negative surge	= a situation with a considerable negative set-up.
internal surge	= surge generated by meteorological phenomena inside the North Sea area.
external surge	= surge generated by meteorological phenomena outside the North Sea area.

Deviation of the water-level is a general term for the above conceptions.

The definition of surge is rather wide. Wemelsfelder [1960] introduced a classification by distinguishing between low, normal, high, extraordinary and extreme surges.

As remarked the set-up is obtained by subtracting the astronomical tide from the observed tide. This implies no interaction between the astronomical and the meteorological component of the tide. This is not quite acceptable in very shallow waters (depth less than 30 m). Under these circumstances interaction may cause a set-up, which is not quite representative for the meteorological effect. However, in most cases such an interaction is of minor importance, so that the meteorological effect on the water-level can be determined in a satisfactory way by subtracting the astronomical tide from the observed tide.

3 The investigations of the government committee 'Rotterdamse Waterweg', Schalkwijk and Weenink

3.0 The investigations are based on the assumption of the simple superposition of meteorological and astronomical effects. The Staatscommissie Rotterdamse Waterweg [1920] (Committee for the Waterweg) related differences between observed water-levels and water-levels predicted on an astronomical basis at Hook of Holland to the registered wind at Hook of Holland. This is not very satisfactory, the windfield over the North Sea being characterized by one wind-parameter only. Schalkwijk [1947] made an attempt to improve the method by relating the windfield over three districts, viz. North, South and Channel (see Fig. 3.0.1) to differences of water-levels obtained in the way indicated above. Following theoretical considerations Schalkwijk assumed a quadratic relationship between wind-velocity and wind-effect. He used a stationary model and wrote the wind-effect at Hook of Holland as a sum of contributions of the sectors North, South and Channel:

$$h = a_N V_N^2 \cos(\psi_N - \varepsilon_N) + a_Z(\psi_Z) V_Z^2 + a_K V_K^2 \cos(\psi_K - \varepsilon_K) \qquad (3.0.1)$$

For the meaning of the symbols one is referred to the list on page 102. When the coefficients a_N, a_Z, a_K, ε_N, ε_K and the wind over the districts North, South and Channel are known, relation 3.0.1 can be applied for the computation of the wind-effect. The coefficients were computed by Schalkwijk with the aid of the least-squares method from 14 storm surges that occurred in the period 1920-1940. He determined the wind-effect at Hook of Holland and the windfields over the districts North, South and Channel as accurately as possible, but it is obvious that the sample effect on the coefficients must not be neglected, the more so as the meteorological material was rather poor.

A serious shortcoming of the Schalkwijk-method is the limited applicability to a region near Hook of Holland. Besides, the representation of the windfield over the North Sea by two parameters is insufficient.

3.1 Especially after the storm surge of 1953 the necessity was felt to develop a method based on a more detailed analysis of the windfield and valid for more places along the Netherlands coast. Along the lines given by Schalkwijk the processing of the material for each station taken into account and a considerable extension of the material due to an increased number of wind parameters would have been necessary. In order to avoid these difficulties Weenink [1958] gave his investigation a more physical and dynamical basis. He examined the Navier-Stokes equations of motion for a turbulent, incompressible fluid and the equation of continuity. He integrated the differential equations in a vertical sense from the sea surface to the bottom. See Weenink [1958] and also Timmerman [1969]. From a practical point of view this integration is admissible, because the vertical distribution of the stream is of minor importance with respect to the storm surge problem. The integrated equations describing the transport of water and the resulting deviations of the water-level (the astronomical aspect is omitted) read as follows:

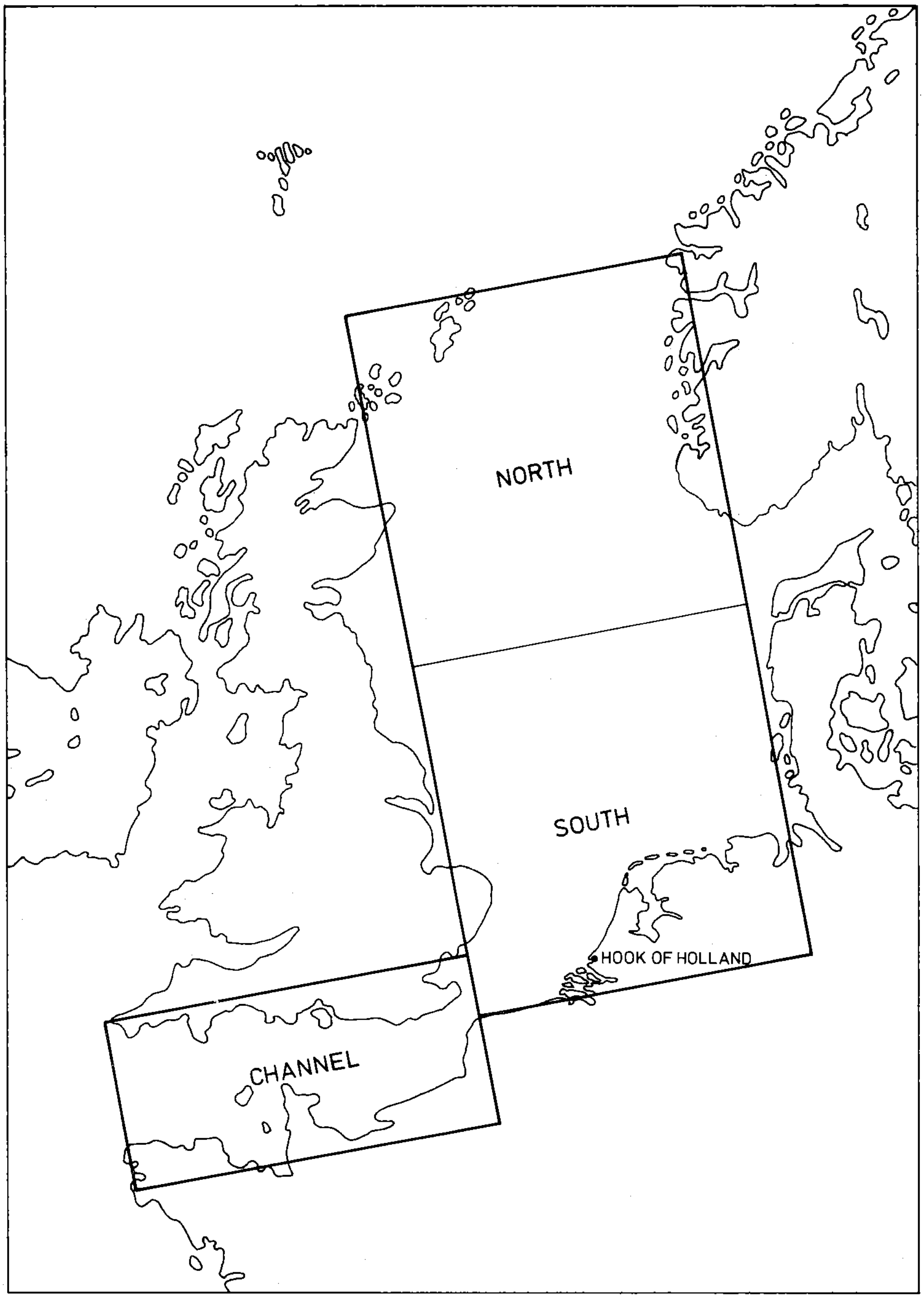

Fig. 3.0.1 Districts method Schalkwijk.

$$\frac{\partial U}{\partial t} = fV - g(H + h)\frac{\partial h}{\partial x} + \frac{\tau_o^{zx}}{\rho_s} - \frac{\tau_b^{zx}}{\rho_s} - \frac{H + h}{\rho_s}\frac{\partial p(h)}{\partial x}$$

$$\frac{\partial V}{\partial t} = -fU - g(H+h)\frac{\partial h}{\partial y} + \frac{\tau_o^{zy}}{\rho_s} - \frac{\tau_b^{zy}}{\rho_s} - \frac{H + h}{\rho_s}\frac{\partial p(h)}{\partial y} \qquad (3.1.1.)$$

$$\frac{\partial h}{\partial t} = -\frac{\partial U}{\partial x} - \frac{\partial V}{\partial y}$$

To answer the question whether this set of equations meets practical requirements, it must be examined how far the factors causing deviations of the water-level are incorporated in 3.1.1. The most important factors are:

1) wind stress
2) Coriolis effects
3) bottom stress
4) configuration of the coast
5) configuration of the bottom
6) air pressure effect
7) wave set-up

It appears from the set of equations 3.1.1 that the factors 1, 2, 3, 5 and 6 are taken into account, while the configuration of the coast can be described by boundary conditions. Mean horizontal transports of water and momentum are associated with the waves. This transport of water can be considered simply as a contribution to the vector describing the water transport U and V in the equations 3.1.1. Horizontal gradients in the wave-induced transport of momentum, however, give rise in a direct way to extra gradients in the mean water-level. See Phillips [1966]. This phenomenon is of importance mainly in the surf zone, where a 'wave set-up' in the direction of the coast may occur. For a gently sloping beach and waves perpendicular to the coast the wave set-up near the coastline is one to two tenths of the wave-height outside the surf zone. This effect is strongly determined by local conditions and can, therefore, hardly be quantified. It is conceivable that due to the effect tide gauges, situated for instance in a harbour, give an extra set-up of some decimeters compared with the water-level at some distance outside the coast. During storm surges the wave set-up gives a positive contribution, which can be taken account of by a somewhat higher value of the drag-coefficient C_d of the wind stress. See Chapter 4. Apart from the wave set-up it may be concluded that the set of equations 3.1.1 includes all terms of importance with respect to the variations of the sea-level other than those related to the astronomical forces.

In the set of equations 3.1.1 the convective terms $U\frac{\partial U}{\partial x}$, $U\frac{\partial V}{\partial x}$, $V\frac{\partial U}{\partial y}$, $V\frac{\partial V}{\partial y}$ and the viscosity terms $\frac{\partial \tau^{xx}}{\partial x}$, $\frac{\partial^{xy}}{\partial x}$, $\frac{\partial^{yx}}{\partial y}$, and $\frac{\partial \tau^{yy}}{\partial y}$ are neglected. Though the contribution of these terms is very small, the viscosity terms control the dissipation of energy in such a way that these terms may not be neglected in long-term computations.

To solve the set of equations 3.1.1 Weenink was obliged to use analytical solutions. Therefore it was necessary to introduce simplifications and to consider a stationary and linear set of equations. The following modifications were therefore made:

1. Replacing of H + h by H. This is allowed if $h \ll H$. Certainly this supposition is correct if the depth of the sea is more than, say, 30 m.

2. $\frac{\partial U}{\partial t} = \frac{\partial V}{\partial t} = \frac{\partial h}{\partial t} = 0.$

3. τ_b^{zx} and τ_b^{zy} are composed of a linear function of the transport of water and of a fraction m (about 0.1) of τ_o^z.

4. Introduction of an analytical function for the bottom profile.

5. $\frac{\partial p(h)}{\partial x} = \frac{\partial p(h)}{\partial y} = 0.$

Introducing these simplifications the set of equations reads as follows:

$$
\begin{aligned}
& fV - gH\frac{\partial h}{\partial x} + \frac{(1+m)\tau_o^{zx}}{\rho_s} - \frac{rU}{H} = 0 \\
& -fU - gH\frac{\partial h}{\partial y} + \frac{(1+m)\tau_o^{zy}}{\rho_s} - \frac{rV}{H} = 0 \qquad (3.1.2) \\
& \frac{\partial U}{\partial x} + \frac{\partial V}{\partial y} = 0.
\end{aligned}
$$

The terms τ_o^{zx} and τ_o^{zy} represent the x- and y-component of the stress τ_o^z exerted by the atmosphere on the surface of the sea. It is usual to put $\tau_o^z = C_d \rho \, |\vec{v}| \, \vec{v}$, where $\vec{v}$ is the wind vector at a certain height, for instance at 10 m, averaged over 10 minutes. Because C_d is related to the square of the wind velocity, its value is of vital importance. However, C_d is known only approximately and not independent of the wind velocity. In Chapter 4 the wind stress is discussed in more detail.

The modified set of equations 3.1.2 can only give a solution valid for a stationary state. Such a solution was computed by Weenink for the effect of the wind over the district South (see Fig. 3.0.1) on the water-levels at Hook of Holland. C_d was taken as a variable quantity and computed with the method of least-squares by comparison of the results with those obtained by using the Schalkwijk-method as well. Consequently, the value C_d determined by Weenink is dependent of the sampling errors of the coefficients a_N, a_Z and a_K of Schalkwijk, which, as remarked already, are not negligible. Weenink found $C_d = 0.0034$, valid at a difference in temperature between air and sea-water of -2 °C. According to present-day views this value of C_d is rather large.

Applying $C_d = 0.0034$ Weenink computed the stationary wind effect at Flushing, Hook of Holland, Den Helder and Borkum as a function of a constant and homogeneous wind field over the districts North, South 1, South 2, South 3 and Channel. See Fig. 3.1.1. Finally, the total effect of the sea area taken into consideration is obtained by simply adding the partial contributions of the districts. This is admissible due to the linearity of the differential equations 3.1.2.

The contribution of district North, as computed by Weenink, appeared to be about twice as large as the one determined by Schalkwijk. Weenink did not relate this difference to a high

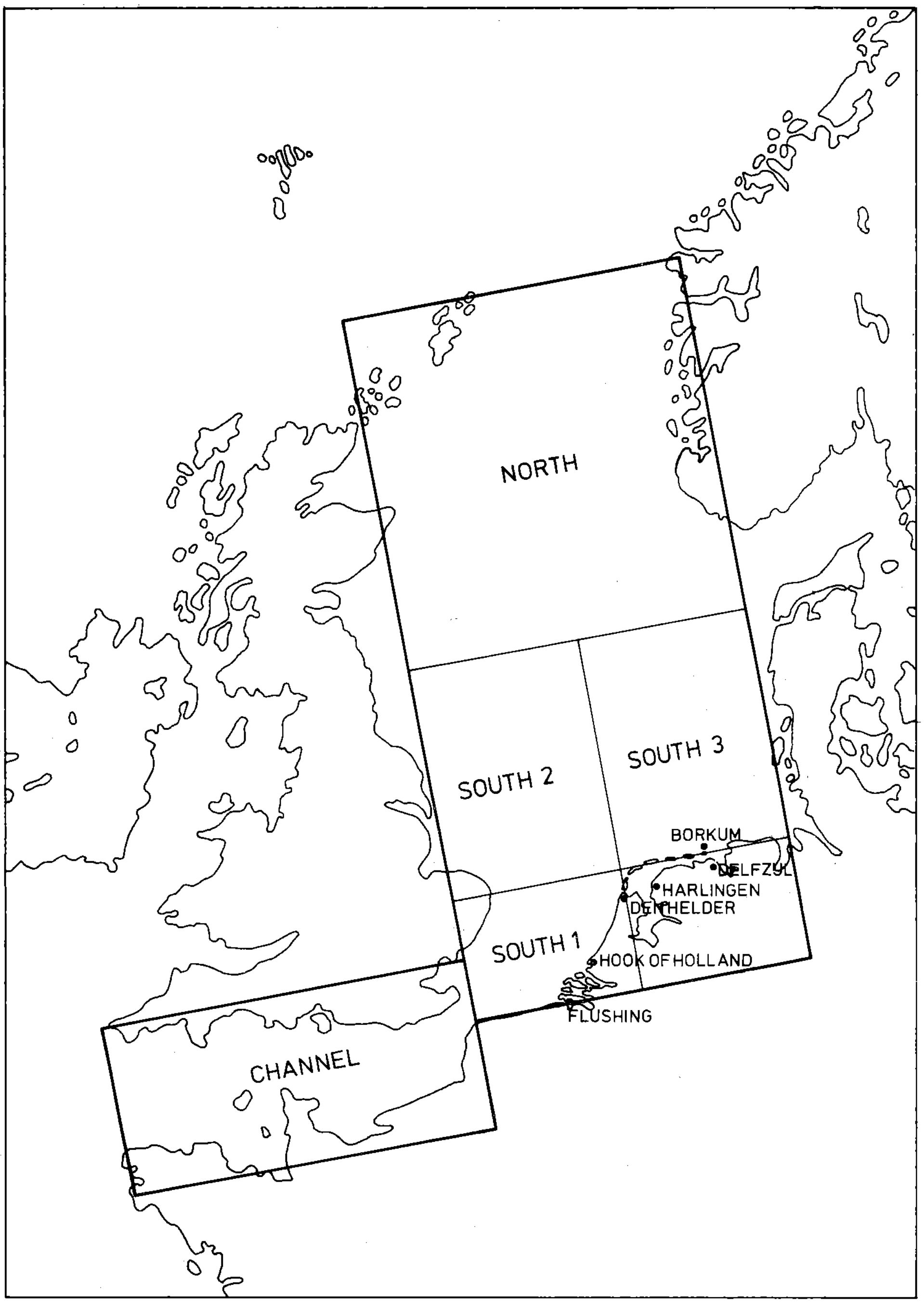

Fig. 3.1.1 Districts method Weenink.

value of C_d, but to an insufficient determination of the corrections for a non-stationary state and to the inaccurate description of the bottom profile by an analytical function, of importance especially to the districts North and Channel. For this reason Weenink accepted the results of Schalkwijk for the districts North and Channel. This means that the method used for practical purposes in the period 1954-1971 is based on the statistical investigation by Schalkwijk as far as the districts North and Channel are concerned, and on the theoretical investigation by Weenink as far as the districts South 1, South 2 and South 3 are concerned. However, it must be remarked that in the work of Weenink the results of Schalkwijk also play an important part, because the value of C_d, used by Weenink, originates from the work of Schalkwijk.

In accordance with the Warning Service for storm surges the water-levels at Harlingen and Delfzijl (see Fig. 3.1.1) need to be computed as well. These levels are partly determined by the shallow waters of the Frisian Sea and the Eems estuary. The bottom topography in these waters is rather complicated, so that a statistical method for determining the meteorological effect at Harlingen and Delfzijl seems to be more convenient than a method based on the hydrodynamical equations. Verploegh and Groen [1955] made such a statistical investigation by relating the difference in set-up between Harlingen and Den Helder to the wind over the Frisian Sea, and by relating the difference in set-up between Delfzijl and Borkum to the wind over the Eems estuary. Bakker [1969] carried out a new investigation for Harlingen with the aid of more recent material. On the basis of the foregoing Weenink composed tables which could be used for practical applications.

3.2 The tables of Weenink were tested by Timmerman [1965] for situations during the years 1958-1962 defined by a set-up of 8 dm or more. The meteorological effect (O), determined by subtracting the astronomical high tide from the observed tidal heights, was compared with the computed set-up according to the method developed by Weenink (C_W). It turned out that there were almost no systematic differences between O and C_W. The standard deviation of the differences was about 2½-3 dm. Table 3.2.1 gives a survey of the five stations Flushing, Hook of Holland, Den Helder, Harlingen and Delfzijl.

Table 3.2.1 Verification of the tables of Weenink.

$\overline{O - C_W}$ = mean value of $O - C_W$,
σ_W = standard deviation of $O - C_W$.

	$\overline{O - C_W}$	σ_W
Flushing	—0.8 dm	2.9 dm
Hook of Holland	—0.2 dm	2.5 dm
Den Helder	—0.3 dm	2.8 dm
Harlingen	—0.8 dm	3.1 dm
Delfzijl	+0.5 dm	2.8 dm
mean	—0.3 dm	2.8 dm

Another test was related to situations during the period January 1965 to July 1970 inclusive, selected on a basis of a lowering of tidal heights of 5 dm or more. Here too, no systematic differences between observed and computed values were found. The standard deviation was about 1½ dm. The verification was carried out only for the stations Flushing and Hook of Holland.

These results are fairly satisfactory, the more so as with respect to the standard deviation, measuring errors of the water-levels and inaccuracy of the tide-table are of some importance. Following W. J. A. Kuipers (verbal communication) the error of measurement can be estimated by means of autocorrelation in a time-series.*) A computation based on halfhourly observations of tidal heights during the storm surge of 9 November 1970, gave a standard deviation of the measuring error of 0.25 dm. Bakker [1967] investigated the accuracy of the tide-tables for Flushing and Hook of Holland in the years 1963-1965. During calm periods over the North Sea he found for both stations differences with systematic variations in time and with a standard deviation of 1-1½ dm.

Still some situations showed considerable differences between observed and computed set-up. These differences may be brought about by the simplifications of the equations or by an insufficient fit of the model to the geographical conditions of the North Sea. It is possible that the analytical expression of the depth of the North Sea is too inaccurate. The partition of the North Sea into a number of districts prevents the inclusion of sufficient details in the description of the windfield; notably district North is very large. Furthermore, it is not satisfactory that the results are obtained with an obviously too large value of C_d. Finally, the time-lag between the wind over a certain section and the maximum effect along the Netherlands coast is only known by a rough approximation.

So further investigations were necessary. These are treated in Chapters 5-9. First, however, in Chapter 4 attention is given to the wind stress, which is of paramount importance when studying the influence of the wind on the sea.

*) The variance of the differences between two observed values, with an arbitrary but fixed time-lag Δt, is dependent on both the autocorrelation coefficient ρ and the error of measurement. The variance of the error of measurement can be computed by assuming a model for the autocorrelation coefficient as a function of time (f.i. $\rho = 1 - a\,(\Delta t)^2$) and by computing these variances for two different values of Δt.

4 The wind stress

4.0 As remarked already, the transfer of momentum and energy from the air to the sea is a crucial link in the generation of deviations of the water-level. Generally the transfer is described by a drag-coefficient C_d and a quadratic relation with wind speed. The latter assumption does not seem to be quite correct. Munk [1955] made it acceptable that the 'drag' is composed of two parts:

1) the 'pure' stress, quadratic in v;
2) the 'form' drag, representing the horizontal component of the mean normal pressure force and which depends therefore on the spectrum of the slopes of the sea surface, proportional to v^3.

Munk's hypothesis leads to the relation: $\tau = \lambda_1 v^2 + \lambda_2 v^3$, where λ_1 and λ_2 are positive constants. If this hypothesis is correct, the application of the relation $\tau = C_d \rho v^2$ implies that C_d has no constant value, but increases linearly with wind speed. However, this dependency cannot be strong, since it is known that the wind mainly affects a limited high-frequency part of the wave spectrum. Nevertheless, recently the idea has gained ground that a rough distinction should be made between a low drag-coefficient for low wind speeds and a high drag-coefficient for high wind speeds. According to Kraus [1972], in case of a wind speed exceeding 15 ms^{-1}, a second effect with respect to the transfer of energy from the atmosphere to the sea becomes important. With these higher wind speeds a mechanical tearing off of the crests of the waves (spray, spin-drift) occurs. Now these water particles are carried away by the wind. Returning to the sea they may bring about an intensified transfer of energy from the atmosphere to the sea. However, the dependency of C_d on the wind speed may also be caused simply by the fact that in sea models time-averaged winds are used instead of momentaneous winds, giving rise to an error which increases with increasing gustiness of the wind, the latter being larger at high than at low wind speeds. Furthermore, averaging in space may introduce similar errors.

4.1 Besides on the wind, C_d also depends on the distribution of temperature in the lower layers of the atmosphere. It is possible to determine C_d by applying profiles of wind, temperature and humidity in the boundary layer of the atmosphere. Panofsky [1963] showed that in case of neutral vertical stratification the relation 4.1.1 is valid:

$$C_d = k^2[\ln (z/z_o)]^2 \qquad (4.1.1)$$

The roughness parameter z_o is considerably smaller over sea than over land. Again according to Panofsky, a function of stability ψ has to be added if the stratification deviates from neutral conditions.

$$C_d = k^2[\ln (z/z_o) - \psi(z/L)]^2 \qquad (4.1.2)$$

In 4.1.2 z/L is a function of the Richardson number Ri_v, defined by

$$Ri_v = \frac{g}{\theta_v} \frac{\partial\theta_v}{\partial z} \left(\frac{\partial |\vec{v}|}{\partial z}\right)^2 \qquad (4.1.3)$$

Ri_v can be determined with the aid of measurements of wind speed and virtual temperature in the lowest layers of the atmosphere. The function ψ is given by Brocks and Krügermeyer [1970], using the 'Keyps'-profile for unstable vertical structure (Panofsky [1963]) and the 'log-linear' profile (Webb [1970]).

The equation 4.1.2. gives the opportunity to compute C_d as a function of the Richardson number. The results derived from data given by Brocks and Krügermeyer are shown in Table 4.1.1.

Table 4.1.1 Relation between C_d and the number of Richardson.

Ri_v	—1	—0.5	—0.1	—0.05	—0.01	+0.01	+0.05	+0.1	+0.15	+0.2
C_d* 10^3	5.5	4.1	2.2	1.7	1.4	1.2	0.8	0.4	0.2	0.02

The Richardson numbers, valid for a height of 3.3 m, were computed by Brocks and Krügermeyer with the aid of wind-, temperature- and humidity measurements. Table 4.1.2 gives the highest and lowest computed values of C_d for a wind speed between 3 ms^{-1} and 13 ms^{-1} measured at a height of 10 m. In addition, the associated stresses τ_1 and τ_2 are mentioned, computed with the formula $\tau = C_d \rho v^2$.

Table 4.1.2 Relation between wind speed, the number of Richardson and the stress.

v	Ri_v max.	Ri_v min.	$C_{d1} \cdot 10^3$ min.	$C_{d2} \cdot 10^3$ max.	$\tau_1 \cdot 10^3$ min.	$\tau_2 \cdot 10^3$ max.
3 ms^{-1}	+0.1	—0.5	0.4	4.1	4.5	46 Nm^{-2}
4 ms^{-1}	+0.1	—0.5	0.4	4.1	6.4	82 Nm^{-2}
5 ms^{-1}	+0.1	—0.5	0.4	4.1	10.0	128 Nm^{-2}
6 ms^{-1}	+0.1	—0.4	0.4	3.3	14.4	137 Nm^{-2}
7 ms^{-1}	+0.1	—0.3	0.4	3.0	19.6	173 Nm^{-2}
8 ms^{-1}	+0.1	—0.1	0.4	2.2	25.6	206 Nm^{-2}
9 ms^{-1}	+0.05	—0.1	0.8	2.2	81	218 Nm^{-2}
10 ms^{-1}	+0.05	—0.05	0.8	1.8	100	219 Nm^{-2}
11 ms^{-1}	+0.02	—0.02	1.1	1.4	168	220 Nm^{-2}
12 ms^{-1}	+0.01	—0.01	1.2	1.4	216	245 Nm^{-2}
13 ms^{-1}	+0.01	—0.01	1.2	1.4	254	287 Nm^{-2}

It appears from Table 4.1.2 that at low wind speeds the vertical structure of temperature influences the stress exerted by the atmosphere on the sea surface to a high degree. At high wind speeds, however, the distribution of temperature is of minor importance and the stress is mainly determined by the wind speed. For a wind speed between 10 and 13 ms^{-1} Brocks and Krügermeyer give $C_d = 0.0013$.

In the numerical model described in this treatise the dependency of C_d on the difference in temperature between air and sea is given by a correction factor F, introduced by Weenink, to be applied to C_d, giving the influence of variations in difference between the temperature of air and sea. This correction factor F reads as follows:

$$F = 1 - 0.044(T_a - T_s) \qquad (4.1.4)$$

4.2 As remarked already it is assumed that C_d increases if the wind speed exceeds 15 ms^{-1}. For high wind speeds Wilson [1960] and Roll [1965] take $C_d = 0.0025$. As mentioned in Chapter 3, Weenink applied $C_d = 0.0034$, which seems to be much too large.

Based on measurements over southern Lake Flevo (former Zuiderzee) Wieringa [1973] found the relation $C_d = 0.0007\bar{u}_{10}^{0.3}$ for a wind speed between 5 and 15 ms^{-1}, yielding $C_d =$ $C_d = 0.0016$ if $\bar{u}_{10} = 15$ ms^{-1}, where $\bar{u}_{10}$ is an averaged wind speed at a height of 10 m.

Peeck [1974] developed a numerical model for the southern Lake Flevo and computed by the least squares method that value of C_d that gave the best agreement between observed and computed water-levels. For a wind speed less than 14 ms^{-1} it turned out that $C_d = 0.0018$ was a reliable upper limit.

So the value of C_d is still open to questions. Table 4.2.1 gives C_d in dependence of two classes of wind speed, < 15 ms^{-1} and > 20 ms^{-1} (with linear interpolation for the wind speed between the two values). These values were applied during the periods September 1973 till June 1974 and October 1974 till June 1975, respectively.

Table 4.2.1 The value of $C_d \cdot 10^3$ for two classes of wind speed

	1973-74	1974-75
< 15 ms^{-1}	1.8	1.7
> 20 ms^{-1}	2.7	2.5

It will appear from 9.1.1 that the values of C_d taken for the period 1974-75 are somewhat too low.

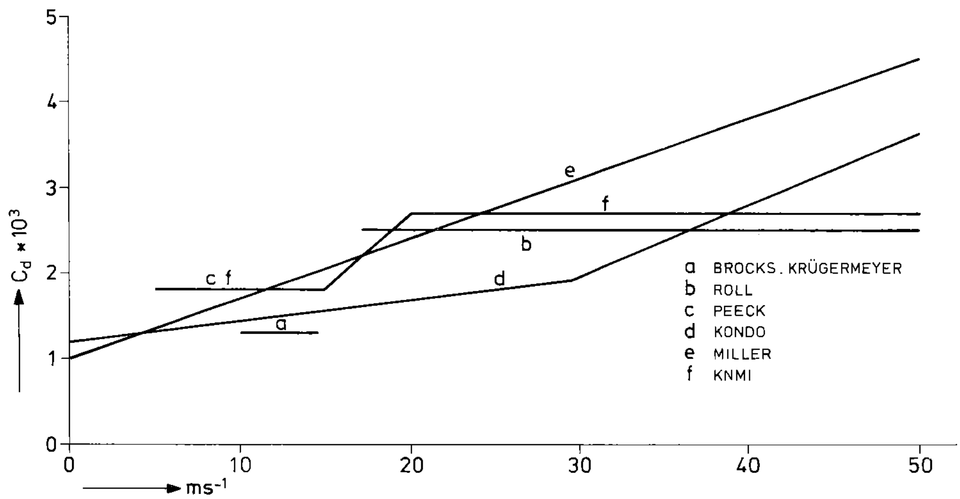

Fig. 4.3.1 Survey of drag coefficients.

4.3 Recently Kondo [1975] proposed the following relations:
$C_d = (1.2 + 0.025 * \overline{u}_{10}) * 10^{-3}$ for $5 < \overline{u}_{10} < 30\ ms^{-1}$ and
$C_d = 0.073 * \overline{u}_{10} * 10^{-3}$ for $\overline{u}_{10} > 30\ ms^{-1}$. These results were based on a high-speed wind flume experiment (Kunishi and Imasato [1966]) and on momentum budgets of the hurricanes Helene, Donna (Miller [1966]) and Hilda (Hawkins and Rubsam [1968]). Especially for wind speeds between 20 and 35 ms^{-1} the values of C_d according to Kondo are appreciably lower than those applied in the KNMI-model. Miller, Chase and Jarvinen [1972] gave the following formula: $C_d = (1.0 + 0.07 * \overline{u}_{10}) * 10^{-3}$. Kondo as well as Miller indicate that C_d increases with increasing wind speed. This is of importance when considering the meteorological effect under very extreme conditions. See for instance Chapter 10. Figure 4.3.1 gives a survey in graphical form of some values of C_d mentioned in this chapter. The three curves clearly show that with respect to C_d there is much uncertainty, especially for high wind speeds. However, applying sea models, it is only of importance that the value of C_d is chosen in such a way that the agreement between observed and computed tidal heights is satisfactory.

5 The numerical model for the North Sea and environment

5.0 Numerical computational methods, characterized by the solution of a set of difference equations corresponding to the differential equations describing physical processes, make use of staggered grids. Water models, based for instance on the set of equations 3.1.1, often make use of two or three grids. In the case of two grids h will be computed in one grid, U and V in the other. Using three grids h, U and V are computed in separate grids. The models of Lauwerier [1963], Van der Houwen [1966] and Heaps [1969] are examples of the first type, while the second type was applied by Hansen [1966] and Leendertse [1967]. Approximating the differential quotients with the aid of three grids is more accurate than by two grids, but when studying a large area such as the North Sea the coastal profiles can better be fitted by two grids, because a three-grid model can describe the coast only in a stepped way.

The investigation by Peeck for Lake Flevo, mentioned in the previous chapter, is a three-grid model, while the model which will be discussed now and which is used for the computation of storm surges (Timmerman [1975]), makes use of two grids. Fig. 5.0.1 gives an illustration of a two-grid model.

The sea-area on which the interest is focussed should be covered completely by grids. It is not necessary that the meshsize is the same all over the grid. It is possible to divide the sea-area in a number of areas with grids of a different mesh-size. Generally, the mesh-size will be larger with increasing distance to the Netherlands coast. The different grids may be coupled by means of interpolation of values of h. Oscillations created by this coupling appeared to be of little importance.

The boundary of the considered area may be composed of U, V-points or h-points. The boundary conditions must be formulated accordingly. For a closed boundary the boundary condition reads that no current perpendicular to the coast is allowed. Therefore, for a coastal boundary the current is prescribed to have a direction parallel to the coast. Generally open boundaries are composed of h-points, which for the sake of simplicity are equated to zero throughout the computation. This introduces an error, which may be minimized by moving the boundary towards more remote regions.

5.1 Solution of the difference equations implies that the functions U, V and h are computed in the grid points at discrete moments: $t_0+n\Delta t$ $(n=0, 1, 2, \ldots)$. The values of the functions for an arbitrary moment are determined with the aid of values computed previously. Besides, it is possible to continue a computation, formerly adjourned because no new meteorological data were available. If no computed values of U, V and h are available, U, V, and h are taken zero as an initial condition.

The set of difference equations to be solved can be derived from a somewhat modified set of equations 3.1.1. The present problem does not deal with details connected with the structure of shallow coastal areas, but with the transport of large quantities of water, causing surges. For this reason h can be neglected with respect to H. Generally it can be remarked that this omission is admissible if H exceeds 30 m.

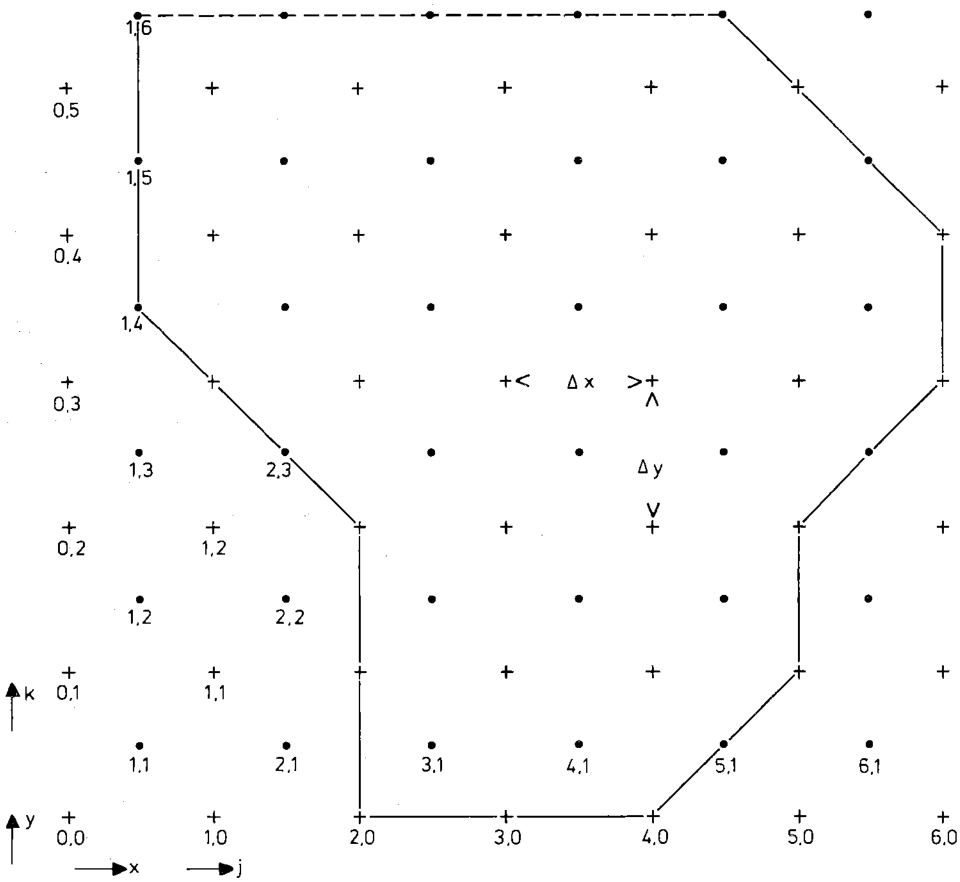

Fig. 5.0.1 Example of a two-grid model. +U,V-point. • h-point. The boundary of the model is indicated by —— (closed boundary) or by – – – (open boundary).

As indicated in Chapter 4, τ_o is given by $C_d \rho v^2$. The bottom stress depends on the bottom velocity in a similar way:

$$\tau_b = C_b \rho_s V_b^2 \tag{5.1.1}$$

However, V_b is not well known and usually replaced by a stream velocity $\overline{V}$ averaged in the vertical. This approximation does not introduce a large error, because the order of magnitude of the bottom stress is smaller than the order of magnitude of some other terms of 3.1.1. It is even acceptable to consider τ_b as a linear function of $\overline{V}$. According to Bowden [1953] a term related to the surface stress must then be added:

$$\frac{\tau_b}{\rho_s} = r\overline{V} + \frac{m\tau_o}{\rho_s} \tag{5.1.2}$$

The last term is of little importance, however, and is generally omitted.

The set of equations now reads as follows:

$$\frac{\partial U}{\partial t} = fV - gH\frac{\partial h}{\partial x} - \frac{rU}{H} + C_d\frac{\rho}{\rho_s}v_x|\vec{v}| - \frac{H}{\rho_s}\frac{\partial p(h)}{\partial x}$$

$$\frac{\partial V}{\partial t} = -fU - gH\frac{\partial h}{\partial y} - \frac{rV}{H} + C_d\frac{\rho}{\rho_s}v_y|\vec{v}| - \frac{H}{\rho_s}\frac{\partial p(h)}{\partial y} \qquad (5.1.3)$$

$$\frac{\partial h}{\partial t} = -\frac{\partial U}{\partial x} - \frac{\partial V}{\partial y}$$

Following Weenink [1958] r is taken as 0.0024 ms^{-1}.

The values of the functions U, V and h in the grid points $j\Delta x$, $k\Delta y$ and at the point of time $n\Delta t$ are indicated as follows (see also figure 5.0.1):

$$U(j\Delta x, k\Delta y, n\Delta t) = U^n_{j,k}$$

$$V(j\Delta x, k\Delta y, n\Delta t) = V^n_{j,k} \qquad (5.1.4)$$

$$h(j\Delta x, k\Delta y, n\Delta t) = h^n_{j,k}$$

A depth $H_{j,k}$ is added to each U, V point. This depth is related to actual depths within a square with angular points $(j+\frac{1}{2}, k+\frac{1}{2})$, $(j+\frac{1}{2}, k-\frac{1}{2})$, $(j-\frac{1}{2}, k+\frac{1}{2})$ and $(j-\frac{1}{2}, k-\frac{1}{2})$. For the grid and the depth distribution reference is made to Fig. 5.1.1 and 5.1.2.

From the set of equations 5.1.3 the following set of difference equations can be derived:

$$U^{n+1}_{j,k} = U^n_{j,k} + \Delta t * \left[fV^n_{j,k} - gH_{j,k}\left(\frac{h^n_{j+1,k+1} + h^n_{j+1,k} - h^n_{j,k+1} - h^n_{j,k}}{2\Delta x}\right) - \frac{rU^n_{j,k}}{H_{j,k}} + \right.$$

$$\left. + C_d\frac{\rho}{\rho_s}v_x|\vec{v}| - \frac{H_{j,k}}{\rho_s}\frac{\partial p(h)}{\partial x}\right]$$

$$V^{n+1}_{j,k} = V^{j,k}_{n} + \Delta t * \left[-fU^n_{j,k} - gH_{j,k}\left(\frac{h^n_{j+1,k+1} + h^n_{j,k+1} - h^n_{j+1,k} - h^n_{j,k}}{2\Delta y}\right) - \frac{rV^n_{j,k}}{H_{j,k}} + \right. \qquad (5.1.5)$$

$$\left. + C_d\frac{\rho}{\rho_s}v_y|\vec{v}| - \frac{H_{j,k}}{\rho_s}\frac{\partial p(h)}{\partial y}\right]$$

$$h^{n+1}_{j,k} = h^n_{j,k} - \Delta t * \left[\frac{U^{n+1}_{j,k} + U^{n+1}_{j,k-1} - U^{n+1}_{j-1,k} - U^{n+1}_{j-1,k-1}}{2\Delta x} + \frac{V^{n+1}_{j,k} + V^{n+1}_{j-1,k} - V^{n+1}_{j,k-1} - V^{n+1}_{j-1,k-1}}{2\Delta y}\right]$$

The computational scheme 5.1.5 can be simply applied to internal points of the grid. However, special provisions must be made for U-, V- or h-points located on the boundary. This kind of provisions is clarified in Figure 5.1.3, showing part of a boundary. When for instance $h_{j,k}$ is lacking, the difference $h^n_{j+1,k+1} + h^n_{j+1,k} - h^n_{j,k+1} - h^n_{j,k}$ is replaced by $2 * (h^n_{j+1,k+1} - h^n_{j,k+1})$. After each time step the stream vector at a coastal point is resolved in a component parallel and a component perpendicular to the coast. The latter is equated zero, so the new stream vector can be identified with the component parallel to the coast.

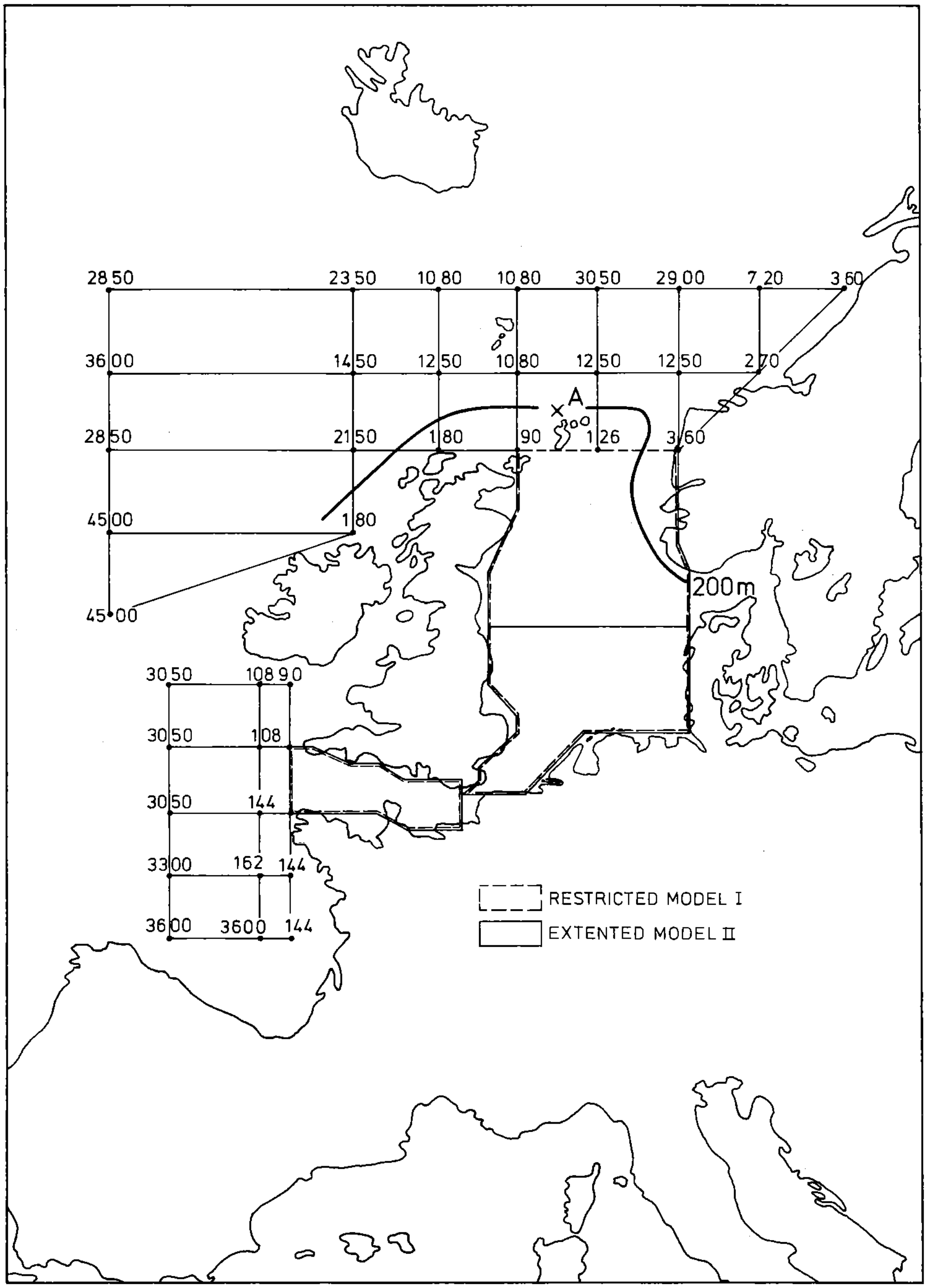

Fig. 5.1.1 Grid, covering the North Sea, the Channel and adjacent regions of the Atlantic Ocean. Depth in m.

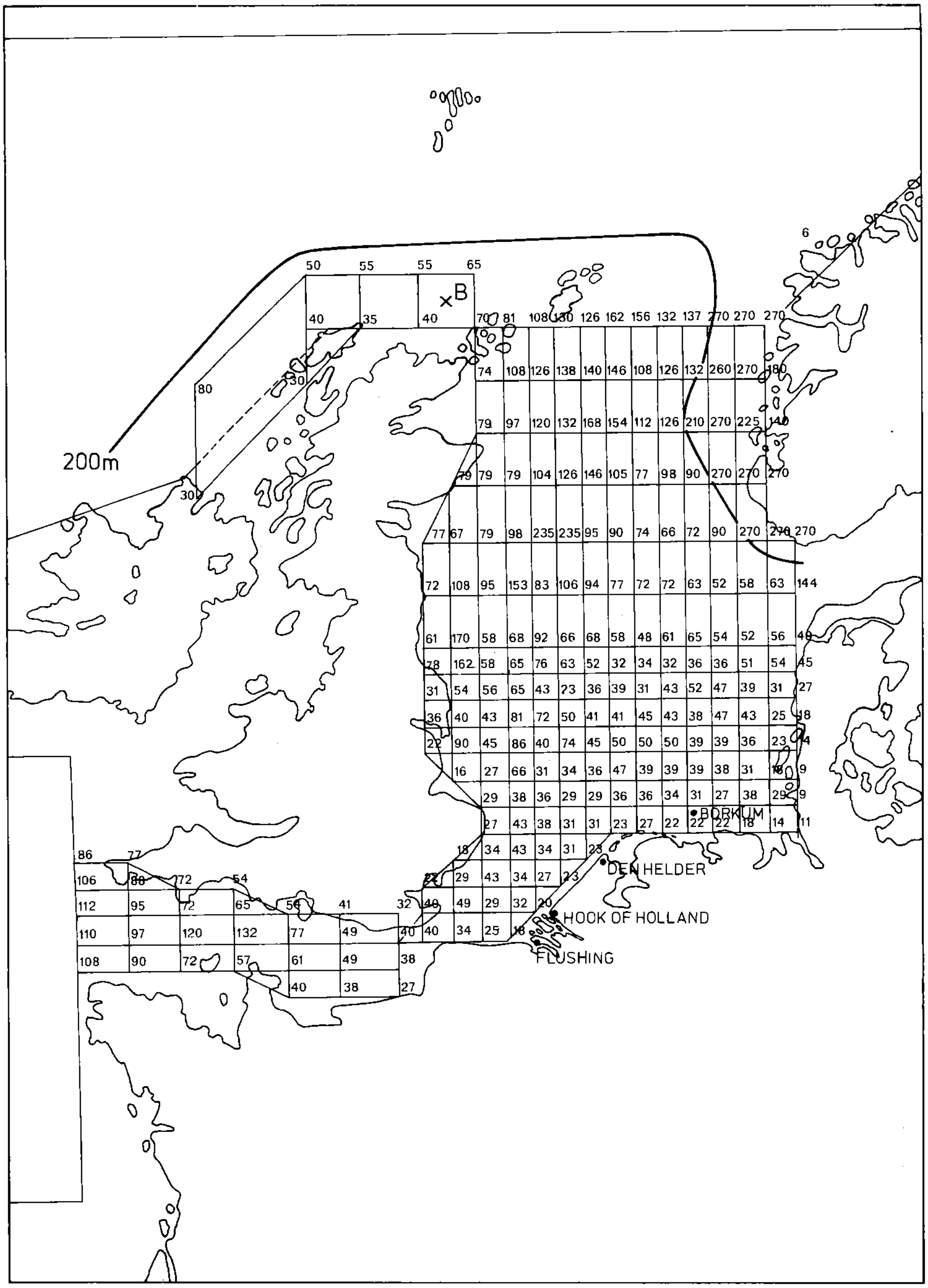

Fig. 5.1.2 Grid, covering the North Sea, the Channel and the shallow areas to the North and West of Scotland. Depth in m.

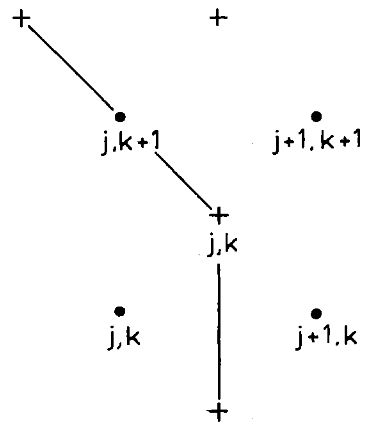

Fig. 5.1.3 Example of a boundary. + U,V-point. • h-point. —— boundary.

In the foregoing it is indicated in which way $U^n_{j,k}$, $V^n_{j,k}$ and $h^n_{j,k}$ can be computed starting from the initial values $U^o_{j,k}$, $V^o_{j,k}$ and $h^o_{j,k}$ with due reference to the boundary conditions.

The numerical stability of the set of difference equations 5.1.5 was investigated by Lauwerier and Damsté [1963] and Van der Houwen [1966]. The most important limitation as far as the choice of Δx, Δy and Δt is concerned is given by the stability condition for the coast.
This condition reads:

$$\Delta t \leq \frac{1}{2\sqrt{gH}} \frac{\Delta x\ \Delta y}{|s|\Delta x + |c|\Delta y} \tag{5.1.6}$$

This is shown by Van der Houwen, provided that U^{n+1} and V^{n+1} are used when computing h^{n+1}.

A flow diagram of the iteration process is given in Figure 5.1.4.

5.2 The programme for the computer has been written in such a way that the geometric characteristics can be altered during the execution of the program. Due to this the program is suitable for the investigation of sea areas of different shapes and proportions. However, too large dimensions are not allowed, because the curvature of the earth is not taken into account.

The investigation for improving the tables used in practical service to compute the deviations of the water-level was carried out with a grid covering the North Sea and the Channel. (Restricted model I). These tables were given for a number of stations as a function of the wind over the North Sea and the Channel and are based on the method of Weenink. See Fig. 5.1.1 and 5.1.2 (Chapter 6). Also the application to the 16 surges in the period 1958-1962 (Timmerman [1965]) was carried out with this restricted model (Chapter 8). The grid was

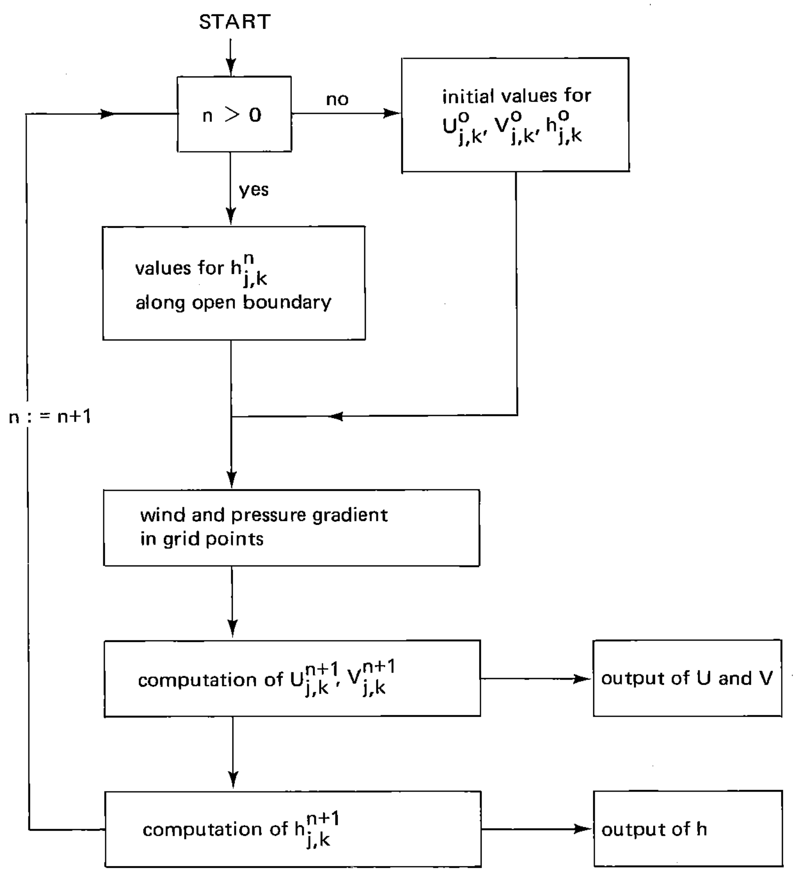

Fig. 5.1.4 Flow diagram of iteration process.

adapted to the real geographical conditions, especially on the southern part of the North Sea, by taking a length of 42 km. For reasons of stability in more remote parts of the North Sea and in the Channel the mesh length in one of the directions was raised to 84 km. Furthermore, $\Delta t = 450$ s.

The recent model, operating on a semi-operational basis, covers a much larger area and includes besides the area of the restricted model I also parts of the Atlantic Ocean (Extended model II). See Fig. 5.1.1 (Chapter 7).

The grids could be represented on a square matrix of 23 * 19 points, after a rotation of 90 degrees of some of them.

6 Tables for operational use in computing deviations of water-levels

6.0 As described in Chapter 3 Weenink computed the stationary windeffect for a number of stations along the Netherlands coast as a function of a homogeneous windfield over five districts in the North Sea and the Channel area. It turned out that a number of objections could be raised, which can be summarized as follows:

a) The computed values for the district North appear to be about twice as large as the values determined by Schalkwijk.
b) The district North is much too large for a specification of the wind.
c) The geography of the North Sea and the distribution of its depth is presented rather poorly.
d) The value of the drag coefficient C_d is too large.
e) The time-lag between a windfield over a sector and the maximum effect on the Netherlands' coast is only roughly known.

When computers became available, the differential equations could be solved without the restrictions necessary to obtain an analytical solution. Such computations were carried out with the restricted model I, given in Fig. 5.1.1, solving the set of equations 6.0.1.

$$\frac{\partial U}{\partial t} = fV - gH \frac{\partial h}{\partial x} - \frac{rU}{H} + C_d \frac{\rho}{\rho_s} v_x |\vec{v}|$$

$$\frac{\partial V}{\partial t} = -fU - gH \frac{\partial h}{\partial y} - \frac{rV}{H} + C_d \frac{\rho}{\rho_s} v_y |\vec{v}| \qquad (6.0.1)$$

$$\frac{\partial h}{\partial t} = -\frac{\partial U}{\partial x} - \frac{\partial V}{\partial y}$$

This set of equations corresponds with 5.1.3 after omitting the two pressure terms.

The grid was divided into 6 districts, namely North-W, North-E, Mid-W, Mid-E, South and Channel. The districts Mid-W and Mid-E correspond with the former districts South 1 and South 3, while the districts North-W and North-E represent a partition of the district North. See Fig. 6.0.1. At different wind speeds and wind directions the stationary effect on the water-levels at Flushing, Hook of Holland, Den Helder and Borkum of each district separately was computed. This was attained by assuming a constant windfield over a district for a sufficiently long period, so that the corresponding wind effect remained constant as well. Moreover, computations carried out in this way give the time-lag between the occurrence of a windfield over a certain district and the effect on the Netherlands coast. C_d was taken 0.0028. Along these lines the new tables 6.0.1-6.0.4 for the computation of the wind effect at these stations were composed. Due to the linearity of the equations the total effect can be achieved by a simple addition of the partial contributions of the districts. The computation of the wind effect of the Frisian Sea and the Eems-estuary for the case of Harlingen and Delfzijl has remained unaltered.

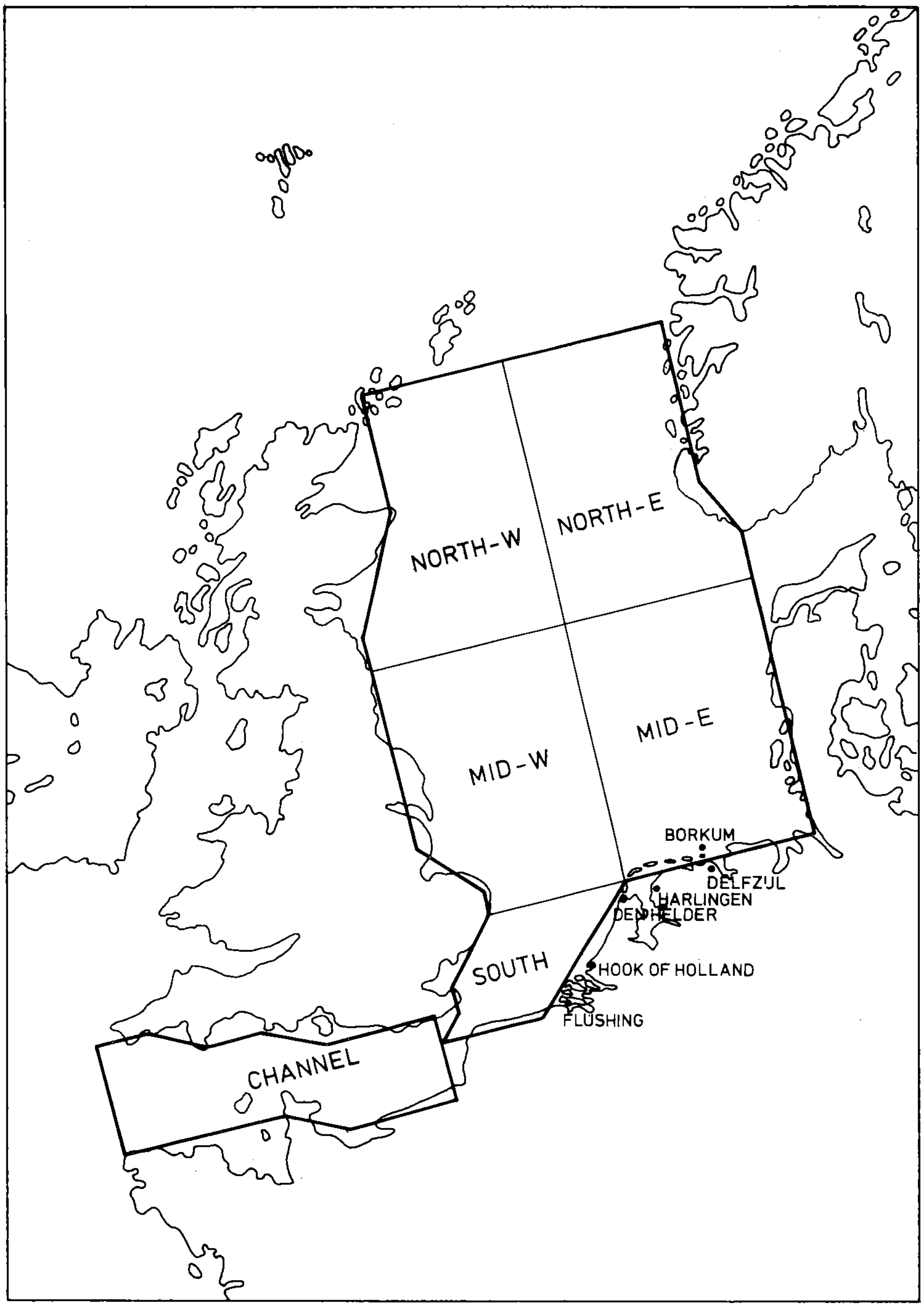

Fig. 6.0.1 Districts method, operational since September 1971.

Table 6.0.1

WIND EFFECT (in dm) FLUSHING

Timelag in hrs ↓		kts ↓	Direction of isobars → 180	200	220	240	260	280	300	320	340	360	020	040	060	080	100	120	140	160
9	NORTH-W	20	-½	-½	-½	0	0	0	½	½	½	½	½	½	0	0	0	-½	-½	-½
		25	-1	-½	-½	0	0	½	½	½	1	1	½	½	0	0	-½	-½	-½	-1
		30	-1	-1	-½	-½	0	½	1	1	1	1	1	½	½	0	-½	-1	-1	-1
		35	-1½	-1½	-1	-½	0	½	1	1½	1½	1½	1½	1	½	0	-½	-1	-1½	-1½
		40	-2	-1½	-1	-½	0	1	1½	2	2	2	1½	1	½	0	-1	-1½	-2	-2
		45	-2½	-2	-1½	-1	0	1	2	2½	2½	2½	2	1½	1	0	-1	-2	-2½	-2½
		50	-3	-2½	-2	-1	0	1½	2½	3	3	3	2½	2	1	0	-1½	-2½	-3	-3
		55	-4	-3	-2½	-1	0	1½	2½	3	4	4	3	2½	1	0	-1½	-2½	-3½	-4
		60	-5½	-4	-2½	-1½	½	2	3½	4	4½	4½	4	2½	1½	-½	-2	-3½	-4	-4½
9	NORTH-E	20	0	0	0	0	0	0	0	0	0	0	0	0	0	0	0	0	0	0
		25	0	0	0	0	0	0	0	0	0	0	0	0	0	0	0	0	0	0
		30	-½	-½	0	0	0	0	0	½	½	½	½	0	0	0	0	0	-½	-½
		35	-½	-½	-½	0	0	0	½	½	½	½	½	½	0	0	0	-½	-½	-½
		40	-½	-½	-½	0	0	0	½	½	½	½	½	½	0	0	0	-½	-½	-½
		45	-1	-½	-½	-½	0	0	½	½	1	1	½	½	½	0	0	-½	-½	-1
		50	-1	-1	-½	-½	0	0	½	1	1	1	1	½	½	0	0	-½	-1	-1
		55	-1	-1	-½	-½	0	0	½	1	1	1	1	½	½	0	0	-½	-1	-1
		60	-1½	-1	-1	-½	0	½	1	1	1½	1½	1	1	½	0	-½	-1	-1	-1½
6	MID-W	20	-1½	-1	-½	-½	0	½	1	1½	1½	1	1	½	½	0	-½	-1	-1½	-1½
		25	-2	-1½	-1	-½	½	1	1½	2	2	2	1½	1	½	-½	-1	-1½	-2	-2
		30	-3	-2½	-1½	-½	½	1½	2½	3	3	3	2½	1½	½	-½	-1½	-2½	-3	-3
		35	-4	-3½	-2	-1	½	2	3	4	4½	4	3½	2	1	-½	-2	-3	-4	-4½
		40	-5½	-4½	-3	-1	1	3	4	5	5½	5½	4½	3	1	-1	-3	-4	-5	-5½
		45	-6½	-5½	-3½	-1½	1	3½	5½	6½	7	6½	5½	3½	1½	-1	-3½	-5½	-6½	-7
		50	-8½	-7	-4½	-1½	1½	4½	6½	8	8½	8½	7	4½	1½	-1½	-4½	-6½	-8	-8½
		55	-10	-8	-5½	-2	1½	5½	8	10	10½	10	8	5½	2	-1½	-5½	-8	-10	-10½
		60	-12	-10	-6½	-2½	2	6½	9½	12	12½	12	10	6½	2½	-2	-6½	-9½	-11½	-12½
3	MID-E	20	0	0	0	0	0	0	0	0	0	0	0	0	0	0	0	0	0	0
		25	0	-½	-½	-½	-½	0	0	0	0	0	½	½	½	½	0	0	0	0
		30	-½	-½	-½	-½	-½	-½	0	0	0	½	½	½	½	½	½	0	0	0
		35	-½	-½	-½	-½	-½	-½	-½	0	0	½	½	½	½	½	½	½	0	0
		40	-½	-½	-1	-1	-1	-½	-½	0	0	½	½	1	1	1	½	½	0	0
		45	-1	-1	-1	-1	-1	-1	-½	0	½	1	1	1	1	1	1	½	0	-½
		50	-1	-1	-1½	-1½	-1½	-1	-½	0	½	1	1	1½	1½	1½	1	½	0	-½
		55	-1	-1½	-1½	-1½	-1½	-1	-½	0	½	1	1½	1½	1½	1½	1	½	0	-½
		60	-1½	-1½	-2	-2	-2	-1½	-1	0	½	1½	1½	2	2	2	1½	1	0	-½
3	SOUTH	20	-1½	-1	-½	0	½	1	1	1½	1½	1½	1	½	0	-½	-1	-1	-1½	-1½
		25	-2	-1½	-1	0	½	1½	2	2	2	2	1½	1	0	-½	-1½	-2	-2	-2
		30	-3	-2	-1½	-½	1	2	2½	3	3	3	2	1½	½	-1	-2	-2½	-3	-3
		35	-4	-3	-2	-½	1	2½	3½	4	4½	4	3	2	½	-1	-2½	-3½	-4	-4½
		40	-5	-4	-2½	-½	1½	3½	4½	5½	5½	5	4	2½	½	-1½	-3½	-4½	-5½	-5½
		45	-6½	-5	-3	-½	2	4	6	7	7	6½	5	3	½	-2	-4	-6	-7	-7
		50	-8	-6	-4	-1	2½	5	7	8½	9	8	6	4	1	-2½	-5	-7	-8½	-9
		55	-10	-7½	-4½	-1	2½	6	8½	10½	10½	10	7½	4½	1	-2½	-6	-8½	-10½	-10½
		60	-11½	-9	-5½	-1	3½	7½	10½	12	13	11½	9	5½	1	-3½	-7½	-10½	-12	-13
6	CHANNEL	20	0	½	1	1	1	1	1	½	0	0	-½	-1	-1	-1	-1	-1	-½	0
		25	0	1	1½	1½	1½	1½	1½	1	0	0	-1	-1½	-1½	-1½	-1½	-1½	-1	0
		30	½	1½	2	2½	2½	2½	2	1	½	-½	-1½	-2	-2½	-2½	-2½	-2	-1	-½
		35	1	2	2½	3	3½	3	2½	1½	½	-1	-2	-2½	-3	-3½	-3	-2½	-1½	-½
		40	1	2½	3½	4	4	4	3	2	½	-1	-2½	-3½	-4	-4	-4	-3	-2	-½
		45	1	3	4½	5	5½	5	4	2½	1	-1	-3	-4½	-5	-5½	-5	-4	-2½	-1
		50	1½	4	5½	6½	6½	6½	5	3	1	-1½	-4	-5½	-6½	-6½	-6½	-5	-3	-1
		55	2	4½	7	8	8	8	6	3½	1	-2	-4½	-7	-8	-8	-8	-6	-3½	-1
		60	2	5½	8	9	9½	9	7	4½	1½	-2	-5½	-8	-9	-9½	-9	-7	-4½	-1½

Sept. 1971

Table 6.0.2

WIND EFFECT (in dm) HOOK OF HOLLAND

Timelag in hrs ↓	kts ↓	Direction of isobars → 180	200	220	240	260	280	300	320	340	360	020	040	060	080	100	120	140	160
9 NORTH-W	20	-½	-½	-½	0	0	0	½	½	½	½	½	½	0	0	0	-½	-½	-½
	25	-1	-1	-½	-½	0	½	½	1	1	1	1	½	½	0	-½	-½	-1	-1
	30	-1½	-1½	-1	-½	0	½	1	1½	1½	1½	1½	1	½	0	-½	-1	-1½	-1½
	35	-2	-1½	-1	-½	0	½	1½	1½	2	2	1½	1	½	0	-½	-1½	-1½	-2
	40	-2½	-2	-1½	-1	0	1	1½	2	2½	2½	2	1½	1	0	-1	-1½	-2	-2½
	45	-3	-3	-2	-1	0	1	2	3	3	3	3	2	1	0	-1	-2	-3	-3
	50	-4	-3½	-2½	-1	0	1½	2½	3½	4	4	3½	2½	1	0	-1½	-2½	-3½	-4
	55	-4½	-4	-3	-1½	0	1½	3	4	4½	4½	4	3	1½	0	-1½	-3	-4	-4½
	60	-5½	-5	-3½	-2	0	2	4	5	5½	5½	5	3½	2	0	-2	-4	-5	-5½
9 NORTH-E	20	0	0	0	0	0	0	0	0	0	0	0	0	0	0	0	0	0	0
	25	-½	-½	0	0	0	0	0	½	½	½	½	0	0	0	0	0	-½	-½
	30	-½	-½	-½	0	0	0	0	½	½	½	½	½	0	0	0	0	-½	-½
	35	-½	-½	-½	0	0	0	½	½	½	½	½	½	0	0	0	-½	-½	-½
	40	-1	-½	-½	-½	0	0	½	½	½	1	½	½	½	0	0	-½	-½	-½
	45	-1	-1	-½	-½	0	0	½	1	1	1	1	½	½	0	0	-½	-1	-1
	50	-1	-1	-1	-½	0	0	½	1	1	1	1	1	½	0	0	-½	-1	-1
	55	-1½	-1	-1	-½	0	0	½	1	1	1½	1	1	½	0	0	-½	-1	-1
	60	-2	-1½	-1	-½	-½	½	1	1½	1½	2	1½	1	½	½	-½	-1	-1½	-1½
6 MID-W	20	-1½	-1	-1	-½	0	½	1	1½	1½	1½	1	1	½	0	-½	-1	-1½	-½1
	25	-2½	-2	-1½	-½	½	1	2	2½	2½	2½	2	1½	½	-½	-1	-2	-2½	-2½
	30	-3½	-3	-2	-½	½	1½	2½	3½	3½	3½	3	2	½	-½	-1½	-2½	-3½	-3½
	35	-4½	-4	-2½	-1	½	2	3½	4½	5	4½	4	2½	1	-½	-2	-3½	-4½	-5
	40	-6	-5	-3½	-1½	1	3	4½	6	6½	6	5	3½	1½	-1	-3	-4½	-6	-6½
	45	-7½	-6½	-4½	-1½	1	3½	6	7½	8	7½	6½	4½	1½	-1	-3½	-6	-7½	-8
	50	-9½	-8	-5½	-2	1	4½	7½	9	10	9½	8	5½	2	-1	-4½	-7½	-9	-10
	55	-11½	-9½	-6½	-2½	1½	5½	9	11	12	11½	9½	6½	2½	-1½	-5½	-9	-11	-12
	60	-13½	-11	-7½	-3	2	6½	10½	13½	14	13½	11	7½	3	-2	-6½	-10½	-13½	-14
3 MID-E	20	-½	-½	-½	-½	-½	0	0	0	0	½	½	½	½	½	0	0	0	0
	25	-½	-½	-½	-½	-½	-½	0	0	½	½	½	½	½	½	½	0	0	-½
	30	-½	-1	-1	-1	-½	-½	0	0	½	½	1	1	1	½	½	0	0	-½
	35	-1	-1	-1	-1	-1	-½	0	0	½	1	1	1	1	1	½	0	0	-½
	40	-1	-1½	-1½	-1½	-1	-½	-½	½	1	1	1½	1½	1½	1	½	½	-½	-1
	45	-1½	-2	-2	-2	-1½	-1	-½	½	1	1½	2	2	2	1½	1	½	-½	-1
	50	-2	-2½	-2½	-2½	-2	-1	-½	½	1	2	2½	2½	2½	2	1	½	-½	-1
	55	-2	-2½	-2½	-2½	-2	-1	-½	½	1½	2	2½	2½	2½	2	1	½	-½	-1½
	60	-2½	-3½	-3½	-3½	-2½	-1½	-½	½	2	2½	3½	3½	3½	2½	1½	½	-½	-2
3 SOUTH	20	-1	-½	0	0	½	1	1	1½	1	1	½	0	0	-½	-1	-1	-1½	-1
	25	-1½	-1	-½	½	1	1½	2	2	2	1½	1	½	-½	-1	-1½	-2	-2	-2
	30	-2½	-1½	-½	½	1½	2½	2½	3	3	2½	1½	½	-½	-1½	-2½	-2½	-3	-3
	35	-3	-2	-½	½	2	3	3½	4	4	3	2	½	-½	-2	-3	-3½	-4	-4
	40	-4	-2½	-1	1	2½	4	5	5½	5	4	2½	1	-1	-2½	-4	-5	-5½	-5
	45	-5	-3½	-1	1	3½	5	6	6½	6½	5	3½	1	-1	-3½	-5	-6	-6½	-6½
	50	-6½	-4	-1½	1½	4	6½	7½	8	8	6½	4	1½	-1½	-4	-6½	-7½	-8	-8
	55	-7½	-5	-1½	1½	5	7½	9	10	9½	7½	5	1½	-1½	-5	-7½	-9	-10	-9½
	60	-9	-6	-2	2	6	9	11	12	11	9	6	2	-2	-6	-9	-11	-12	-11
6 CHANNEL	20	0	0	1	1	1	1	½	½	0	0	0	-1	-1	-1	-1	-½	-½	0
	25	½	1	1	2	2	1½	1	½	0	-½	-1	-1	-2	-2	-1½	-1	-½	0
	30	½	1	1½	2	2	2	1½	1	½	-½	-1	-1½	-2	-2	-2	-1½	-1	-½
	35	½	1½	2½	3	3	2½	2	1½	½	-½	-1½	-2½	-3	-3	-2½	-2	-1½	-½
	40	1	2	3	3½	3½	3½	3	2	½	-1	-2	-3	-3½	-3½	-3½	-3	-2	-½
	45	1	2½	4	4½	4½	4½	3½	2½	½	-1	-2½	-4	-4½	-4½	-4½	-3½	-2½	-½
	50	-1½	3½	5	6	6	5½	4½	2½	1	-1½	-3½	-5	-6	-6	-5½	-4½	-2½	-1
	55	1½	4	6	7	7	7	5½	3½	1	-1½	-4	-6	-7	-7	-7	-5½	-3½	-1
	60	2	5	7	8½	8½	8	6½	4	1½	-2	-5	-7	-8½	-8½	-8	-6½	-4	-1½

Table 6.0.3

WIND EFFECT (in dm) DEN HELDER-HARLINGEN

Timelag in hrs ↓		kts ↓	Directions of isobars → 180	200	220	240	260	280	300	320	340	360	020	040	060	080	100	120	140	160
9	NORTH-W	20	-1	-1	-½	-½	0	½	½	½	1	1	½	½	½	0	-½	-½	-½	-1
		25	-1	-1	-1	-½	0	½	1	1	1	1	1	1	½	0	-½	-1	-1	-1
		30	-2	-1½	-1	-½	0	½	1	1½	2	2	1½	1	½	0	-½	-1	-1½	-2
		35	-2½	-2	-1½	-1	0	1	1½	2	2½	2½	2	1½	1	0	-1	-1½	-2	-2½
		40	-3	-3	-2	-1	0	1	2	3	3	3	3	2	1	0	-1	-2	-3	-3
		45	-4	-3½	-2½	-1½	0	1½	2½	3½	4	4	3½	2½	1½	0	-1½	-2½	-3½	-4
		50	-5	-4½	-3½	-1½	0	1½	3	4½	5	5	4½	3½	1½	0	-1½	-3	-4½	-5
		55	-6	-5½	-4	-2	0	2	4	5½	6	6	5½	4	2	0	-2	-4	-5½	-6
		60	-7	-6½	-5	-2½	0	2½	4½	6½	7	7	6½	5	2½	0	-2½	-4½	-6½	-7
9	NORTH-E	20	0	0	0	0	0	0	0	0	0	0	0	0	0	0	0	0	0	0
		25	-½	-½	-½	0	0	0	0	½	½	½	½	½	0	0	0	0	-½	-½
		30	-½	-½	-½	0	0	0	½	½	½	½	½	½	0	0	0	-½	-½	-½
		35	-½	-½	-½	-½	0	0	½	½	½	½	½	½	½	0	0	-½	-½	-½
		40	-1	-1	-½	-½	0	½	½	1	1	1	1	½	½	0	-½	-½	-1	-1
		45	-1	-1	-1	-½	0	½	½	1	1	1	1	1	½	0	-½	-½	-1	-1
		50	-1½	-1½	-1	-½	0	½	1	1	1½	1½	1½	1	½	0	-½	-1	-1	-1½
		55	-2	-2	-1½	-1	-½	½	1	1½	2	2	2	1½	1	½	-½	-1	-1½	-2
		60	-2	-2	-1½	-1	-½	½	1	2	2	2	2	1½	1	½	-½	-1	-2	-2
6	MID-W	20	-1½	-1	-½	0	½	1	1½	1½	1½	1½	1	½	0	-½	-1	-1½	-1½	-1½
		25	-2	-2	-1	-½	½	1½	2	2½	2½	2	2	1	½	-½	-1½	-2	-2½	-2½
		30	-3	-2½	-1½	-½	1	2	3	3½	3½	3	2½	1½	½	-1	-2	-3	-3½	-3½
		35	-4½	-3½	-2	-½	1	2½	4	4½	5	4½	3½	2	½	-1	-2½	-4	-4½	-5
		40	-5½	-4½	-3	-½	1½	3½	5	6	6½	5½	4½	3	½	-1½	-3½	-5	-6	-6½
		45	-7½	-5½	-3½	-1	2	4½	6½	7½	8	7½	5½	3½	1	-2	-4½	-6½	-7½	-8
		50	-9	-7	-4½	-1	2½	5½	8	9½	10	9	7	4½	1	-2½	-5½	-8	-9½	-10
		55	-11	-8½	-5½	-1½	3	6½	9½	11½	12	11	8½	5½	1½	-3	-6½	-9½	-11½	-12
		60	-13	-10	-6½	-1½	3½	8	11½	13½	14	13	10	6½	1½	-3½	-8	-11½	-13½	-14
3	MID-E	20	-½	-1	-1	-1	-½	-½	0	½	½	½	1	1	1	½	½	0	-½	-½
		25	-1	-1½	-1½	-1	-1	-½	0	½	½	1	1½	1½	1	1	½	0	-½	-1
		30	-1½	-2	-2	-1½	-1½	-½	0	½	½	1½	2	2	1½	1½	½	0	-½	-1½
		35	-2	-2½	-2½	-2½	-1½	-1	0	1	1½	2	2½	2½	2½	1½	1	0	-1	-1½
		40	-3	-3½	-3½	-3	-2½	-1	0	1	2½	3	3½	3½	3	2½	1	0	-1	-2½
		45	-3½	-4½	-4½	-4	-3	-1½	0	1½	3	3½	4½	4½	4	3	1½	0	-1½	-3
		50	-4½	-5½	-5½	-5	-3½	-2	0	2	3½	4½	5½	5½	5	3½	2	0	-2	-3½
		55	-5½	-6½	-6½	-6	-4½	-2½	0	2½	4½	5½	6½	6½	6	4½	2½	0	-2½	-4½
		60	-6½	-8	-8	-7	-5	-2½	0	2½	5	6½	8	8	7	5	2½	0	-2½	-5
3	SOUTH	20	0	0	½	1	1	1	1	1	½	0	0	-½	-1	-1	-1	-1	-1	-½
		25	-½	½	1	1½	2	2	2	1½	1	½	-½	-1	-1½	-2	-2	-2	-1½	-1
		30	-½	½	1½	2	2½	3	2½	2	1½	½	-½	-1½	-2	-2½	-3	-2½	-2	-1½
		35	-½	½	2	3	3½	4	3½	3	2	½	-½	-2	-3	-3½	-4	-3½	-3	-2
		40	-1	1	2½	3½	4½	5	4½	4	2½	1	-1	-2½	-3½	-4½	-5	-4½	-4	-2½
		45	-1	1	3	4½	6	6	6	5	3	1	-1	-3	-4½	-6	-6	-6	-5	-3
		50	-1½	1	3½	6	7½	7½	7½	6	4	1½	-1	-3½	-6	-7½	-7½	-7½	-6	-4
		55	-2	1½	4½	7	9	9½	9	7½	5	2	-1½	-4½	-7	-9	-9½	-9	-7½	-5
		60	-2	2	5½	8½	10½	11	10½	8½	5½	2	-2	-5½	-8½	-10½	-11	-10½	-8½	-5½
9	CHANNEL	20	0	½	½	½	½	½	½	½	0	0	-½	-½	-½	-½	-½	-½	-½	0
		25	0	½	½	1	1	1	½	½	0	0	-½	-½	-1	-1	-1	-½	-½	0
		30	½	½	1	1	1	1	1	½	0	-½	-½	-1	-1	-1	-1	-1	-½	0
		35	½	1	1½	1½	1½	1½	1	1	½	-½	-1	-1½	-1½	-1½	-1½	-1	-1	-½
		40	½	1	2	2	2	2	1½	1	½	-½	-1	-2	-2	-2	-2	-1½	-1	-½
		45	½	1½	2	2½	2½	2½	2	1½	½	-½	-1½	-2	-2½	-2½	-2½	-2	-1½	-½
		50	1	1½	2½	3	3½	3	2½	1½	½	-1	-1½	-2½	-3	-3½	-3	-2½	-1½	-½
		55	1	2	3½	3½	4	3½	3	2	½	-1	-2	-3½	-3½	-4	-3½	-3	-2	-½
		60	1	2½	4	4½	5	4½	3½	2½	1	-1	-2½	-4	-4½	-5	-4½	-3½	-2½	-1
			wind direction																	
0	WADDENZEE	20	0	0	0	1	1	1	1	1	1	0	0	0	-1	-1	-1	-1	0	0
		25	0	0	1	1	2	2	2	1	1	0	-1	-1	-2	-2	-2	-1	-1	0
		30	0	1	1	2	3	3	3	2	1	0	-1	-2	-2	-3	-2	-2	-1	0
		35	0	1	2	3	4	4	4	3	1	0	-1	-2	-3	-3	-3	-2	-1	0
		40	0	2	2	4	5	5	5	3	2	0	-2	-3	-4	-5	-4	-3	-2	0
		45	1	2	3	5	6	6	6	4	2	0	-2	-4	-6	-6	-5	-4	-2	-1
		50	1	3	4	6	7	8	7	5	2	0	-3	-5	-7	-7	-6	-5	-3	-1
		55	1	3	5	7	9	10	9	6	3	0	-4	-6	-8	-9	-7	-6	-4	-1
		60	1	4	6	9	10	11	10	7	3	0	-4	-8	-10	-10	-9	-7	-4	-4

Sept. 1971

Table 6.0.4

WIND EFFECT (in dm) BORKUM-DELFZIJL

Timelag in hrs ↓		kts ↓	180	200	220	240	260	280	300	320	340	360	020	040	060	080	100	120	140	160
			Direction of isobars →																	
9	NORTH-W	20	–1	–1	–1	–½	0	½	½	1	1	1	1	½	½	0	–½	–½	–1	–1
		25	–1½	–1½	–1	–½	0	½	1	1½	1½	1½	1½	1	½	0	–½	–1	–1½	–1½
		30	–2½	–2	–1½	–1	0	1	1½	2	2½	2½	2	1½	1	0	–1	–1½	–2	–2½
		35	–3	–2½	–2	–1	0	1	2	2½	3	3	2½	2	1	0	–1	–2	–2½	–3
		40	–4	–3½	–2½	–1½	0	1½	2½	3½	4	4	3½	2½	1½	0	–1½	–2½	–3½	–4
		45	–5	–4½	–3	–1½	0	1½	3½	4½	5	5	4½	3	1½	0	–1½	–3½	–4½	–5
		50	–6½	–5½	–4	–2	0	2	4	5½	6½	6½	5½	4	2	0	–2	–4	–5½	–6½
		55	–7½	–7	–5	–2½	0	2½	5	7	7½	7½	7	5	2½	0	–2½	–5	–7	–7½
		60	–9	–8	–5½	–3	0	3	6	8	9	9	8	5½	3	0	–3	–6	–8	–9
9	NORTH-E	20	–½	–½	0	0	0	0	0	½	½	½	½	0	0	0	0	0	–½	–½
		25	–½	–½	–½	0	0	0	½	½	½	½	½	½	0	0	0	–½	–½	–½
		30	–1	–½	–½	–½	0	½	½	½	1	1	½	½	½	0	–½	–½	–½	–1
		35	–1	–1	–½	–½	0	½	½	1	1	1	1	½	½	0	–½	–½	–1	–1
		40	–1½	–1	–1	–½	0	½	1	1	1½	1½	1	1	½	0	–½	–1	–1	–1½
		45	–1½	–1½	–1	–1	0	½	1	1½	1½	1½	1½	1	1	0	–½	–1	–1½	–1½
		50	–2	–2	–1½	–1	0	½	1½	2	2	2	2	1½	1	0	–½	–1½	–2	–2
		55	–2½	–2½	–1½	–1	0	1	1½	2½	2½	2½	2½	1½	1	0	–1	–1½	–2½	–2½
		60	–3	–2½	–2	–1½	0	1	2	2½	3	3	2½	2	1½	0	–1	–2	–2½	–3
6	MID-W	20	–½	–½	0	½	1	1	1½	1	1	½	½	0	–½	–1	–1	–1½	–1	–1
		25	–1	–½	0	1	1½	1½	2	2	1½	1	½	0	–1	–1½	–1½	–2	–2	–1½
		30	–1½	–1	0	1	2	2½	3	3	2½	1½	1	0	–1	–2	–2½	–3	–3	–2½
		35	–2½	–1	0	1½	2½	3½	4	4	3	2½	1	0	–1½	–2½	–3½	–4	–4	–3
		40	–3	–1½	½	2	3½	4½	5	5	4	3	1½	–½	–2	–3½	–4½	–5	–5	–4
		45	–4	–2	½	2½	4½	5½	6½	6	5½	4	2	–½	–2½	–4½	–5½	–6½	–6	–5½
		50	–4½	–2½	½	3	5½	7	8	7½	6½	4½	2½	–½	–3	–5½	–7	–8	–7½	–6½
		55	–5½	–3	½	3½	6½	8½	9½	9½	8	5½	3	–½	3	–6½	–8½	–9½	–9½	–8
		60	–6½	–3½	½	4½	7½	10	11½	11	9½	6½	3½	–½	–4½	–7½	–10	–11½	–11	–9½
3	MID-E	20	–2	–2	–1	–½	½	1	1½	2	2	2	2	1	½	–½	–1	–1½	–2	–2
		25	–3½	–3	–2	–1	½	1½	2½	3	3½	3½	3	2	1	–½	–1½	–2½	–3	–3½
		30	–5	–4	–3	–1	½	2½	3½	4½	5	5	4	3	1	–½	–2½	–3½	–4½	–5
		35	–6½	–5½	–4	–1½	1	3	5	6½	7	6½	5½	4	1½	–1	–3	–5	–6½	–7
		40	–8½	–7	–5	–2	1	4	6½	8	9	8½	7	5	2	–1	–4	–6½	–8	–9
		45	–11	–9	–6	–2½	1½	5	8½	10½	11½	11	9	6	2½	–1½	–5	–8½	–10½	–11½
		50	–13½	–11	–7½	–3½	1½	6½	10½	13	14	13½	11	7½	3½	–1½	–6½	–10½	–13	–14
		55	–16	–13½	–9½	–4	2	7½	12½	15½	17	16	13½	9½	4	–2	–7½	–12½	–15½	–17
		60	–19	–16	–11	–4½	2½	9	15	18½	20	19	16	11	4½	–2½	–9	–15	–18½	–20
3	SOUTH	20	0	½	½	½	½	½	½	0	0	0	–½	–½	–½	–½	–½	–½	0	0
		25	0	½	½	1	1	1	½	½	0	0	–½	–½	–1	–1	–1	–½	–½	0
		30	½	1	1	1	1	1	1	½	0	–½	–1	–1	–1	–1	–1	–1	–½	0
		35	½	1	1½	1½	1½	1½	1	½	0	–½	–1	–1½	–1½	–1½	–1½	–1	–½	0
		40	½	1½	2	2	2	2	1½	1	0	–½	–1½	–2	–2	–2	–2	–1½	–1	0
		45	1	1½	2½	2½	2½	2½	2	1	0	–1	–1½	–2½	–2½	–3	–2½	–2	–1	0
		50	1	2	3	3½	3½	3	2½	1½	0	–1	–2	–3	–3½	–3½	–3	–2½	–1½	0
		55	1	2½	3½	4	4	3½	3	1½	½	–1	–2½	–3½	–4	–4	–3½	–3	–1½	–½
		60	1½	3	4	4½	4½	4½	3½	2	½	–1½	–3	–4	–4½	–4½	–4½	–3½	–2	–½
9	CHANNEL	20	0	0	½	½	½	½	0	0	0	0	0	–½	–½	–½	–½	0	0	0
		25	0	½	½	½	½	½	½	0	0	0	–½	–½	–½	–½	–½	–½	0	0
		30	0	½	½	½	1	1	½	½	0	0	–½	–½	–½	–1	–1	–½	–½	0
		35	½	½	1	1	1	1	½	½	0	–½	–½	–1	–1	–1	–1	–½	–½	0
		40	½	½	1	1	1½	1½	1	½	0	–½	–½	–1	–1	–1½	–1½	–1	–½	0
		45	½	1	1½	1½	2	2	1	½	0	–½	–1	–1½	–1½	–2	–2	–1	–1	0
		50	½	1	1½	2	2½	2	1	1	0	–½	–1	–1½	–2	–2½	–2	–1	–1	0
		55	½	1½	2	2½	3	2½	1½	1	0	–½	–1½	–2	–2½	–3	–2½	–1½	–1	0
		60	1	1½	2½	3	3½	2½	1½	1	½	–1	–1½	–2½	–3	–3½	–2½	–1½	–1	–½
			wind direction																	
0	EEMS-ESTUARY	20	–1	–1	–1	0	0	0	1	1	1	1	1	1	0	0	–1	–1	–1	–1
		25	–1	–1	–1	0	0	0	1	1	1	1	1	1	1	0	–1	–1	–1	–1
		30	–2	–2	–1	–1	0	1	1	2	2	2	2	2	1	0	–1	–2	–2	–2
		35	–2	–2	–2	–1	0	1	2	3	3	3	3	2	1	0	–2	–3	–3	–3
		40	–4	–3	–2	–1	0	1	3	4	4	4	4	3	2	0	–3	–4	–4	–4
		45	–5	–4	–3	–1	0	2	3	5	5	5	5	4	3	0	–4	–5	–6	–5
		50	–6	–5	–4	–2	0	2	4	6	7	7	6	5	3	0	–4	–7	–7	–7
		55	–8	–6	–4	–2	1	3	5	7	9	9	8	6	4	0	–6	–9	–9	–9
		60	–9	–7	–5	–3	2	3	6	9	11	11	9	7	5	0	–7	–11	–11	–10

Sept. 1971

Some of the objections mentioned on page 28 could be overcome, viz.:

a) The windfield over the northern part of the North Sea could be specified into greater detail.
b) Fairly accurate fitting of the model to the geography of the North Sea and the depths of the North Sea was possible.
c) The computations yielded a time-lag between the windfield over a district and the subsequent maximum effect on the Netherlands coast.
d) A lower value of C_d was used.

6.1 In accordance with the test of the Weenink-tables the new tables were applied to 16 surges during the period 1958-1962 as well. (See Chapter 3.) Again, the observed meteorological effect (O) during high tide was compared with the computed set-up (C_T), according to the new tables, for the stations Flushing, Hook of Holland, Den Helder, Harlingen and Delfzijl. The results of the comparison are given in Table 6.1.1, which contains Table 3.2.1 also.

Table 6.1.1 Verification of the tables of Weenink and Timmerman.

$\overline{O - C_W}$, $\overline{O - C_T}$ = mean values of $O - C_W$ resp. $O - C_T$.
σ_W, σ_T = standard deviations of $O - C_W$ resp. $O - C_T$.

	$\overline{O - C_W}$	σ_W	$\overline{O - C_T}$	σ_T
Flushing	—0.8 dm	2.9 dm	+0.1 dm	2.3 dm
Hook of Holland	—0.2 dm	2.5 dm	+0.3 dm	2.1 dm
Den Helder	—0.3 dm	2.8 dm	+0.2 dm	2.6 dm
Harlingen	—0.8 dm	3.1 dm	+0.6 dm	2.1 dm
Delfzijl	+0.5 dm	2.8 dm	—0.1 dm	2.8 dm
mean	—0.3 dm	2.8 dm	+0.2 dm	2.4 dm

Table 6.1.1 shows in general that the new tables give better results than the old ones. See for instance the stations Flushing and Harlingen. In the mean the methods are of equal merit as far as the systematic differences are concerned, however, σ_T is smaller than σ_W.

Comparing the two sets of tables it appears that there are substantial differences. For instance the contributions of the districts North-W and North-E are much larger with respect to the former district North, whereas the contribution of the district Mid-W is much smaller with respect to the former district South 1.

An example of these differences is given in Table 6.1.2.

Table 6.1.2 Comparison of the tables of Weenink and Timmerman. As an example the contribution of the indicated districts for Hook of Holland has been chosen by a wind of 340° and 60 kts.

	districts	340/60	districts	340/60
Weenink	North	4 dm	South	18 dm
Timmerman	North-W and North-E	7 dm	Mid-W	14 dm

Furthermore, 75% of the total contribution of the districts North-W and North-E originates from district North-W.

It is useful to check the effect of the new tables in situations with an important difference in wind over the districts North-W and North-E. To perform this check a number of situations

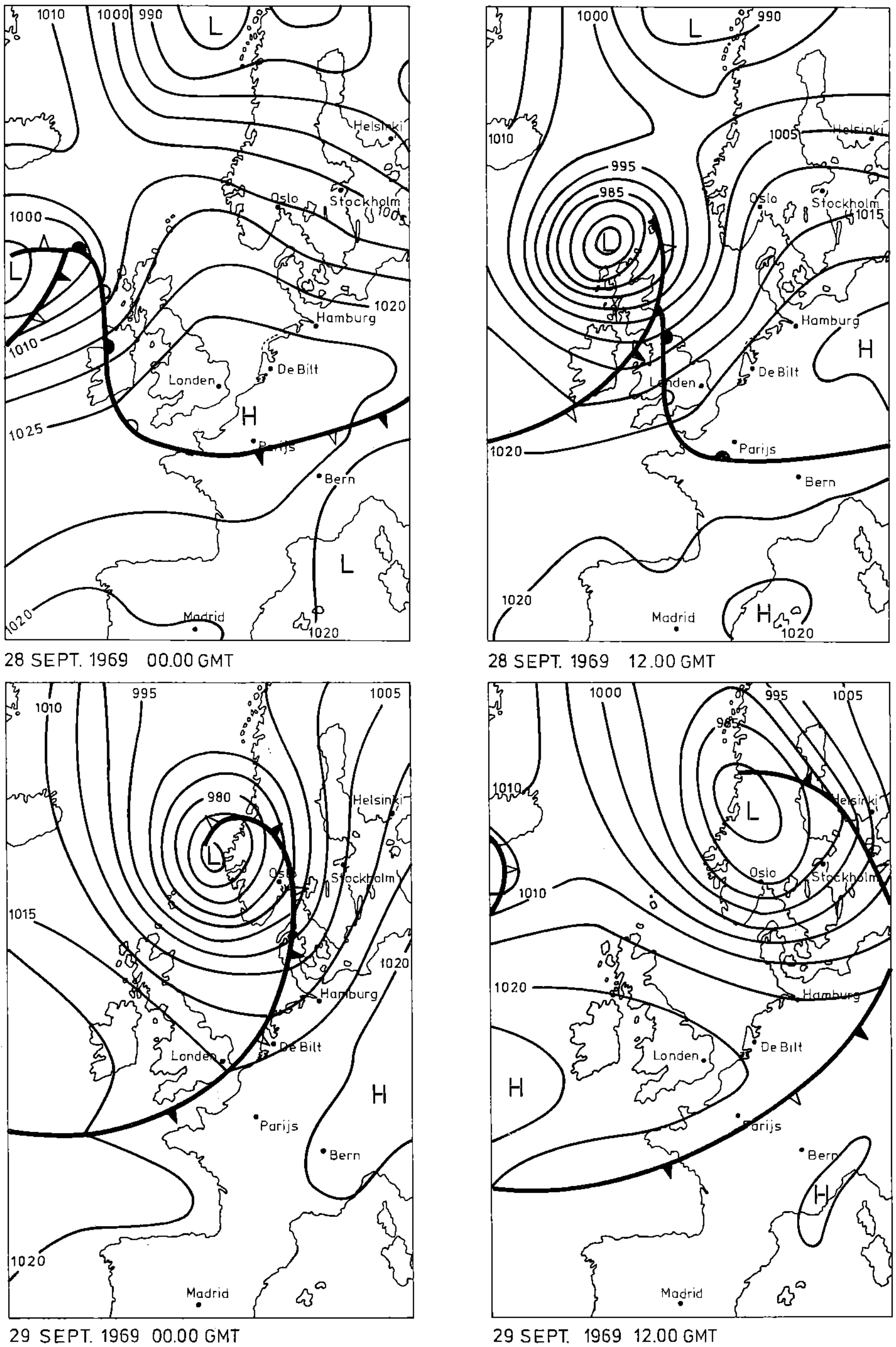

Fig. 6.2.1 Weather charts of 28 and 29 September 1969.

have been selected, characterized by a difference in wind speed over the districts North-W and Mid-W of at least 10 knots. It appeared that the old tables gave a standard deviation of 3.1 dm and the new tables of 2.5 dm only.

6.2 The surge of 28-29 September 1969, connected with a deep depression moving north of Scotland towards the southern part of Norway, was characterized by a considerable difference in wind over the sectors North-W and Mid-W. (See Fig. 6.2.1.) The severe northwesterly gale was confined to the districts North-W and North-E. The wind effect has been computed with both the old and the new set of tables. The results are given in Table 6.2.1.

Table 6.2.1 Observed and computed set-up on 28-29 September 1969.

	O	old set (Weenink)	new set (Timmerman)
Flushing	11½ dm	7½ dm	10 dm
Hook of Holland	13½ dm	8 dm	12 dm
Den Helder	10 dm	8½ dm	12½ dm
Harlingen	12 dm	7½ dm	10½ dm
Delfzijl	14½ dm	11½ dm	14½ dm
Flushing	7½ dm	7 dm	7½ dm
Hook of Holland	10 dm	7½ dm	10½ dm
mean	11.4 dm	8.2 dm	11.1 dm

This table clearly shows that the surge of 28-29 September 1969 is an example illustrating the suitability of the new method for computing the set-up caused by a windfield that is strongly inhomogeneous over the northern part of the North Sea.

6.3 Summarizing it can be ascertained that the new tables are more accurate than the old, especially in situations with an inhomogeneous windfield over the North Sea. Furthermore, they are based on a more acceptable value of the drag-coefficient C_d. The new tables were introduced in the operational service in September 1971.

It must be stated that in the foregoing no account has been taken of non-stationary effects. These effects may be of importance. See for instance Timmerman [1971]. Also external effects from the Atlantic Ocean have not been considered, and the windfield has not been specified in as much detail as possible.

Incorporating these desirabilities implies the necessity of a meteorological data input in an automatic way. The problems connected with these automation are dealt with in the next chapter.

7 Automation of meteorological input in numerical sea models

7.0 In recent years W. J. A. Kuipers (KNMI, to be published) developed a method for an objective analysis of pressure fields including wind observations. He represents the pressure field by a finite and incomplete Fourier-series with data-dependent coefficients. Actual data can be obtained directly from the international data communication channels, while data connected with historical surges can be derived from weather maps, for instance with the aid of a pencil-follow-apparatus. Information of the pressure field at arbitrary moments can be acquired by means of an interpolation of the data-dependent coefficients. The analytical description of the pressure field makes it possible to compute the pressure at each point that is desired, for instance at the grid points of the sea model. The computations which are discussed in Chapters 8 and 9 are based on a quadratic interpolation in time and on a meteorological input at every grid point with a time interval of one hour.

7.1 It is necessary to compute the wind from the analytical expression of the pressure field. In this study the method given by Hesselberg [1915] is used. Hesselberg gave a solution of somewhat simplified equations of motion, in which among others vertical motions had been neglected. These equations relate the horizontal components of the acceleration of an air-particle to the horizontal components of the pressure-gradient force, the Coriolis force and a linearized friction force. The equations of Hesselberg read as follows:

$$\frac{dv_x}{dt} = G_x + lv_y - cv_x$$
$$\frac{dv_y}{dt} = G_y - lv_x - cv_y \qquad (7.1.1)$$

v_x and v_y are related to the wind at a height of 10 meters.
$l = f(1+b \sin \beta)$ en $c = fb \cos \beta$. See Fig. 7.1.1.

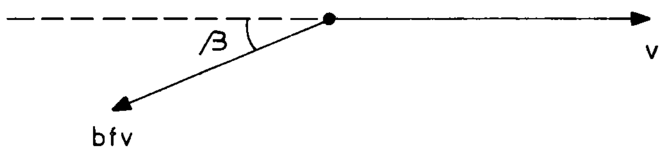

Fig. 7.1.1 Wind velocity v with friction angle β and friction coefficient b.

A solution of 7.1.1 can be obtained by total differentiation of 7.1.1 with respect to time, while neglecting the second-order timederivatives of v_x and v_y, and considering ρ, l and c as constants.

$$v_x = \frac{l}{c^2+l^2} G_y + \frac{c}{c^2+l^2} G_x - \frac{2cl}{(c^2+l^2)^2} \frac{dG_y}{dt} - \frac{c^2-l^2}{(c^2+l^2)^2} \frac{dG_x}{dt}$$

$$v_y = \frac{c}{c^2+l^2} G_y - \frac{l}{c^2+l^2} G_x - \frac{c^2-l^2}{(c^2+l^2)^2} \frac{dG_y}{dt} + \frac{2cl}{(c^2+l^2)^2} \frac{dG_x}{dt} \tag{7.1.2}$$

7.1.2 can be transformed into 7.1.3 by applying $\frac{d}{dt} = \frac{\partial}{\partial t} + \vec{v} \cdot \Delta$:

$$v_x = \begin{vmatrix} A_1 & A_5 \\ A_2 & A_4 \end{vmatrix} \Big/ \begin{vmatrix} A_3 & A_5 \\ A_6 & A_4 \end{vmatrix} \text{ and } v_y = \begin{vmatrix} A_3 & A_1 \\ A_6 & A_2 \end{vmatrix} \Big/ \begin{vmatrix} A_3 & A_5 \\ A_6 & A_4 \end{vmatrix} \tag{7.1.3}$$

where

$$A_1 = \frac{cG_x}{c^2+l^2} + \frac{lG_y}{c^2+l^2} - \frac{c^2-l^2}{(c^2+l^2)^2} \frac{\partial G_x}{\partial t} - \frac{2cl}{(c^2+l^2)^2} \frac{\partial G_y}{\partial t}$$

$$A_2 = \frac{-lG_x}{c^2+l^2} + \frac{cG_y}{c^2+l^2} + \frac{2cl}{(c^2+l^2)^2} \frac{\partial G_x}{\partial t} - \frac{c^2-l^2}{(c^2+l^2)^2} \frac{\partial G_y}{\partial t}$$

$$A_3 = 1 + \frac{c^2-l^2}{(c^2+l^2)^2} \frac{\partial G_x}{\partial x} + \frac{2cl}{(c^2+l^2)^2} \frac{\partial G_y}{\partial x}$$

$$A_4 = 1 - \frac{2cl}{(c^2+l^2)^2} \frac{\partial G_x}{\partial y} + \frac{c^2-l^2}{(c^2+l^2)^2} \frac{\partial G_y}{\partial y}$$

$$A_5 = \frac{c^2-l^2}{(c^2+l^2)^2} \frac{\partial G_x}{\partial y} + \frac{2cl}{(c^2+l^2)^2} \frac{\partial G_y}{\partial y}$$

$$A_6 = \frac{-2cl}{(c^2+l^2)^2} \frac{\partial G_x}{\partial x} + \frac{c^2-l^2}{(c^2+l^2)^2} \frac{\partial G_y}{\partial x}$$

As can be seen from the coefficients A_i, the solution accounts for the curvature of isobars and for the isallobaric wind.

The quantities l and c depend on the stability of the lowest layers of the atmosphere and on the temperature difference between air and sea ($T_a - T_d$), therefore. Bijvoet [1957] computed some values of $\frac{fl}{c^2+l^2}$, $\frac{fc}{c^2+l^2}$, $\frac{2f^2cl}{(c^2+l^2)^2}$ and $\frac{f^2(c^2-l^2)}{(c^2+l^2)^2}$ as a function of $T_a - T_s$, applying empirical relations between the surface wind at 10 m and the geostrophic wind. These quantities are not mutually independent. If indicated by a_1, a_2, a_3 and a_4, respectively, it appears that $a_3 = 2a_1a_2$ and $a_4 = a_2^2 - a_1^2$. The values of a_1, a_2, a_3 and a_4 as determined by Bijvoet are given in Table 7.1.1.

Outside the interval $-4 \leqslant T_a - T_s \leqslant +2$ the values of a_1, a_2, a_3 and a_4 must be extrapolated. The coefficients are exclusively valid over sea and not over land.

As an illustration the components of the wind can easily be computed under conditions with straight, parallel and equidistant isobars and the x-axis parallel to the isobars. Then G_x

Table 7.1.1 Coefficients a_1, a_2, a_3 and a_4.

$T_a - T_s \rightarrow$	—4°	—2°	0°	+2°
a_1	0.77	0.71	0.64	0.58
a_2	0.16	0.18	0.20	0.21
a_3	0.25	0.26	0.26	0.25
a_4	—0.56	—0.48	—0.38	—0.29

and all derivatives of G_x and G_y are zero. Taking $T_a - T_s = -2$ °C the solution reads: $v_x = \frac{0.71}{f} G_y$ and $v_y = \frac{0.18}{f} G_y$. This means that the computed wind is about 73% of the geostrophic wind, while the angle between the wind and the isobars is about 10° in the direction of the low pressure area.

An example of a weather map and the wind, computed in the grid-points of the restricted model I, is shown in Fig. 7.1.2 and Table 7.1.2.

Table 7.1.2 Example of computed windfield 25 September 1974, 1200 GMT. Numbers representing wind direction in tenths of degrees and wind speed in knots. For position grid points see fig. 5.1.2.

Windfield North Sea

0	0	3414	3314	3315	3315	3316	3316	3317	3417	3315	3413	3511	3608	0
0	0	3411	3211	3215	3114	3217	3117	3218	3218	3315	3313	3310	3306	0
0	0	3308	3209	3113	3114	3117	3118	3120	3120	3117	3214	3211	3007	0
0	0106	3505	3307	3209	3112	3115	3117	3120	3120	3118	3115	3012	2910	0
0409	0508	0306	0106	3507	3309	3212	3114	3117	3217	3115	3013	2812	2713	2412
0511	0510	0509	0408	0307	0107	3507	3208	3111	3211	3011	2811	2612	2415	2417
0510	0610	0610	0610	0609	0507	0406	0204	3203	2703	2406	2210	2413	2316	2220
0509	0609	0610	0610	0609	0608	0506	0504	0902	1802	2105	2209	2212	2316	2319
0307	0507	0608	0709	0709	0708	0807	1006	1305	1506	1707	1909	2112	2215	2217
3605	0305	0606	0707	0707	0908	1108	1208	1409	1409	1610	1711	1913	2014	2217
3207	3505	0404	0805	0905	1108	1209	1310	1512	1414	1514	1614	1814	1914	2115
0	3107	3203	0902	1104	1307	1409	1411	1514	1617	1517	1617	1716	1815	2014
0	0	3006	2702	1703	1506	1510	1513	1616	1618	1620	1620	1618	1717	1914
0	0	2910	2605	2105	1808	1711	1714	1717	1720	1721	1722	1720	1718	0
0	2918	2813	2609	2308	2010	1813								
2928	2822	2816	2612	2310	2112	0								
2931	2824	2819	2615	2314	0	0								
2932	2825	2720	2517	0	0	0								

Windfield Channel

3233	3131	0	0	0	0	0
3230	3029	2933	2841	0	0	0
3128	2928	2834	2843	2846	2848	0
3126	2928	2735	2842	2846	2851	2933
3024	2827	2735	2842	2847	2851	2940
0	0	0	0	2847	2949	0

7.2 The accuracy of the computed windfield depends on the objective analysis of the pressure field and on the method by which the wind is computed. To get an impression of this accuracy, computed winds need to be compared with observed winds. Such a comparison was carried out for the periods 15 October 1973 till 8 June 1974 and 4 October 1974 till 1 June 1975. During these periods analysis of the 1000 mbar level were carried out using data from the international communication channels directly and four times a day. The observed winds

O originated from (see Fig. 7.2.1) the light-vessels Noord-Hinder (NH), Texel (T), Terschellingerbank (TB), the light-island Goeree (G), the Norwegian ship at 57.5 N and 4.0 E (not indicated in the figure) and from measurements on piles at Cadzand (C), Roggeplaat (R), Katwijk (K) and Texelhors (TH). The computed winds at grid points adjacent to these observation points were considered as the computed winds C at these stations. In this way it was possible to determine every six hours the difference between observed and computed winds

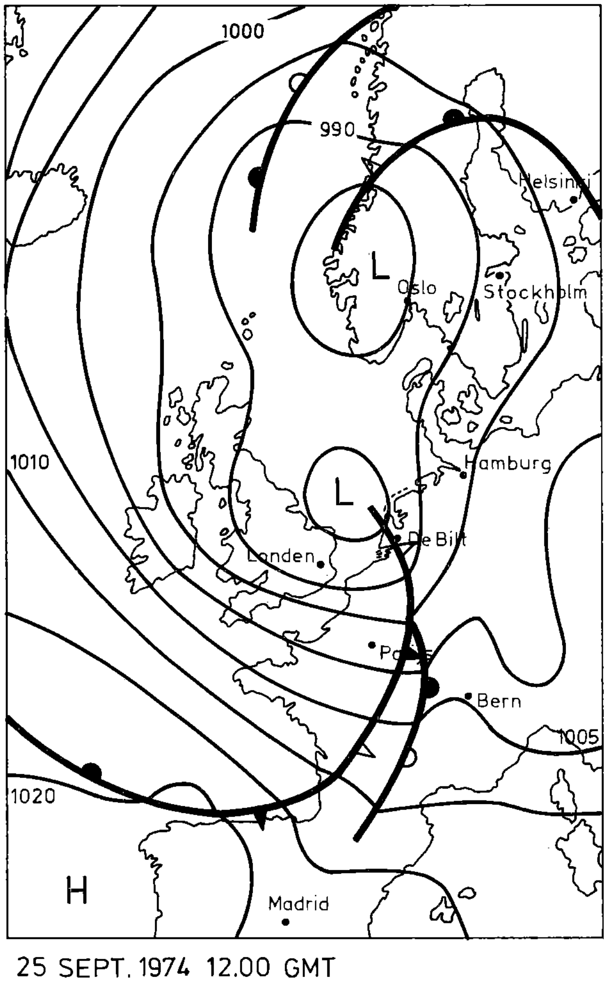

Fig. 7.1.2 Weather chart of 25 September 1974, 1200 GMT.

both with respect to direction and to speed. The material was divided into the following three classes:

a) observed wind 10-24 kts;
b) observed wind 25-34 kts;
c) observed wind $\geqslant$ 35 kts;

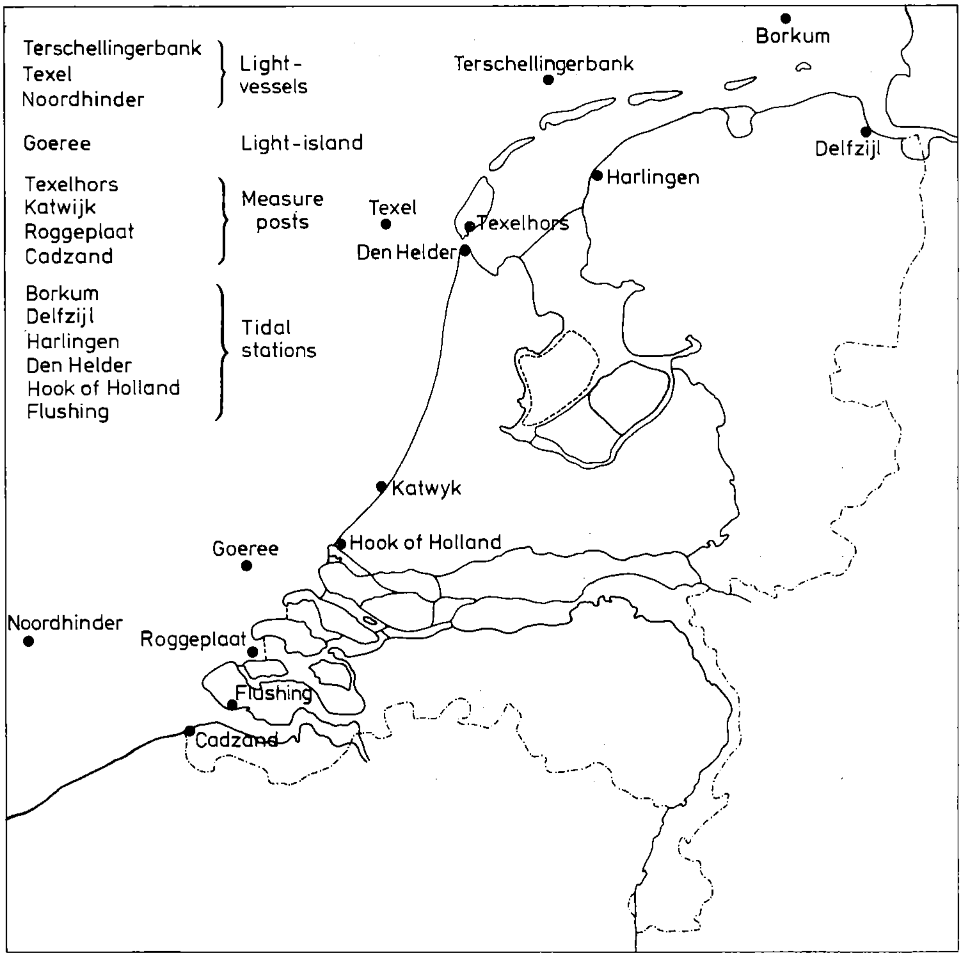

Fig. 7.2.1 Survey of stations.

Table 7.2.1 Verification of wind direction and wind speed in the periods 15 October 1973 till 8 June 1974 (I) and 4 October 1974 till 1 June 1975 (II).

	Light-vessels						Light-island	
	NH		T		ʕTB		G	
Wind direction in degrees	I	II	I	II	I	II	I*	II
10-24 kts $\overline{O-C}$	+2	+6	+6	+9	+5	+8	—13	—7
σ	21	25	15	18	19	18	19	19
number of observations	537	597	535	547	490	377	406	591
25-34 kts $\overline{O-C}$	+4	+7	—1	+5	+8	+4	—19	—8
σ	24	21	19	16	15	13	18	14
number of observations	114	124	86	104	110	114	52	93
⩾ 35 kts $\overline{O-C}$	+5	+4	+6	+12	+6	+10	—17	—7
σ	18	18	17	17	12	15	14	6
number of observations	35	39	34	54	41	45	4	7
Wind speed in knots								
10-24 kts $\overline{O-C}$	—1.2	—0.5	—1.6	—1.0	—0.7	+0.2	—0.7	—0.6
σ	4.3	4.8	4.4	4.4	4.4	4.2	3.9	4.4
number of observations	537	597	535	547	490	377	406	591
25-34 kts $\overline{O-C}$	+3.1	+1.0	+0.1	+0.7	+0.2	—0.0	+0.3	—3.0
σ	5.7	6.2	6.1	4.6	4.9	4.9	5.7	5.0
number of observations	114	124	86	104	110	114	52	93
⩾ 35 kts $\overline{O-C}$	+7.1	+6.8	+3.7	+4.1	+3.7	+7.1	—3.5	—2.6
σ	7.7	7.2	5.4	6.0	8.0	7.1	6.6	3.4
number of observations	35	39	34	54	41	45	4	7

	Measuring posts							Norwegian ship	
	C		R		K		TH	N	
Wind direction in degrees	I	II	I	II	I	II	I	I	II
10-24 kts $\overline{O-C}$	—16	—19	—8	—5	—14	0	+2	+5	+7
σ	23	24	22	22	21	20	23	22	23
number of observations	559	628	396	493	576	605	542	161	294
25-34 kts $\overline{O-C}$	—4	—16	—2	—8	—9	—2	+2	+9	+5
σ	18	19	14	15	17	15	14	20	15
number of observations	85	96	38	93	92	90	119	32	95
⩾ 35 kts $\overline{O-C}$	—15	—11		—3	—8	—6	+8	+7	+6
σ	8	17		5	7	14	14	12	15
number of observations	6	15	0	16	13	18	29	19	28
Wind speed in knots									
10-24 kts $\overline{O-C}$	—1.2	—1.5	—2.7	+0.3	—1.8	—0.8	+0.2	—0.3	—0.7
σ	5.6	5.9	4.9	5.1	4.8	4.7	4.4	5.2	5.5
number of observations	559	628	396	493	576	605	542	161	294
25-34 kts $\overline{O-C}$	+0.2	—1.6	—5.6	—2.1	—1.8	—2.0	+1.6	+0.3	+0.8
σ	6.4	5.3	5.3	5.1	3.8	4.9	5.9	5.7	4.2
number of observations	85	96	38	93	92	90	119	32	95
⩾ 35 kts $\overline{O-C}$	—2.3	+1.1		—1.9	—1.9	—1.8	+0.2	+6.3	+3.2
σ	7.2	5.1		4.0	5.3	6.3	6.0	7.1	6.8
number of observations	6	15	0	16	13	18	29	19	28

* During period I the wind direction of Goeree showed an error.

Observed wind speeds less than 10 kts were not taken into account. Table 7.2.1 gives the mean difference $\overline{O\text{-}C}$ and the standard deviation σ of this difference for the observation points in the two periods mentioned above. The number of observations is indicated as well. No measurements were made at Texelhors during the second period.

The results of Table 7.2.1 are not only determined by the quality of the computation, but also by observational errors. The computed winds are based on coefficients valid over sea, so that the results for the coastal stations are influenced by the neglect of coastal effects. Furthermore, as far as the light-vessels are concerned, the conversion from the scale of Beaufort into wind speeds in knots may introduce an error as well. This may be elucidated as follows: the wind speed on light-vessels is estimated according to Beaufort's scale. The Beaufort-number corresponds to a wind speed in knots according to an international conversion scale. Verploegh [1956] remarked that these equivalents seem to be not quite correct. Application of the equivalents given by Verploegh (see Table 7.2.2) means an increase of the observed wind in knots at lower wind speeds, and a decrease of the observed wind at higher speeds. The order of magnitude of this increase respectively decrease generally agrees with the systematic differences contained in Table 7.2.1.

The wind direction of the light-island Goeree, during the first period, some of the wind speeds of the piles in the class $\geqslant$35 kts and probably the wind speed of Goeree in the classes 25-34 kts and $\geqslant$ 35 kts seem to be influenced by errors of the second category.

The computed winds were also compared with the observed winds in the case of some very severe gales, for instance the gale of 1 February 1953. It turned out that differences between observed and computed values increase with increasing wind speed. For this reason a correction of the computed winds exceeding 56 kts was introduced:

$$C_{corrected} = 56 + 0.4 * (C_{computed} - 56) \qquad (7.2.1)$$

where $C_{corrected}$ is the corrected value of the wind speed and $C_{computed}$ the uncorrected computed value of the wind speed, both given in knots. The formula need not be applied frequently.

However, this correction appeared to be insufficient for extremely high wind speeds. This was clearly demonstrated by the severe gale of 3 January 1976. The maximum speed of the

Table 7.2.2 Equivalents Beaufort ⇆ knots.

wind force in Beaufort	international equivalents (1946)	KNMI equivalents (1956)
0	1	1
1	1- 3	1- 4
2	4- 6	5- 8
3	7-10	9-12
4	11-16	13-16
5	17-21	17-21
6	22-27	22-26
7	28-33	27-31
8	34-40	32-36
9	41-47	37-42
10	48-55	43-48
11	56-63	49-55
12	> 63	> 55

geostrophic wind on that occasion was 130 kts. The maximum speed of the computed wind varied between 70 and 75 kts. The wind observations had given no indication of such high wind speeds. Moreover, the computed set-up of the water-level had a maximum value of 40 dm, while the observed set-up was about 30 dm, again a strong indication that the computed wind speed had been much too high. The actual wind did probably not exceed 65 kts.

It is likely that the discrepancy is caused by the application of a linear friction term in equation 7.1.1. This assumption, which was originally introduced by Guldberg and Mohn [1876] may not be adequate for high wind speeds and should, under such circumstances, probably be replaced by a quadratic term, in agreement with the quadratic expression of the wind stress. This means an enlargement of the friction term and, therefore, a reduction of the computed wind speed, a reduction that will be of more importance the higher the wind speeds. A quadratic friction term suggests a square root correction rather than a linear correction of the wind speed in formula 7.1.1. Similar suggestions are made by Duun-Christensen [1975] and Deacon [1973]. They draw attention to the effect of undetectable small cyclonic curvatures of the trajectories of the air within the friction layer. So there is evidence that the correction formula 7.2.1 can be improved by a formula of the following form:

$$C_{corrected} = v + (C_{computed} - v)^{\frac{1}{2}} \qquad (7.2.2)$$

where v is to be specified with the aid of wind observations made during severe gales. On the basis of the gale of 3 January 1976 the value $v = 60$ kts seems to be reasonable.

As remarked, computational and observational errors are mutually linked. Following a suggestion of W. J. A. Kuipers, the two can be separated if the distance of two observation-stations is small. During the season 1973-74 winds were observed not only on the light-vessel Texel, but also at Texelhors on the island of Texel, 23 km away. In order to separate the computational and the observational errors, the following assumptions must be made:

a) the three wind speeds at both stations are equal;
b) no correlation exists between the computational and observational errors;
c) no correlation exists between the errors in the observations on Texel and Texelhors.

The assumptions seem to be quite reasonable, the more so as the wind observations at both stations are carried out in quite different ways. On the light-vessel Texel the wind force is estimated in Beaufort, while the observations at Texelhors are based on instrumental measurements.

Now if V_T, V_{TH} and C are respectively the observed winds on the light-vessel Texel, the observational station Texelhors and the computed wind at a neighbouring grid point, e_T, e_{TH} and e_C the observational and computational errors and V the (unknown) true wind speed, then:

$$\begin{aligned} V_T &= V + e_T \\ V_{TH} &= V + e_{TH} \\ C &= V + e_C \end{aligned} \qquad (7.2.3)$$

From (7.2.3) it follows that

$$V_T - V_{TH} = e_T - e_{TH}$$
$$C - V_T = e_C - e_T$$
$$C - V_{TH} = e_C - e_{TH}$$

and

$$\begin{aligned} \text{var}\,(V_T - V_{TH}) &= \text{var}\,e_T + \text{var}\,e_{TH} \\ \text{var}\,(C - V_T) &= \text{var}\,e_C + \text{var}\,e_T \\ \text{var}\,(C - V_{TH}) &= \text{var}\,e_C + \text{var}\,e_{TH} \end{aligned} \qquad (7.2.4)$$

The left hand sides of the equations 7.2.4 can be determined from a series of observations and computations, after which var e_T, var e_{TH}, var e_C can be solved, while by taking the square root the standard deviations of the errors of the estimated, the measured and the computed winds can be found as well. The results for both wind direction and wind speed, based on 655 cases subdivided into three classes of wind speed, are shown in Table 7.2.3.

Table 7.2.3 Standard deviation of the error of the estimated wind on light-vessel Texel, of the measured wind at Texelhors and of the computed wind for three classes of wind speed.

wind speed classes	wind direction in degrees			wind speed in knots		
	lv T	mp TH	C	lv T	mp TH	C
10-24 kts	6	15	14	2.7	2.8	3.4
25-34 kts	15	8	11	4.0	3.7	4.5
⩾ 35 kts	12	9	12	3.6	4.5	3.9

It appears from Table 7.2.3 that generally the differences of the standard deviations are not large. The influence of the wind speed on the accuracy of the determination of the wind direction seems to be only of slight importance.

The computational error of about 4 kts, if the wind speed exceeds 24 kts, seems to be a serious handicap for an accurate determination of the water-level during storm surges. Nevertheless, from a comparison between observed and computed water-levels during storm surges (see Chapters 6, 8 and 9) it appears that the rather inaccurate knowledge of the wind speed on a fixed place does not influence the accuracy of the computed water-levels to a high extent. This may be explained by the integrated character of storm surges which are generated by a transport of water over large areas. This transport is determined by a windfield averaged both in space and time.

8 Sixteen storm surges during the period September 1958 till March 1962

8.0 At the beginning of Chapter 7 it was remarked that historical surges may be studied by using data derived from weather maps with the aid of a pencil-follow apparatus. It is obvious to apply this method to the 16 surges during the period 1958-1962, selected already in view of the comparison of the tables of Weenink and Timmerman. (See Chapters 3 and 6.) So pressure fields and windfields were computed. These computed values were compared with values derived from the subjective analyses. The differences appeared to be small. Then the computed values were utilized in a numerical water-model.

The special geographical features of the water-model are indicated in Fig. 5.1.1. The computations were carried out with the restricted model I; so external effects from the Atlantic Ocean were not taken into account. More details of the grid can be found in Fig. 5.1.2. As indicated already in Chapter 5, the grid-length is generally 42 km and the time-step 450 s. Near the Skagerrak an opening in the model was introduced by replacing the boundary conditions for U and V by boundary conditions for h. Provisions were made to account for the difference in temperature between air and sea by taking five values for the North Sea and one for the Channel, each representing a mean value over a district indicated in Fig. 6.0.1.

The set of equations 6.0.1 was solved by taking $C_d = 0.0028$.

8.1 In accordance with the verification of the operational tables in Chapter 6 averages and standard deviations of the differences between observed and computed set-up during the 16 surges were determined. The results are given in Table 8.1.1. For reasons of comparison the results of Table 6.1.1 are indicated also.

Table 8.1.1 Verification of the computation with model I and of computations with the tables Weenink and Timmerman.

	model I		operational tables			
			Weenink		Timmerman	
	$\overline{O-C}$	σ	$\overline{O-C}$	σ	$\overline{O-C}$	σ
Flushing	—0.9 dm	2.5 dm	—0.8 dm	2.9 dm	+0.1 dm	2.3 dm
Hook of Holland	+0.0 dm	2.3 dm	—0.2 dm	2.5 dm	+0.3 dm	2.1 dm
Den Helder	+0.4 dm	2.3 dm	—0.3 dm	2.8 dm	+0.2 dm	2.6 dm
Harlingen	+0.2 dm	2.5 dm	—0.8 dm	3.1 dm	+0.6 dm	2.1 dm
Delfzijl	+0.8 dm	2.2 dm	+0.5 dm	2.8 dm	—0.1 dm	2.8 dm
mean	+0.1 dm	2.4 dm	—0.3 dm	2.8 dm	+0.2 dm	2.4 dm

It appears from Table 8.1.1 that, as far as these 16 storm surges are concerned, the results with model I show no improvement with respect to the operational tables by Timmerman. No doubt this is due to the fact that storm surges are mainly generated by rather homogeneous windfields, so that the influence of non-stationary effects is small.

9 The extended model with applications to some individual cases on a semi-operational basis

9.0 The methods discussed so far do not deal with the influence of the Atlantic Ocean. Under certain conditions, however, the external effects may be of importance. To study these effects the sea area involved needs to be extended considerably. Fig. 5.1.1 shows the extended model (model II), while the depth configuration is given in Fig. 5.1.1 and 5.1.2. It is known that the depth of the Atlantic Ocean is much larger than the depth of the North Sea. The consequences for the time-step Δt, with a view to the computational stability, need to be examined. The stability condition given by Van der Houwen (see formula 5.1.6) reads as follows:

$$\Delta t \leq \frac{1}{2\sqrt{gH}} \frac{\Delta x \, \Delta y}{|s|\Delta x + |c|\Delta y} \qquad (9.0.1)$$

A large value of H implies a small value of Δt. The reduction of the time-step can be limited by enlarging the mesh widths Δx and Δy. For this reason the grid on the Atlantic Ocean is much coarser than the North Sea grid. Under these conditions and by applying some weak smoothing stable computations could be carried out with a time-step $\Delta t = 150$ s.

The coarse grid is not suited to model the shallow part of the sea, just west of Scotland. Therefore the shallow sea area near Scotland was reproduced by a separate subgrid. See Fig. 5.1.2. So the computations are carried out in a number of subgrids. The coupling of the subgrids is achieved by using linearly interpolated water heights as a boundary condition for a corresponding subgrid.

It had become evident that the effect of the air pressure may not be omitted in the transition zone between deep and shallow waters. Consequently the terms $\frac{H}{\rho_s} \frac{\partial p(h)}{\partial x}$ and $\frac{H}{\rho_s} \frac{\partial p(h)}{\partial y}$ were introduced again. (See the set of equations 5.1.3.) From these expressions it is clear that the depth H is of importance with respect to the magnitude of the terms. Therefore the depth of the sea does determine whether the air pressure term may be omitted in relation to the wind term. Both terms are equal, when

$$|\vec{v}| = \frac{f}{0.7 C_d} H \qquad (9.0.2)$$

This equation can easily be derived by equating the two terms and by taking $|\vec{v}| = \frac{0.7|\vec{G}|}{f}$, where 0.7 is an estimate of the friction coefficient. With the aid of equation 9.0.2 Fig. 9.0.1 can be composed, giving the partition into areas, where one of the two terms dominates. Roughly speaking, Fig. 9.0.1 shows for instance that if the wind speed exceeds 30 knots, the effect of the pressure gradient is of more importance than the effect of the wind in those cases where the depth of the sea is more than about 200 m. The relative effect of the pressure gradient increases linearly with increasing depth, so that in a deep ocean area and in the transition zone from deep to shallow waters divergence in the vector field, describing the transport of water, may occur connected with varying pressure gradients. See Timmerman [1975]. The divergence in this vector field may cause changes in the water-level, which may extend over the continental shelf.

The coarse subgrids in the areas north and west of Scotland and west of the English Channel give a very rough representation of the true depths. Preliminary calculations had yielded results that were obviously rendered false by the very high depth gradients along the continental slope. With a view to the computation time refinement of the grid was not possible. So a solution was found by applying a correction to the water transport computed in the grid points outside the continental slopes. In these points the computed component perpendicular to the slope was reduced by a factor given by the ratio between the depths in adjacent U, V-points on the shelf and the depth in the grid point considered. Example: if the depth of the sea is 1000 m and the depth of the adjacent shelf 100 m, only 10 per cent of the computed water transport perpendicular to the continental slope was taken into account for the next computational step. That this procedure needs to be applied only in deep areas outside the continental slope and not in the shallower areas can be justified by making allowance for the

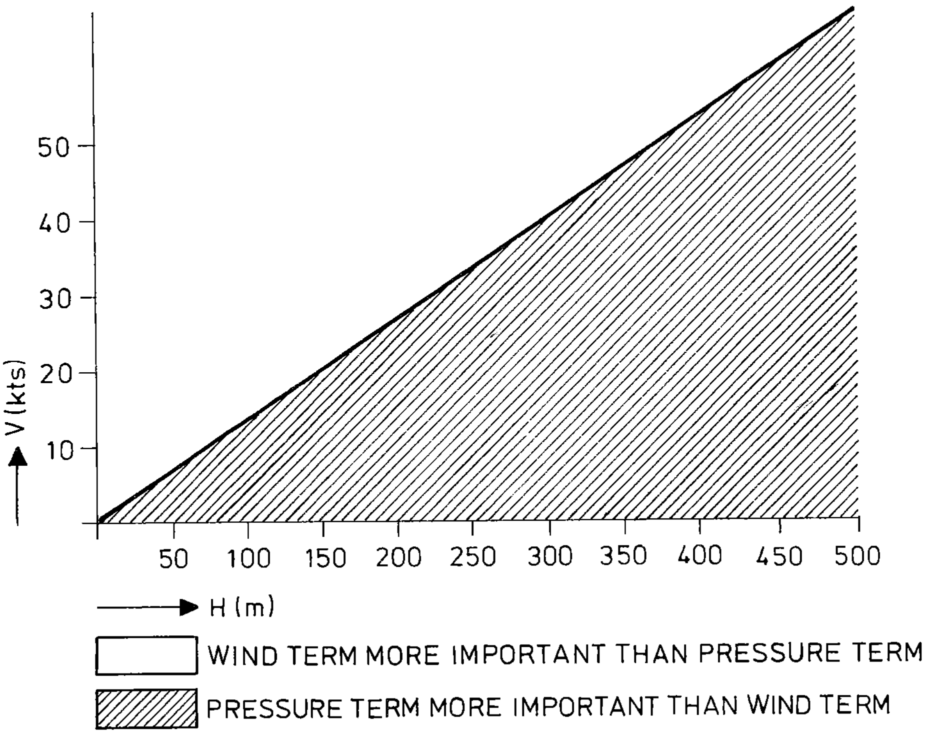

Fig. 9.0.1 Relation between wind term and air pressure term in dependence of depth.

fact that the atmospheric pressure effect, which is predominant in the deep areas, produces currents extending down to the sea bottom, contrary to the windstress effect. The procedure is related to the treatment of the water transport along a closed boundary discussed in Chapter 5.

Experiments with the extended model II are discussed in 9.1 to 9.4.

9.1 Experiments with the extended model II were carried out on a semi-operational basis during the periods 10 September 1973 to 8 June 1974 inclusive and 4 October 1974 to 14 June 1975. The demands that must be made upon a semi-operational model are higher than those upon a model dealing with a single surge. For every new computational cycle is based on the U, V and h field of a previous cycle. Insufficient dissipation of energy, supplied by wind and air pressure, leads to a systematic growth of U, V, resulting in non-realistic U, V and h fields. In the beginning of the experiments with model II these difficulties were really encountered. Insufficient dissipation of energy is connected with the neglect of the viscosity terms. (See Chapter 3). Due to the restricted memory capacity of the computer introduction of the viscosity terms was not possible, so that in order to solve this difficulty a damping factor in some grid points of the northern grid of the North Sea, showing these deficiencies, was introduced. The magnitude of the damping factor had to be chosen on an experimental basis. In this way the problem could be solved satisfactorily.

Furthermore it turned out that the computations in the Atlantic Ocean area showed instability. For this reason it was necessary to introduce a smoothing factor, given by 9.1.1.

$$A^{s}_{j,k} = \alpha\, A_{j,k} + \frac{1-\alpha}{4}\,[A_{j+1,k}+A_{j-1,k}+A_{j,k+1}+A_{j,k-1}] \qquad (9.1.1)$$

where $A^{s}_{j,k}$ is the smoothed value in grid point j,k and α a value between 0 and 1. A suitable value for α appeared to be 0.9.

9.1.1 The results of a verification of the computed values for low tide and high tide at the stations Flushing, Hook of Holland, Den Helder, Harlingen and Delfzijl are presented in Table 9.1.1.1. The material is given for throughout the periods 10 September 1973 to 8 June 1974 and 4 October 1974 to 14 June 1975 for both low tide and high tide. Again, average values and standard deviations of the differences between observed and computed set-up are determined. For each station about 2000 observations were available.

Table 9.1.1.1 Verification of the computations with model II in the periods 10 September 1973 to 8 June 1974 and 4 October 1974 to 14 June 1975. $\overline{O-C}$ and σ in dm.

	1973-1974 low tide		1974-1975 low tide		1973-1974 high tide		1974-1975 high tide	
	$\overline{O-C}$	σ	$\overline{O-C}$	σ	$\overline{O-C}$	σ	$\overline{O-C}$	σ
Flushing	−1.4	2.2	−1.1	1.7	−0.1	1.9	+0.5	1.6
Hook of Holland	−0.2	2.0	−0.0	1.7	+0.6	1.9	+0.3	1.5
Den Helder	−0.9	2.0	−0.3	1.6	−0.3	2.0	+0.2	1.4
Harlingen	−0.9	2.1	−0.3	1.5	−1.6	2.8	−0.8	1.6
Delfzijl	−0.9	2.5	−1.3	2.1	−0.3	2.2	+0.0	1.8
mean	−1.0	2.2	−0.6	1.7	−0.2	2.2	+0.0	1.6

Table 9.1.1.1 shows that the results of the second period are better than those of the first one, which in the first stage of the investigation had been influenced unfavourably by several imperfections in the programs for data extraction, objective analysis of the 1000 mbar field, and computation of wind and water-levels. These imperfections became evident in the course of the computations and were discarded gradually.

The differences between the standard deviations for low-tide and high-tide situations are small, so that the method can be applied to both tides.

The low-tide computations for Flushing and Delfzijl and the high-tide computations for Harlingen seem to give too high results in a systematic way. This may be caused by the model, e.g. by an inaccurate contribution of the Frisian Sea and the Eems-estuary, or by inexact values of the predicted astronomical tide. This last type of error cannot be neglected. In Chapter 3 it has been remarked already that the standard deviation of the error in the predicted astronomical tide for Flushing and Hook of Holland amounts to 1-1½ dm. Taking into account an error in the measurements of about 2-3 cm (see also Chapter 3), the error due to shortcomings in the model, either of meteorological or of oceanographical nature, may be about 1 dm.

It is useful to partition the material from which Table 9.1.1.1 has been computed into a number of classes. The following choice has been made:

class 1	observed set-up	$\leqslant -3$ dm
class 2	observed set-up	> -3 dm and < 4 dm
class 3	observed set-up	$\geqslant 4$ dm and < 8 dm
class 4	observed set-up	$\geqslant 8$ dm

The results are shown in Table 9.1.1.2.

The partition of the material into these four classes shows that the absolute value of the computed set-up is too low compared with the observed set-up in classes 1, 3 and 4. This rather systematic imperfection may be discarded by an increase of the drag-coefficient with about 10%. The effect will be that the systematic differences in classes 3 and 4 will vanish, while in class 1 the systematic difference will decrease to about 1.5 dm. This latter shortcoming may be connected with the fact that the coefficients of the sea-model were tested on situations with positive surges rather than on those with negative ones. Furthermore, negative surges do often occur in situations with southerly to southeasterly winds, which means that the results are rather sensitive with respect to the computed direction of the wind. Further investigation of this problem is necessary.

It is remarkable that the differences between the standard deviations of the four classes are not large. Even in class 2, connected with calm weather, the standard deviation is still about 1.5 dm. This may be caused not only by shortcomings in the predicted astronomical tide, but also by small oscillations as shown by the computed values. From a comparison with Table 8.0.1 it turns out that the standard deviations in class 4 and of the 16 surges that have been investigated are about the same.

The computations carried out so far indicate that the best estimated value of the drag-coefficient for $T_a - T_s = 0°$ is 0.0027 if the wind speed exceeds 20 ms^{-1} and 0.0018 if the wind speed is less than 15 ms^{-1}. In the remaining wind-speed area one may interpolate linearly. (See also Table 4.2.1.)

Table 9.1.1.2 Verification of computations with model II in the periods 10 September 1973 to 8 June 1974 and 4 October 1974 to 14 June 1975. Material distributed over 4 classes: observed set-up ⩽ —3 dm, —3 — +4 dm, 4–8 dm and ⩾ 8 dm. $\overline{O-C}$ and σ in dm. N = number of observations.

class →	1						2						3						4					
observed →	⩽ —3 dm						—3 — +4 dm						4–8 dm						⩾ 8 dm					
	1973-74			1974-75			1973-74			1974-75			1973-74			1974-75			1973-74			1974-75		
low tide	$\overline{O-C}$	σ	N	$\overline{O-C}$	σ	N	$\overline{O-C}$	σ	N	$\overline{O-C}$	σ	N	$\overline{O-C}$	σ	N	$\overline{O-C}$	σ	N	$\overline{O-C}$	σ	N	$\overline{O-C}$	σ	N
Flushing	—3.4	2.8	62	—2.1	1.7	60	—1.4	2.0	408	—1.2	1.5	385	+0.8	3.6	27	+0.5	2.1	24	+2.1	4.1	11	+1.5	2.2	14
Hook of Holland	—2.0	2.6	17	—2.0	1.7	23	—0.2	1.8	436	+0.0	1.6	394	+0.9	2.8	41	+0.2	1.7	52	—0.8	3.4	8	+0.9	1.4	14
Den Helder	—2.5	2.5	38	—1.7	1.6	35	—1.0	1.9	416	—0.5	1.4	370	+1.0	2.6	38	+0.7	1.8	49	+1.4	3.0	13	+1.3	2.1	16
Harlingen	—2.9	2.4	45	—1.5	1.6	43	—0.7	2.1	400	—0.2	1.4	355	—0.7	3.9	43	+0.6	1.7	63	—0.1	3.0	19	+1.0	1.7	21
Delfzijl	—3.0	2.5	109	—2.6	2.0	110	—0.9	2.0	356	—1.4	1.7	310	—0.1	3.2	25	+0.2	2.1	41	+0.7	3.2	21	+2.0	2.1	28
mean	—2.9	2.5		—2.1	1.8		—0.8	1.9		—0.8	1.6		+0.4	3.2		+0.4	1.8		+0.7	3.2		+1.4	1.9	
high tide																								
Flushing	—1.6	4.0	5	—1.8	1.7	11	—0.3	1.7	456	+0.6	1.7	361	+0.8	3.1	40	+0.4	1.4	63	+0.3	3.0	13	+1.0	1.9	14
Hook of Holland	+1.5	1.2	4	—1.2	1.4	15	+0.6	2.0	436	+0.3	1.5	401	+1.9	2.4	52	+0.4	1.7	56	+1.6	3.8	24	+1.5	2.1	10
Den Helder	—1.5	1.6	18	—0.8	1.5	15	—0.5	1.7	422	+0.1	1.2	383	+1.2	3.0	47	+0.5	1.3	54	+0.4	3.0	21	+2.2	2.2	27
Harlingen	—3.8	2.9	85	—1.9	1.6	73	—1.5	1.7	361	—0.8	1.3	345	+0.2	3.3	41	+0.2	1.4	48	+0.3	1.8	23	+1.7	2.7	22
Delfzijl	—1.6	2.2	35	—1.9	2.0	27	—0.4	2.0	402	—0.1	1.5	370	+0.7	3.2	47	+0.5	1.6	79	+1.6	2.9	30	+2.2	2.6	29
mean	—2.8	2.5		—1.7	1.7		—0.4	1.8		+0.3	1.4		+1.0	3.0		+0.4	1.5		+1.2	2.9		+1.9	2.4	

9.2 Computations of water levels and of stream vectors are closely tied. Though the present investigation primarily deals with water levels, it is possible to compare the computed stream vector with a measured stream vector from which the periodical tidal components are eliminated. For some places in the southern North Sea such a comparison has been carried out at the Royal Netherlands Meteorological Institute.

9.3 The period November-December 1973 was characterized by numerous surges. A survey of the observed set-up and the set-up computed with a numerical model during these surges is given in Table 9.3.1. For the five stations Flushing, Hook of Holland, Den Helder, Harlingen and Delfzijl the time of high tide and the observed set-up O in dm, connected to this maximum, are indicated. Furthermore three values C_1, C_2 and C_3 are added, representing computed values in dm related to this high tide. Times are given also, but in contrast to the time mentioned before, these times refer to the observation time of the latest synoptic data available when the computation was carried out. As an average the times valid for C_1, C_2 and C_3 are respectively 7 hours and 1 hour before and 5 hours after the time of high water. The computation which gives C_3 is based on wind- and pressure observations of the 1000 mbar surface only. C_1 and C_2 however are obtained by using a 'prebaratic' as well. This 'prebaratic' is based on the very simple assumption that no change in the pressure distribution will occur after the last time of observation.

Table 9.3.1 Verification of the storm surges in November-December 1973.
O = observed set-up at high tide; C_1, C_2 and C_3 = computed set-up (in dm); t = time in GMT.

FLUSHING		t	O	t	C_1	t	C_2	t	C_3
November	6	09	+ 8.3	00	+ 6.8	06	+ 7.6	12	+ 7.2
	13	14	+10.6	06	+11.7	12	+10.5	18	+10.7
	15	16	+ 8.2	12	+ 7.6	18	+ 6.8	00	+ 6.8
	19	21	+13.1	12	+16.3	18	+18.7	00	+19.0
	25	01	+ 9.8	18	+11.6	00	+10.6	06	+10.6
December	6	22	+13.3	12	+13.0	18	+14.2	00	+13.8
	14	16	+13.1	12	+12.0	18	+13.1	00	+13.1
	15	04	+ 9.9	00	+14.2	06	+15.6	12	+14.3
	16	18	+ 8.5	12	+ 6.1	18	+ 6.0	00	+ 6.1

HOOK OF HOLLAND		t	O	t	C_1	t	C_2	t	C_3
November	6	10	+10.4	06	+ 8.3	12	+ 8.2	18	+ 8.5
	13	03	+10.7	18	+14.4	00	+16.0	06	+15.1
		15	+12.5	06	+12.5	12	+11,3	18	+11.5
	15	17	+10.9	12	+ 8.3	18	+ 7.3	00	+ 7.5
	16	18	+10.4	12	+ 1.9	18	+ 2.8	00	+ 3.3
	19	09	+11.6	00	+ 5.2	06	+ 6.9	12	+ 7.9
		22	+14.9	12	+17.6	18	+19.2	00	+18.7
	25	02	+13.0	18	+12.3	00	+10.1	06	+10.1
		14	+ 8.3	06	+ 7.4	12	+ 7.5	18	+ 7.8
	26	03	+ 8.8	18	+ 9.7	00	+11.3	06	+11.1
		15	+ 8.9	06	+ 9.1	12	+ 9.1	18	+ 9.1
	27	03	+ 9.1	18	+ 9.2	00	+ 9.9	06	+ 9.9
		15	+ 9.0	06	+10.3	12	+10.8	18	+10.5
December	6	00	+14.2	12	+14.2	18	+14.4	00	+13.0
	8	12	+ 8.0	06	— 0.6	12	— 0.2	18	— 0.3
	13	16	+ 9.8	06	+10.9	12	+10.7	18	+11.4
	14	05	+13.6	18	+14.8	·		·	
		17	+15.6	12	+12.9	18	+15.6	00	+14.8
	15	06	+10.2	00	+12.8	06	+14.1	12	+13.3
	16	19	+ 9.2	12	+ 7.6	18	+ 7.9	00	+ 7.9

DEN HELDER		t	O	t	C_1	t	C_2	t	C_3
November	6	02	+ 8.1	18	+ 5.0	00	+ 6.2	06	+ 6.2
	6	16	+12.1	12	+10.9	18	+10.4	00	+10.2
	11	19	+ 9.2	12	+ 6.1	18	+ 7.6	00	+ 7.3
	13	08	+17.6	00	+15.9	06	+18.2	12	+17.9
	13	17	+13.1	12	+ 9.9	18	+10.9	00	+11.3
	15	22	+15.8	18	+10.4	00	+10.7	06	+10.9
	16	22	+ 9.7	18	+ 6.3	00	+ 5.1	06	+ 4.8
	19	14	+14.8	06	+12.4	12	+16.4	18	+16.4
	20	02	+13.2	18	+16.7	00	+16.1	06	+14.9
	24	18	+11.3	12	+10.3	18	+12.1	00	+11.3
	25	06	+11.0	00	+10.3	06	+10.5	12	+10.5
	25	19	+ 9.0	12	+ 7.8	18	+ 9.8	00	+ 9.8
December	6	16	+15.2	06	+11.3	12	+14.1	18	+14.3
	7	03	+14.8	18	+14.0	00	+11.6	06	+11.1
	13	09	+ 9.6	00	+ 9.3	06	+11.1	12	+10.3
	14	22	+12.0	18	+15.9	00	+15.2	06	+14.9

HARLINGEN		t	O	t	C_1	t	C_2	t	C_3
November	6	04	+ 9.7	18	+ 7.7	00	+ 7.2	06	+ 8.5
	6	17	+13.7	12	+16.0	18	+14.0	00	+13.6
	11	20	+11.0	12	+ 8.1	18	+11.8	00	+10.2
	13	09	+20.5	00	+20.2	06	+23.8	12	+22.0
	13	20	+12.1	12	+12.7	18	+14.2	00	+12.4
	15	12	+ 9.6	06	+ 8.0	12	+11.9	18	+10.8
	15	00	+19.4	18	+15.8	00	+17.7	06	+18.1
	16	00	+10.2	18	+11.9	00	+ 7.9	06	+ 8.4
	19	16	+20.7	12	+22.5	18	+21.7	00	+21.1
	19	04	+13.2	00	+16.1	06	+14.2	12	+14.5
	24	21	+14.3	12	+14.8	18	+14.7	00	+13.8
	25	08	+ 9.9	00	+13.5	06	+10.5	12	+10.2
	25	21	+10.9	12	+ 9.9	18	+12.4	00	+12.3
	26	21	+ 8.2	12	+ 9.1	18	+10.2	00	+11.5
December	6	17	+20.8	12	+18.5	18	+19.0	00	+20.5
	6	03	+16.9	18	+19.0	00	+15.6	06	+14.1
	13	11	+10.8	06	+15.6	12	+12.5	18	+13.9
	14	00	+14.5	18	+19.4	00	+16.6	06	+17.7

DELFZIJL		t	O	t	C_1	t	C_2	t	C_3
November	6	06	+ 8.2	00	+ 4.9	06	+ 6.4	12	+ 6.7
	6	20	+15.7	12	+17.3	18	+18.3	00	+18.7
	10	23	+10.3	18	+ 9.6	00	+ 8.3	06	+ 8.4
	13	12	+22.0	06	+22.4	12	+21.5	18	+20.9
	14	00	+10.4	18	+11.5	00	+ 9.1	06	+10.4
	15	14	+11.6	06	+ 5.7	12	+13.5	18	+14.6
	16	02	+22.1	18	+19.0	00	+21.1	06	+20.5
	16	16	+ 9.4	12	+ 3.4	18	+ 5.3	00	+ 5.6
	17	03	+11.8	18	+10.0	00	+ 6.7	06	+ 7.6
	17	16	+ 8.9	12	+10.8	18	+ 9.4	00	+ 8.4
	19	18	+33.4	12	+24.7	18	+30.8	00	+32.4
	20	06	+16.3	00	+21.9	06	+18.2	12	+17.9
	24	21	+16.3	12	+15.0	18	+14.0	00	+13.4
	25	11	+ 9.4	06	+10.2	12	+ 9.8	18	+10.0
	25	23	+13.8	18	+11.8	00	+10.5	06	+10.3
	26	00	+10.4	18	+ 6.7	00	+ 9.8	06	+10.0
	27	12	+10.3	06	+10.0	12	+10.5	18	+10.3
December	6	19	+27.0	12	+19.8	18	+23.7	00	+24.9
	7	07	+16.5	00	+18.0	06	+14.6	12	+15.1
	13	13	+12.1	06	+16.7	12	+15.3	18	+16.6
	14	02	+14.9	18	+16.2	00	+12.1	06	+12.8
	16	16	+ 8.5	12	+ 8.8	18	+ 8.3	00	+ 8.3

A summary of Table 9.3.1 is given in Table 9.3.2, containing average values $\overline{O\text{-}C}$ and standard deviations. For reasons of comparison some results of Table 8.0.1 are given also, indicated with C_c.

Table 9.3.2 Summary of the tables 9.3.1 and 8.0.1.

	$\overline{O - C}$ in dm				σ in dm			
	C_1	C_2	C_3	C_c	C_1	C_2	C_3	C_c
Flushing	—0.5	—0.9	—0.7	—0.9	2.3	2.6	2.4	2.5
Hook of Holland	+1.1	+0.6	+0.7	+0.0	3.2	3.6	3.2	2.3
Den Helder	+1.5	+0.7	+1.9	+0.4	2.2	2.6	2.3	2.3
Harlingen	—0.6	—0.5	—0.4	+0.2	2.6	1.7	1.7	2.5
Delfzijl	+1.1	+1.0	+0.7	+0.8	3.6	2.2	2.1	2.2
mean	+0.5	+0.2	+0.4	+0.1	2.8	2.5	2.3	2.4

It is remarkable that the standard deviations of C_1, C_2 and C_3 for the stations Flushing, Hook of Holland and Den Helder only show small mutual differences, a consequence of the inertia of the sea. Harlingen and Delfzijl, however, are to a great extent influenced by local effects of the Frisian Sea and the Eems estuary, working directly and resulting in stronger varying values of the standard deviations C_1, C_2 and C_3.

The mean values show small differences as well, contrary to the individual stations. It is likely that the values are to some extent influenced by a sampling effect. This is confirmed for instance by Table 9.3.1, showing two cases with important differences between observed and computed values, especially at Hook of Holland, notably on 16 November 1973 and 8 December 1973. From a further investigation it turned out that on the first date a small depression moved over the North Sea in a southeasterly direction. The analysis was hampered by an insufficient number of observations on the North Sea. On 8 December 1973 the winds over the southwestern part of the North Sea were mainly NNE. Under these circumstances the computed set-up is very sensitive to small changes in the computed wind direction. So a relatively small error in the computation of the wind may cause considerable errors in the computed set-up.

On 19 November 1973 Delfzijl showed an extremely high water level. The set-up due to meteorological conditions amounted to 33.4 dm, which is only 0.5 dm less than the value observed during the Hamburg surge of 16 February 1962. The computed value based on the observed pressure- and windfields was 32.4 dm, which indicates a good agreement between observed and computed value.

Incorporating external effects was the main intention of the extension of the model over the Atlantic Ocean. So far the advantage of this extension has not clearly been demonstrated, due to the fact that only average values have been considered, which are mainly dominated by the normal behaviour of the overwhelming majority of the cases. Therefore it is desirable to discuss a number of individual cases.

9.4 The external surges of 11-15 December 1972, 16-17 October 1963, 29 January 1974 and the surge of 16 February 1962.

An external surge in the North Sea can be defined as an upward deviation of the sea level with regard to the normal astronomical tide generated by meteorological forces acting outside the North Sea proper.

The phenomenon was described by Corkan [1948], Rossiter [1958, 1959] and Koopmann [1963]. In the sixties external surges were studied with a numerical model by Schmitz [1962, 1965] and by Heaps [1969]. Schmitz introduced the external surge as a boundary condition of a North Sea model and then examined how the surge propagated over the North Sea. He also performed some computations with regard to the development of a deep-water surge caused by a depression on the Atlantic Ocean, which may enter the North Sea as an external surge. Heaps investigated the mechanism which may cause the phenomenon and concluded that westerly gales over the shallow sea area west of Scotland may bring about external surges.

In these studies no attention was paid to the effect of the air pressure in the transition area between the shallow continental shelf and the much deeper part of the ocean. In such a transition area pressure fields associated for instance with depressions may create a strongly convergent mass transport. This convergence results in changes of the water level, which may extend as an external surge over the North Sea.

It appears that these processes are described in a satisfactory way by the extended numerical model II. This will be demonstrated by three cases with an external surge and by the surge of 16 February 1962, which seems to have been accompanied by a rather important external component. The selection of the first three cases was based on the following considerations:

a) the external surges of 11-15 December 1972 gave bad results when applying model I;
b) the external surge of 16-17 October 1962 is well known in literature and described by Koopmann [1963];
c) the external surge of 29 January 1974 is an example of a computation carried out semi-operationally with model II.

9.4.0 The external surges of 11 to 15 December 1972.

The weather maps (Fig. 9.4.0.1) show two deep storm depressions passing near the continental slope during the period of 11 to 15 December 1972. During the whole period the wind over the North Sea had a southerly component, while the wind speeds over the southern part of the North Sea were small. The depressions caused two external surges arriving at the Netherlands coast on 12 December at approximately 21h00m and on 14 December at 06h00m respectively.

It appears from Fig. 9.4.0.2 that the extended model with air pressure reproduces the external surge fairly well. (See dashed line.) With the restricted model, however, a lowering of the water levels was computed due to the southerly winds. The improvement given by the first model with respect to the second can be given quantitatively by computing the mean differences between observed (O) and computed (C) values during high and low tide and by computing the root mean square of these differences. See Table 9.4.0.1, which is based on 14 successive high and low waters.

Table 9.4.0.1 Computed values with the extended and restricted model.

	extended model with air pressure		restricted model without air pressure	
	O — C	RMS	O — C	RMS
Flushing	+0.0 dm	1.4 dm	+2.2 dm	1.9 dm
Hook of Holland	+1.6	2.1	+3.2	4.0
Den Helder	+1.5	2.3	+3.1	3.9
Harlingen	+1.0	1.4	+2.6	3.7
Delfzijl	+0.1	2.2	+1.9	2.6
mean	+0.8	1.9	+2.6	3.2

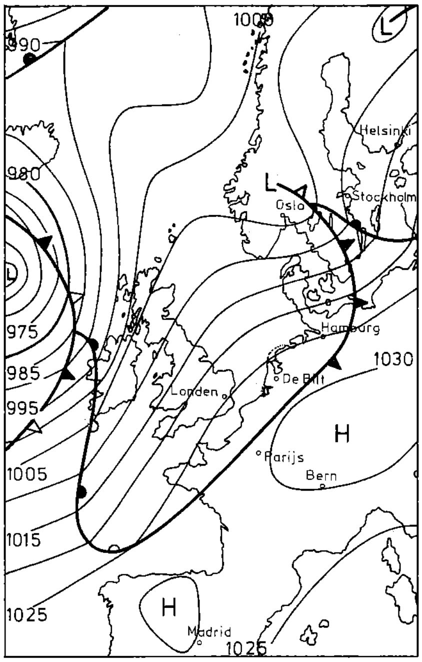

11 DEC. 1972 12.00 GMT

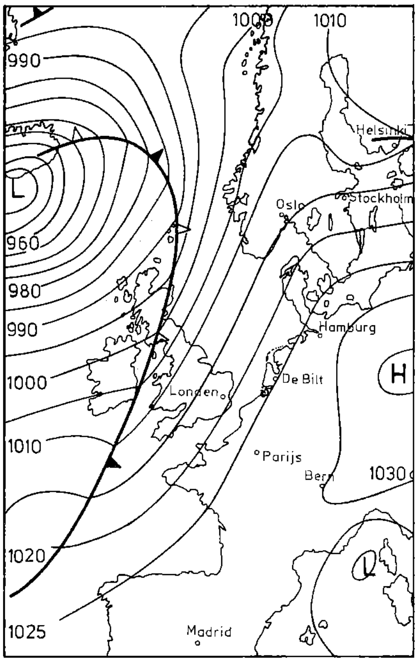

12 DEC. 1972 00.00 GMT

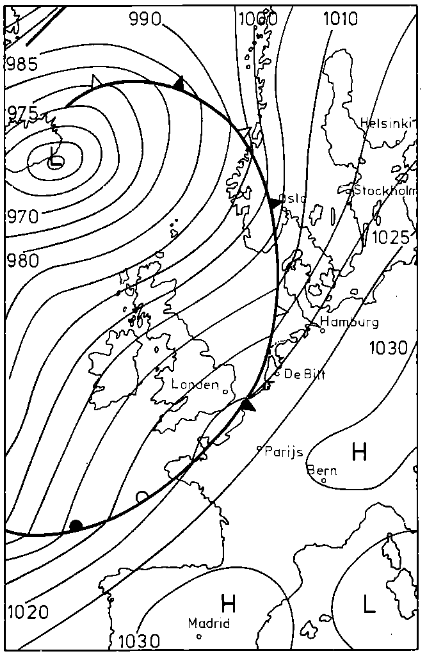

12 DEC. 1972 12.00 GMT

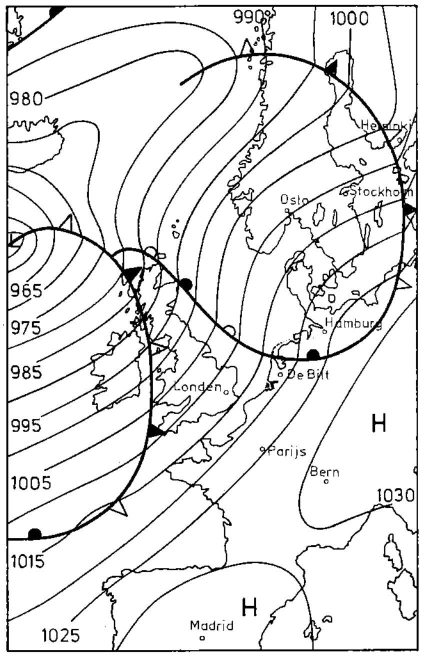

13 DEC. 1972 00.00 GMT

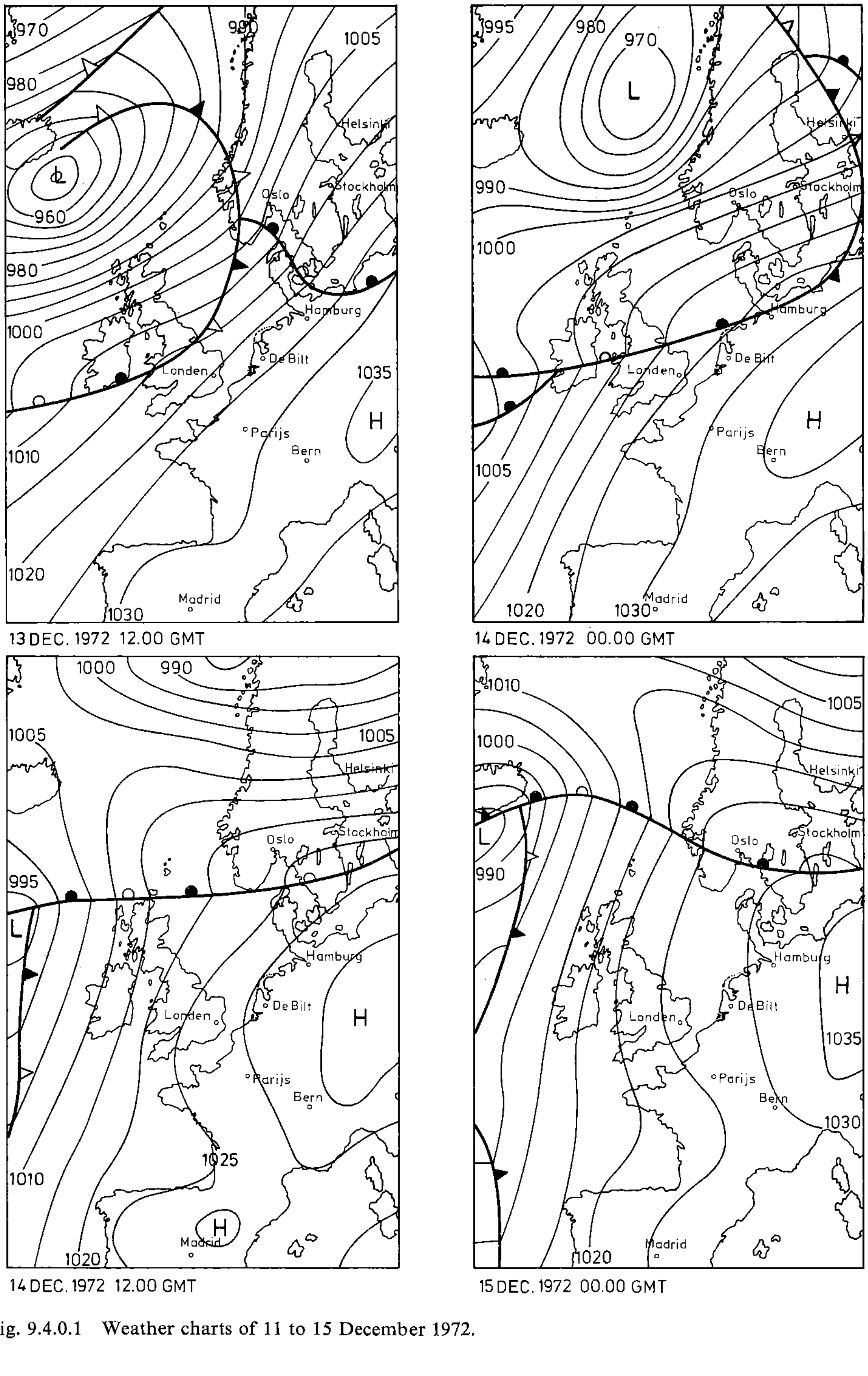

Fig. 9.4.0.1 Weather charts of 11 to 15 December 1972.

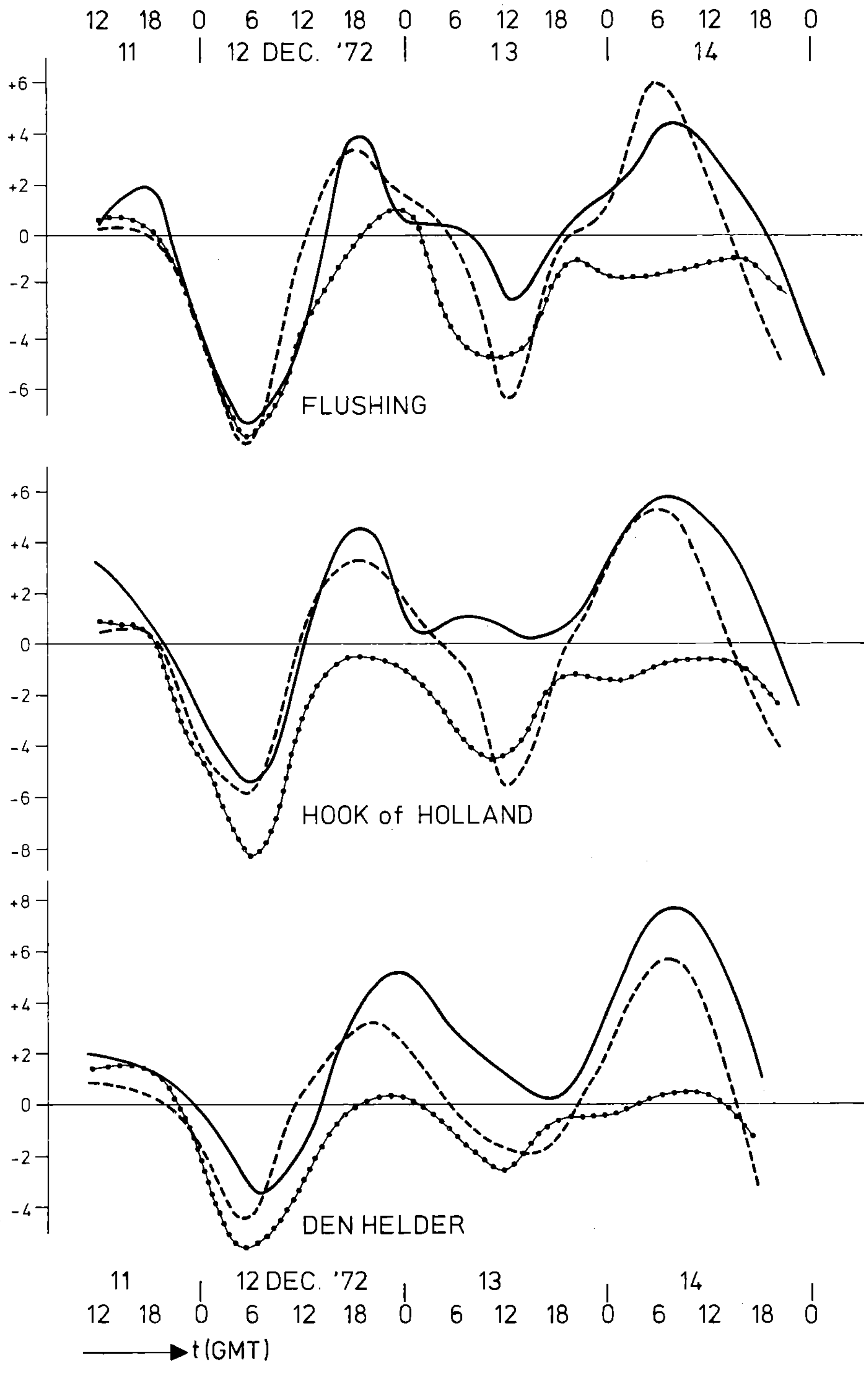
12 18 0 6 12 18 0 6 12 18 0 6 12 18 0
11 | 12 DEC. '72 | 13 | 14 |
+6
+4
+2
0
-2
-4
-6
FLUSHING
+6
+4
+2
0
-2
-4
-6
-8
HOOK of HOLLAND
+8
+6
+4
+2
0
-2
-4
DEN HELDER
11 | 12 DEC. '72 | 13 | 14 |
12 18 0 6 12 18 0 6 12 18 0 6 12 18 0
t (GMT)

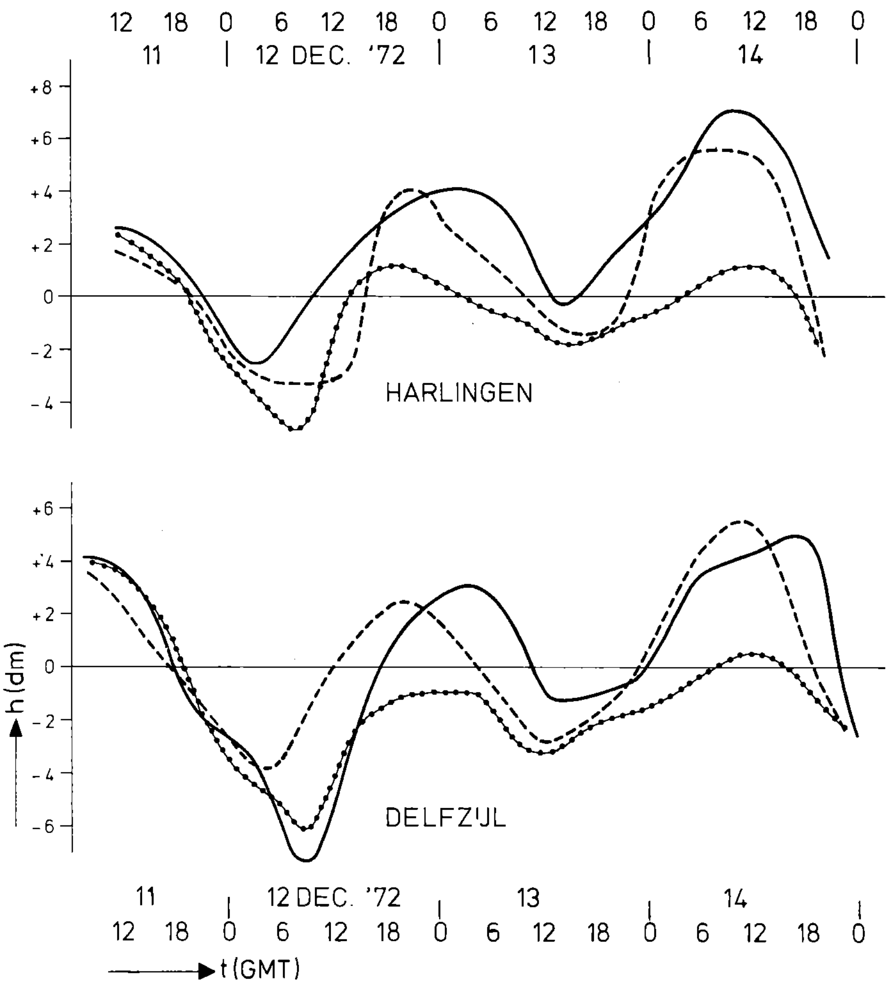

Fig. 9.4.0.2 External surge of 11 to 15 December 1972 at Flushing, Hook of Holland, Den Helder, Harlingen and Delfzijl, respectively.
—— residuals after removal of astronomical tide;
– – – surge, computed with extended model, including air pressure term;
–•–•–•– surge, computed with restricted model, without air pressure term.

It is known from experience that southerly winds blowing over the North Sea can be followed by a rising of the water level along the Netherlands coast. This phenomenon may be explained by the occurrence of an oscillation in the North Sea in such a way that water being swept away by a southerly gale starts to flow back when the gale vanishes and may cause a rise of the water level along the Netherlands coast 15-18 hrs later. Generally, the meteorological phenomenon is accompanied by a front passing the northern part of the North Sea in easterly direction.

Applying this idea to the cold front of 12 December 1972 one would expect a rise of the water level around 21h00m. This rise is indeed confirmed by the observations. Nevertheless it is doubtful whether this theory is correct. Computations with the restricted model show that vanishing southerly winds on the northern part of the North Sea do not account for rising water levels along the Netherlands coast, whereas a rising of the water levels is reproduced by the extended model. See Fig. 9.4.0.2. It may be concluded therefore that the surge is created exclusively by external effects.

The external effects are composed of the pressure effect near the continental slope and of the effect of westerly gales over the shallow part of the ocean near Scotland. Fig. 9.4.0.3 shows the contribution of the wind effect in point B (dashed line) and the contribution of the pressure effect in point A (full line): the location of A and B is indicated in Fig. 5.1.1 and 5.1.2. After midday of 13 December the severe gale around Scotland created a field of increases in water levels of about 2-4 dm. This disturbance propagated along the Orkney Islands, entered the North Sea and moved in about six hours towards the southern part of the North Sea. From 13 December 06h00m to 14 December 04h00m the pressure effect, on the contrary, produced a more permanent rise of the water levels along the northern boundary of the North Sea of about 3-6 dm. See also Fig. 9.4.0.4. The depression of 12 December induced a similar effect on the water levels as can be seen from Fig. 9.4.0.3 and 9.4.0.4. Again, the pressure effect seems to be more important than the wind effect. Furthermore, it becomes evident from the computations that the pressure effect generated a permanent rise along the northern boundary of the North Sea, while the westerly gale near Scotland produced a small field of rising levels moving along the English coast in a southerly direction.

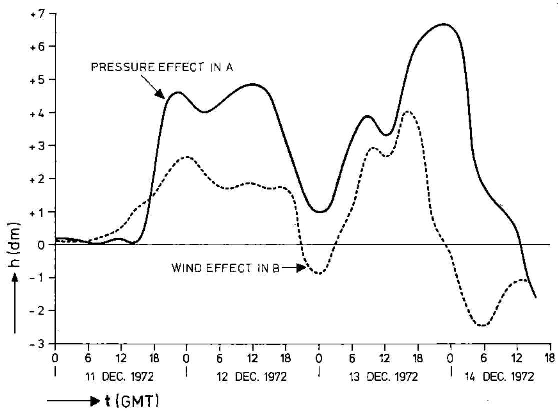

Fig. 9.4.0.3 Pressure effect in A and wind effect in B in the period 11 to 15 December 1972.

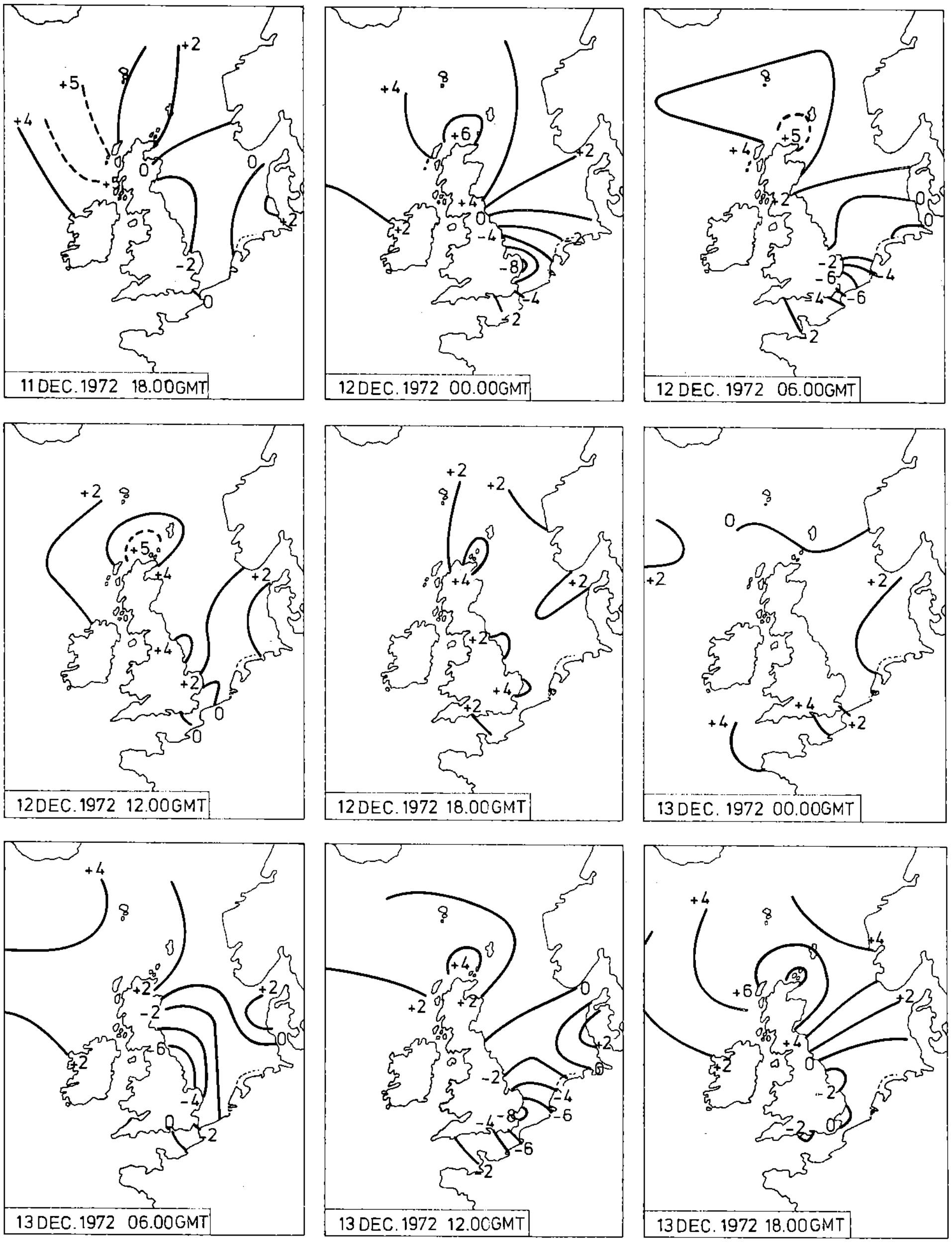

For legend see page 62

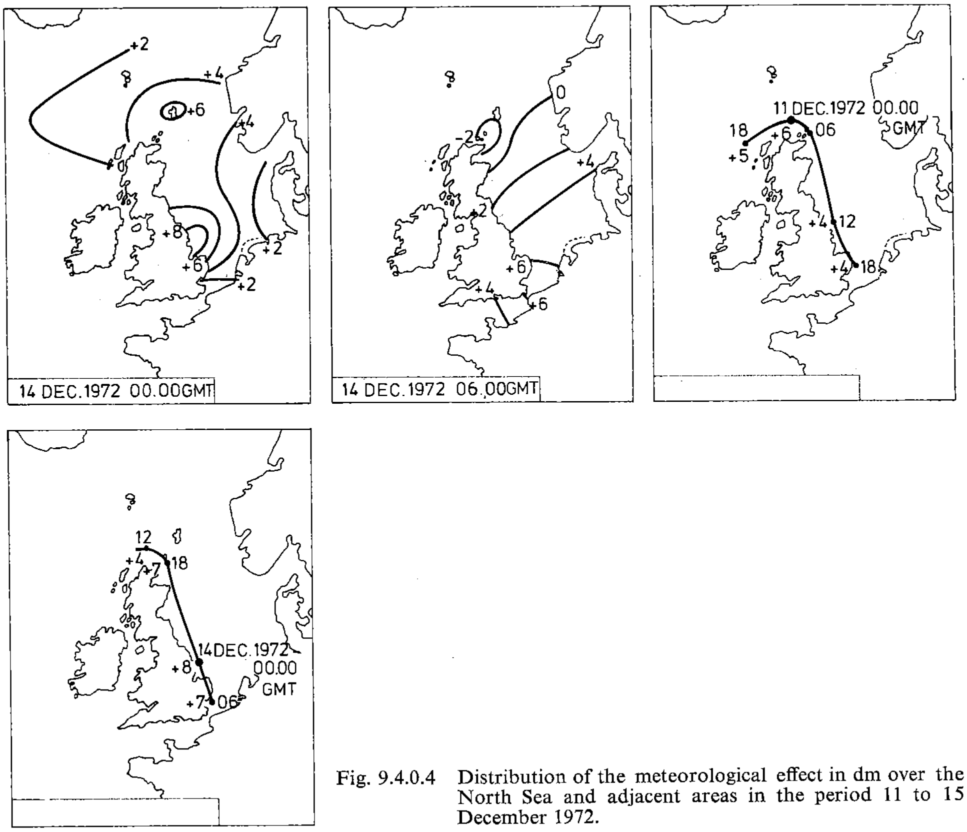

Fig. 9.4.0.4 Distribution of the meteorological effect in dm over the North Sea and adjacent areas in the period 11 to 15 December 1972.

9.4.1 The external surge of 16-17 October 1963.

The external surge of 16-17 October 1963 was described by Koopmann (1963). The rise of the water levels was accompanied by weak southerly winds over the North Sea. Hence this surge also can only be attributed to external effects. It appears from Fig. 9.4.1.1 that again a concentrated storm depression moved in northeasterly direction along the continental slope.

It follows from Fig. 9.4.1.2 that on 15 and 16 October 1963 this depression generated an external surge. As Fig. 9.4.1.3 shows, the external surge consisted of two components, one connected with the air pressure and one with the wind. The air pressure built up an extensive field of about 4 dm bringing about a permanent rise of the water level along the whole northern boundary of the North Sea. The westerly gale however brought about only a small field of 2-3 dm, which on 16 October moved along the English east-coast in southerly direction over the North Sea. After 16 October 15h00m this field could no more be distinguished as a separate field in the southern part of the North Sea. Comparing in Fig. 9.4.1.4 the dashed line with the point-dashed line, the latter obtained by omitting the pressure effects, it appears that the pressure effect cannot be neglected. Generally, it appears that an important part of the external surge is explained by the model. However, it must be recognized that many curves show an indication of an external effect, which is not reproduced by the model.

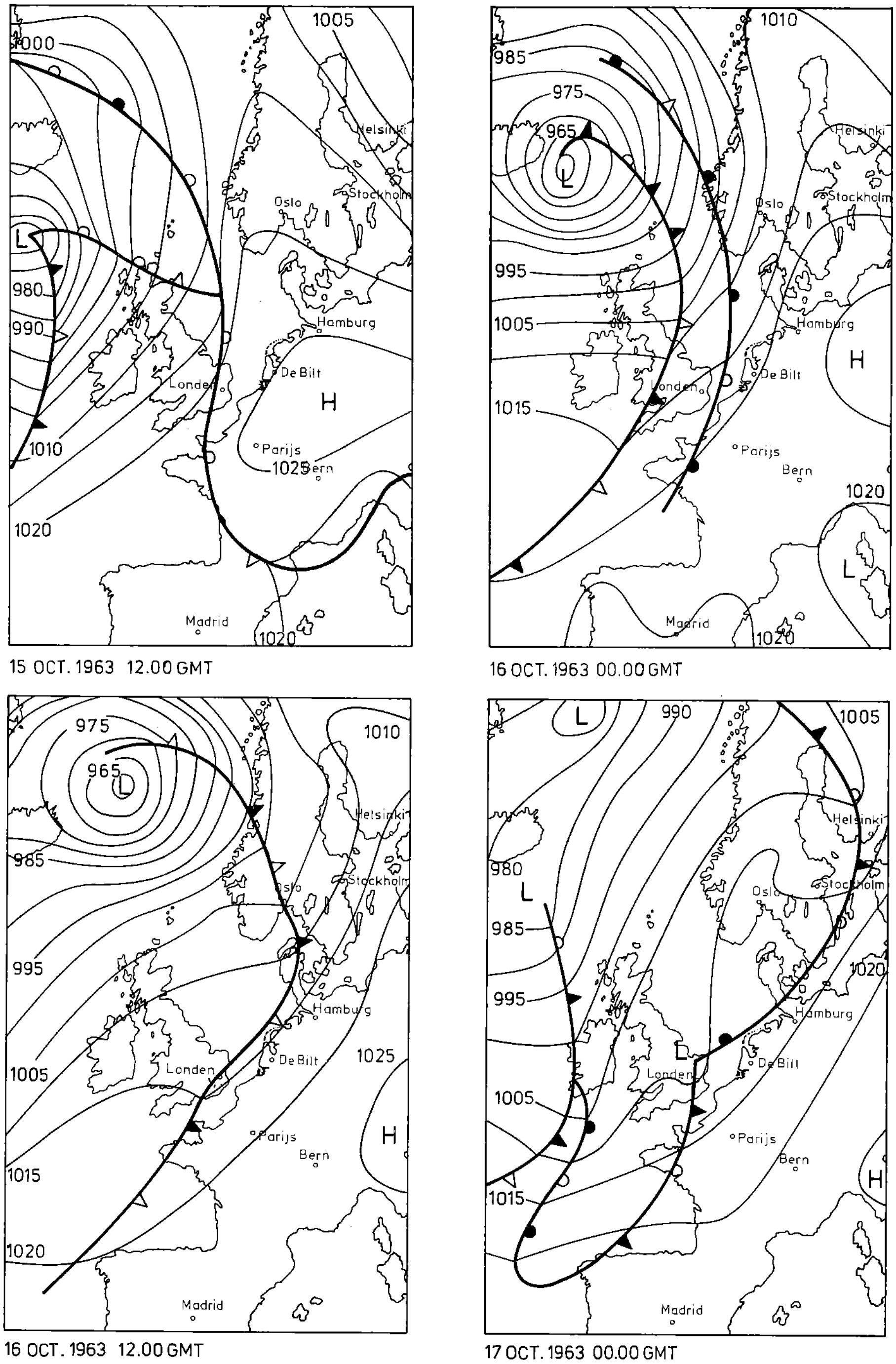

Fig. 9.4.1.1 Weather charts of 15 to 17 October 1963.

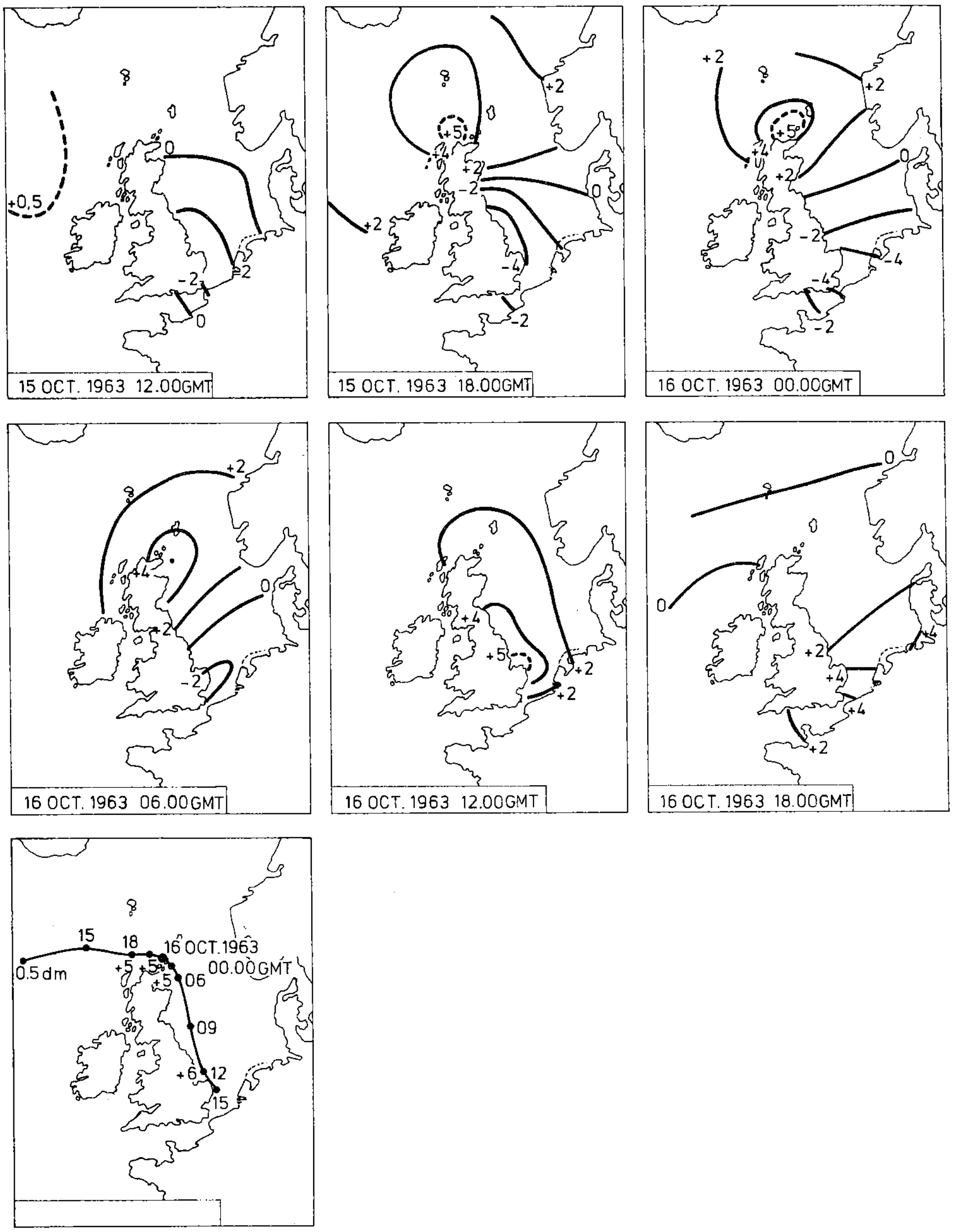

Fig. 9.4.1.2 Distribution of the meteorological effect in dm over the North Sea and adjacent areas in the period 15 to 17 October 1963.

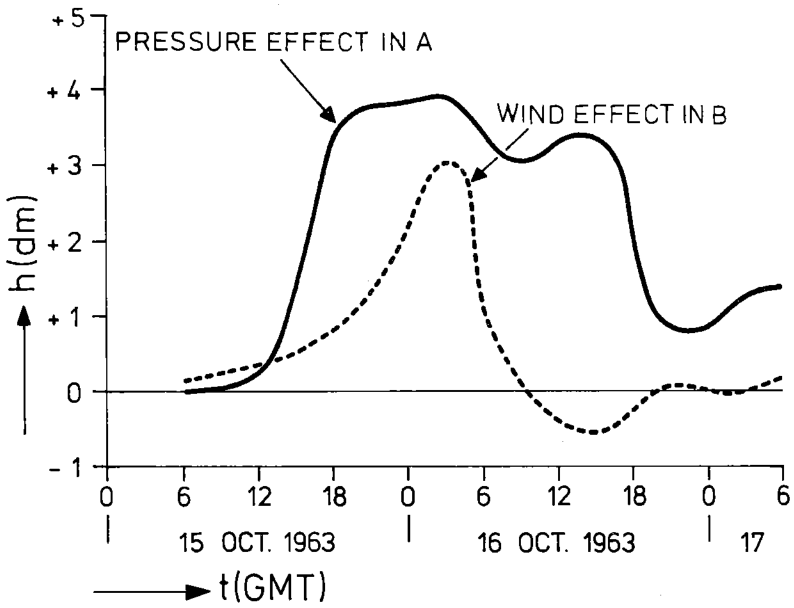

Fig. 9.4.1.3 Pressure effect in A and wind effect in B in the period 15 to 17 October 1963.

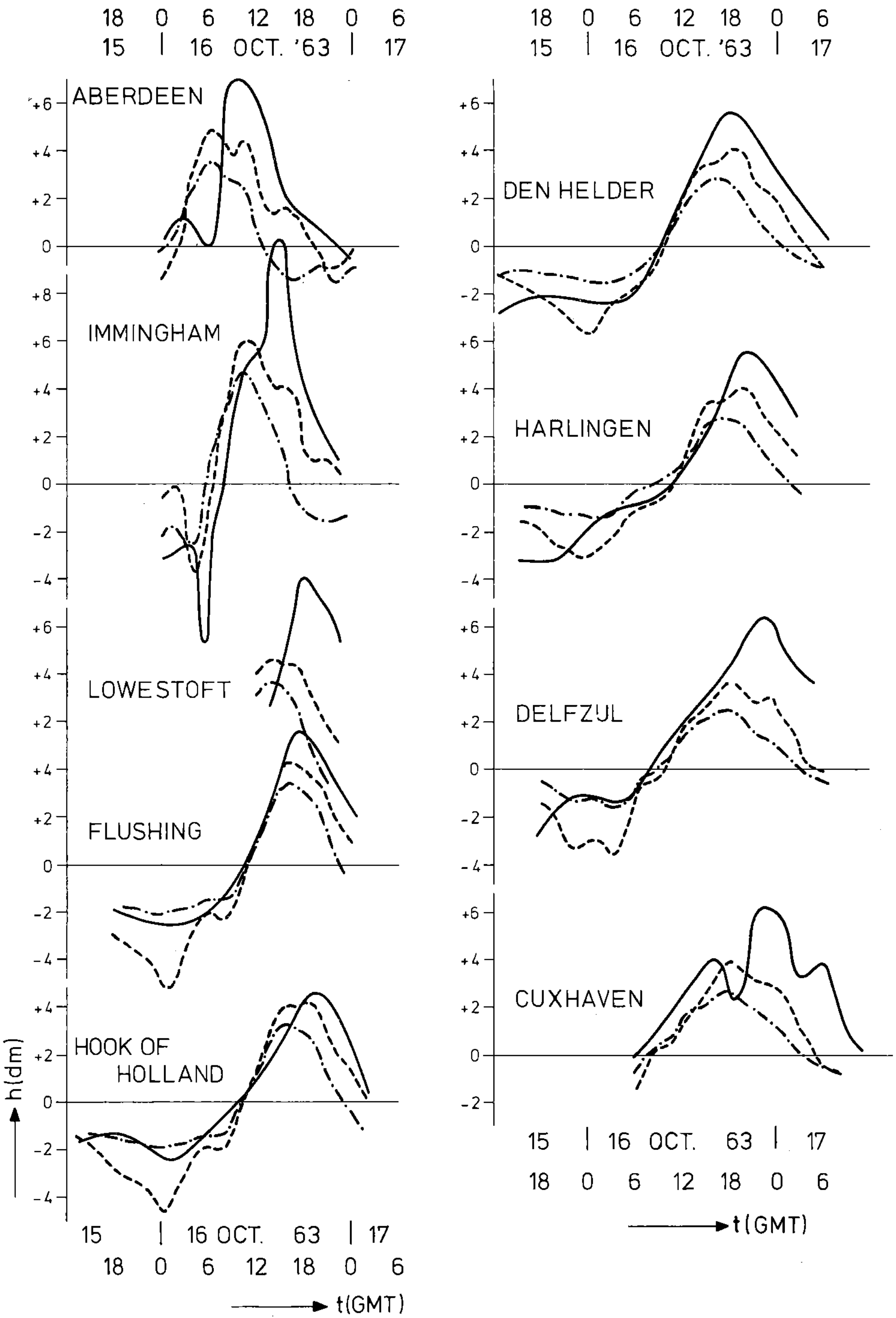
18 0 6 12 18 0 6
15 16 OCT. '63 17
ABERDEEN
IMMINGHAM
LOWESTOFT
FLUSHING
HOOK OF HOLLAND
DEN HELDER
HARLINGEN
DELFZIJL
CUXHAVEN
h(dm)
15 16 OCT. 63 17
18 0 6 12 18 0 6
t(GMT)

9.4.2 The external surge of 29 January 1974.

On 29 January 1974 the occurrence of an external surge was obvious. The weather maps (Fig. 9.4.2.1) showed a storm depression northwest of Scotland, while the wind over the North Sea remained southerly. In spite of these southerly winds a substantial rise of the water levels of about 6 dm took place along the British and Netherlands coasts. (See Fig. 9.4.2.2, solid curve.) The computed water levels given in this figure were produced by the extended model. In contrast with the preceding cases, the westerly gale over the shallow waters near Scotland was only of little importance. So the computed contribution of the wind field near Scotland did not exceed $1\frac{1}{2}$ dm. See Fig. 9.4.2.3. Therefore, this external surge must be ascribed mainly to the pressure effect, which during the first half of 29 January caused a semi-permanent rise of the water-level of about 4-7 dm along the whole northern boundary. See Fig. 9.4.2.4. Furthermore, Fig. 9.4.2.4 shows that the field of rising water levels is built up near Scotland and that this field is extending over the North Sea, not only along the English coast, but over a vast area.

Fig. 9.4.1.4 External surge of 15 to 17 October 1963 at Aberdeen, Immingham, Lowestoft, Flushing, Hook of Holland, Den Helder, Harlingen, Delfzijl, Cuxhaven, respectively.
—— residuals after removal of astronomical tide;
– – – surge, computed with extended model, including air pressure term;
– • – • – • – surge, computed without air pressure term.

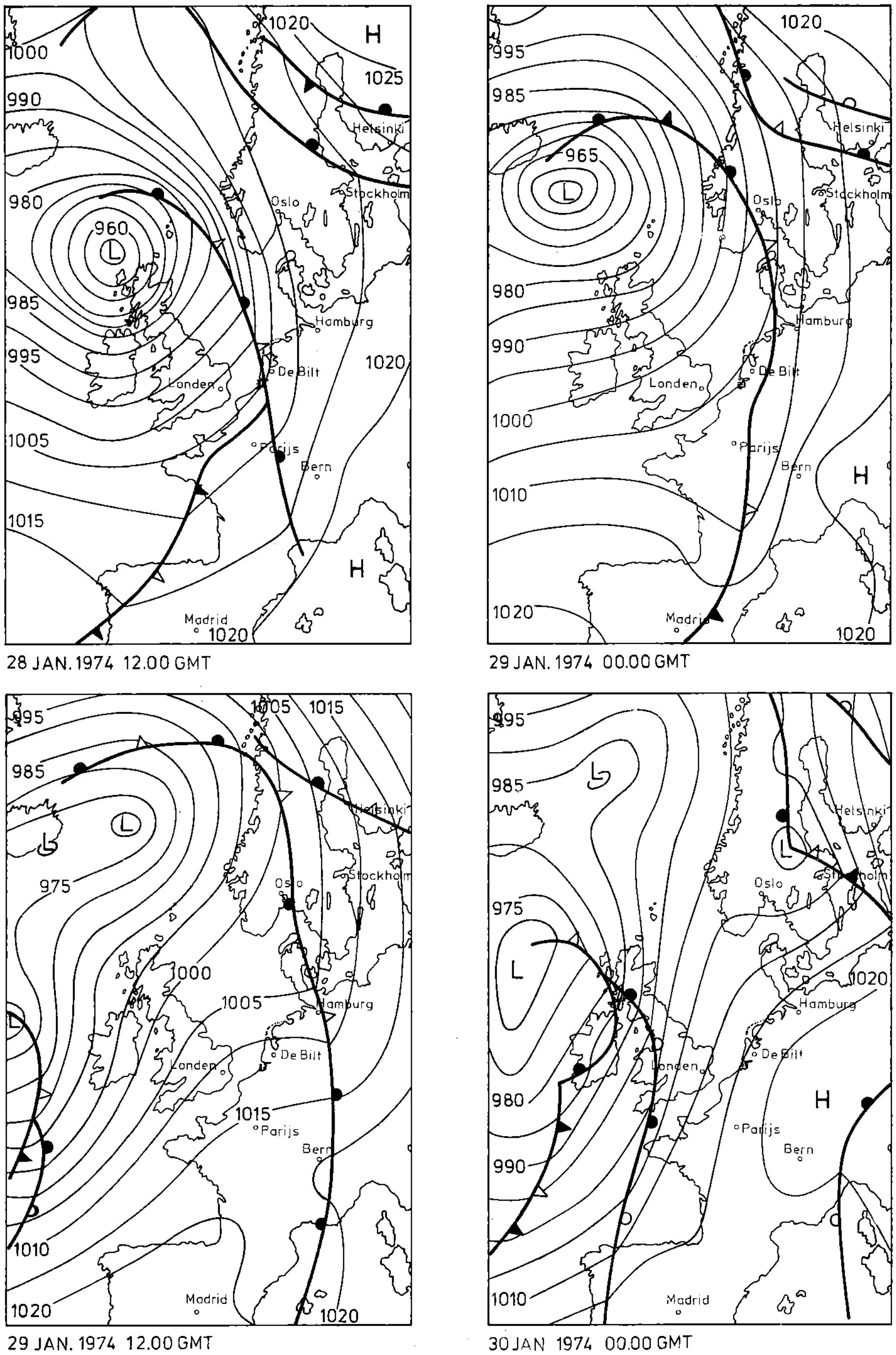

Fig. 9.4.2.1 Weather charts of 28 to 30 January 1974.

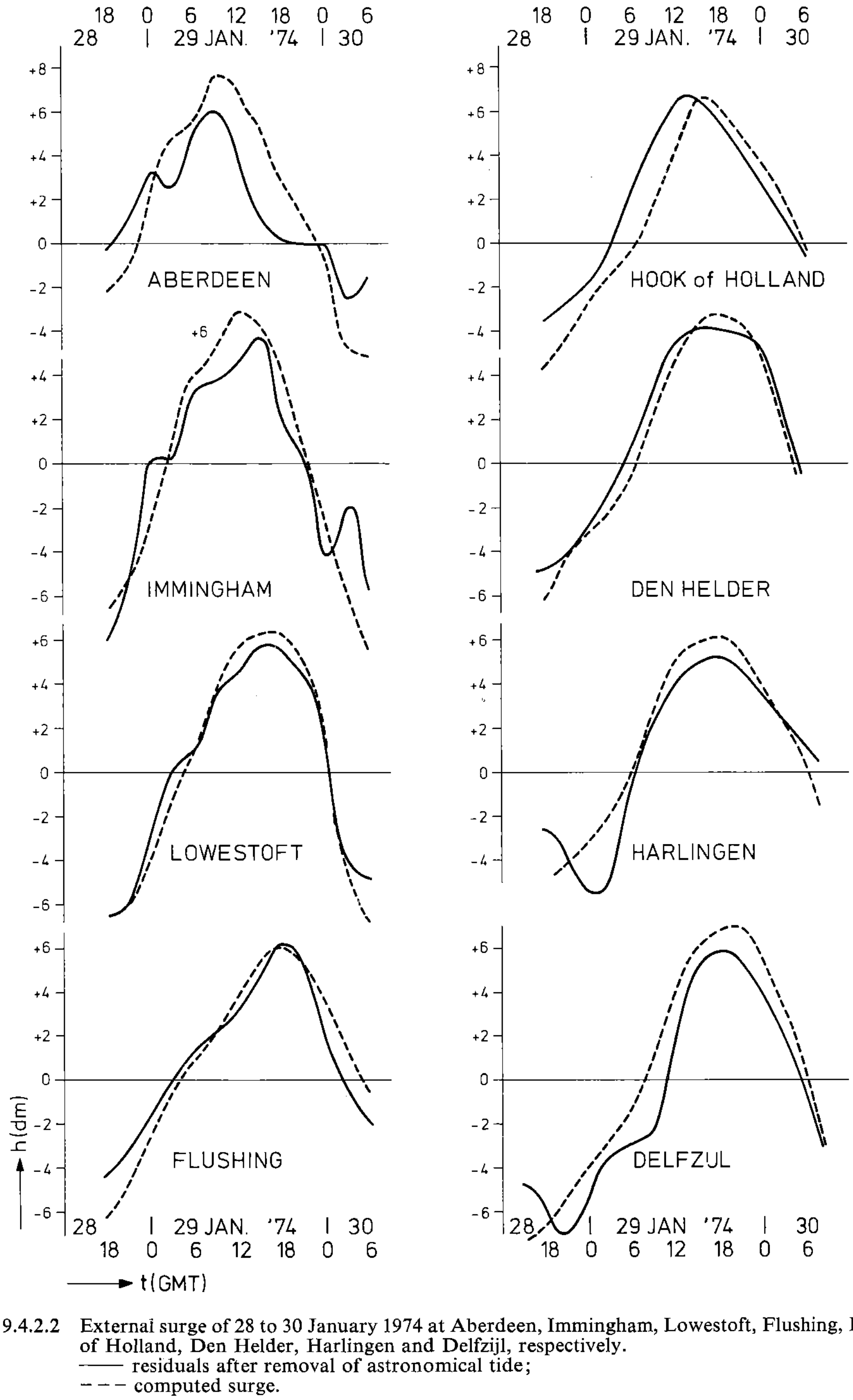

Fig. 9.4.2.2 External surge of 28 to 30 January 1974 at Aberdeen, Immingham, Lowestoft, Flushing, Hook of Holland, Den Helder, Harlingen and Delfzijl, respectively.
—— residuals after removal of astronomical tide;
– – – computed surge.

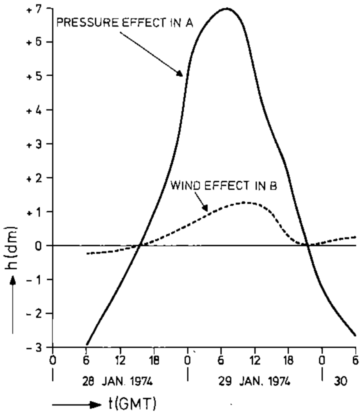

Fig. 9.4.2.3 Pressure effect in A and wind effect in B in the period 28 to 30 January 1974.

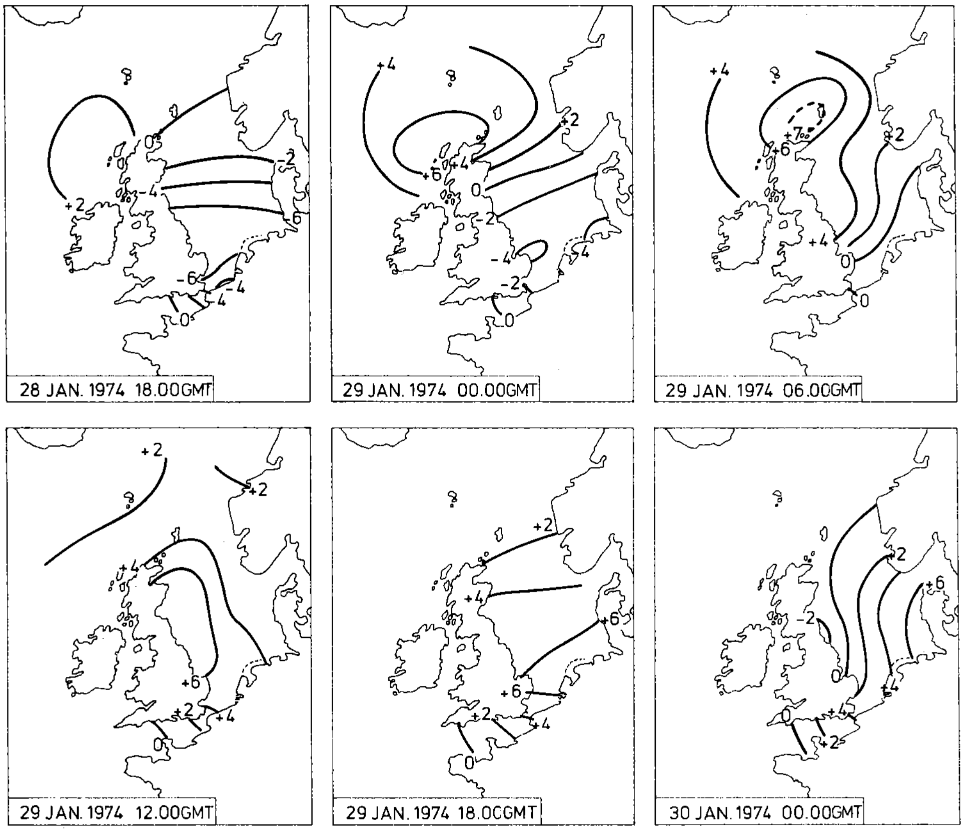

Fig. 9.4.2.4 Distribution of the meteorological effect in dm over the North Sea and adjacent areas in the period 28 to 30 January 1974.

9.4.3 The Hamburg surge of 16 February 1962.

The surge of 16 February 1962 brought about floods in the neighbourhood of Hamburg. In the German Bight the surge effect exceeded $3\frac{1}{2}$m. These levels were highly due to a severe northwesterly storm over the North Sea. See Fig. 9.4.3.1. Part of the surge, however, was connected with external effects, as will be shown later.

Hansen [1966] and Heaps [1969] investigated this surge. Hansen accounted for the external effect by using observations of the water level near the Orkney Islands and Bergen. Heaps moved the boundary of his computational grid in northerly direction, in order to compute the wind effects over the shallow sea area west of Scotland. However, the effect of the air pressure was neglected.

For this surge the pure effect of the air pressure by omitting the wind term was computed. Fig. 9.4.3.2 shows that in the period 15 February 18h00m till 17 February 06h00m the effect of air pressure is a permanent set-up of the water levels along the whole northern boundary of the North Sea. During the maximum effect of the surge in the area of the Frisian Islands and the German Bight, on 17 February 00h00m, the air pressure contributes about 4-5 dm to the set-up.

Fig. 9.4.3.3 shows the curves for Aberdeen and Bergen. Curve a gives values computed with the restricted model without pressure. Here, the boundary condition along the line Orkney Islands-Bergen is chosen as h=0. Curve b gives values computed with the improved KNMI-model with the term of air pressure. The observed values in Aberdeen and Bergen are approximated much better by curve b than by curve a. The Fig. 9.4.3.3 gives observed values and values computed with the recent model for Hook of Holland, Den Helder, Delfzijl and Cuxhaven. The observed and computed values agree to a high extent.

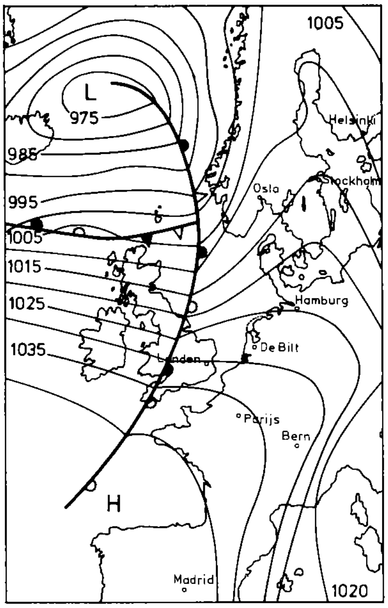

15 FEBR. 1962 12.00GMT

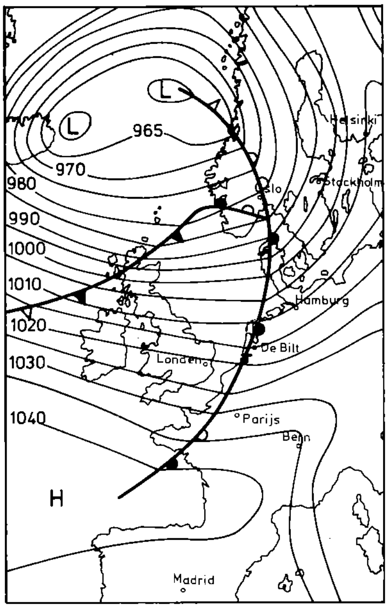

16 FEBR. 1962 00.00 GMT

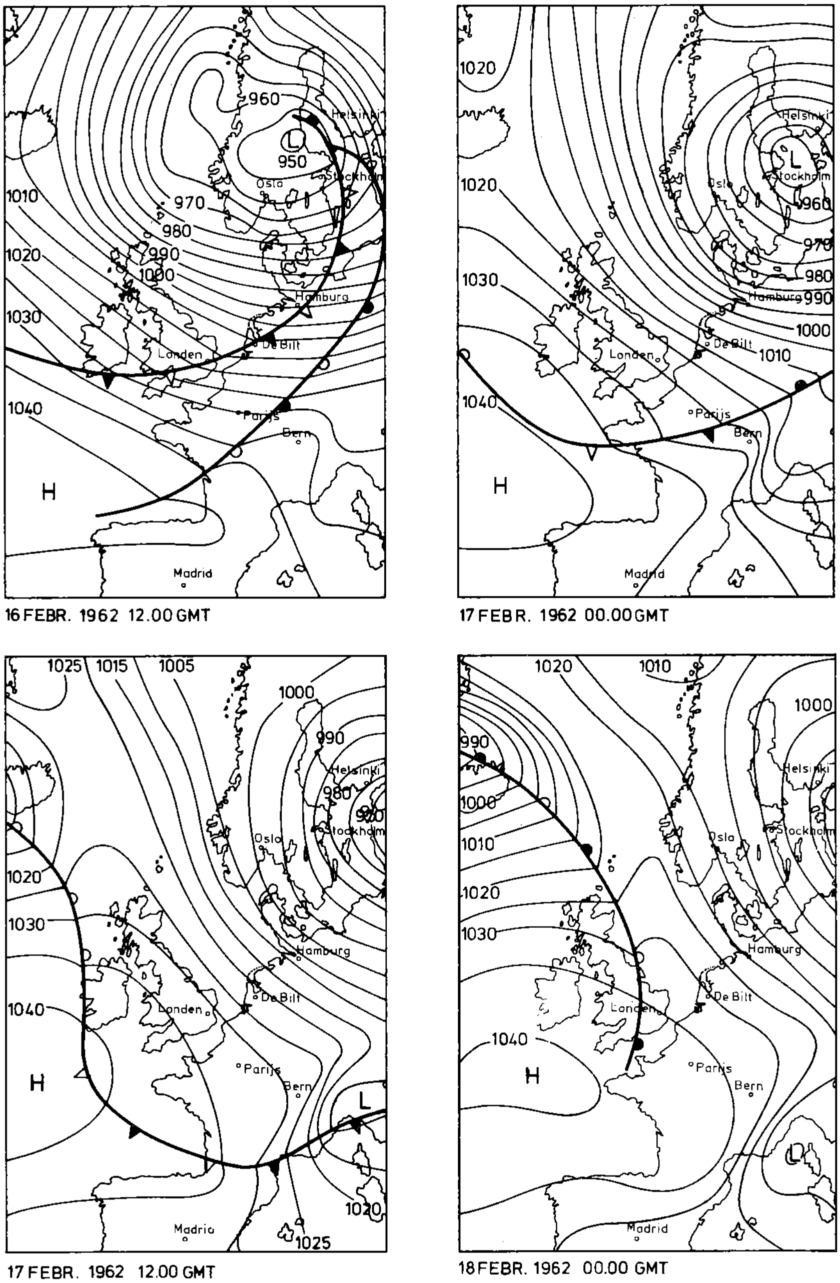

Fig. 9.4.3.1 Weather charts of 15 to 18 February 1962.

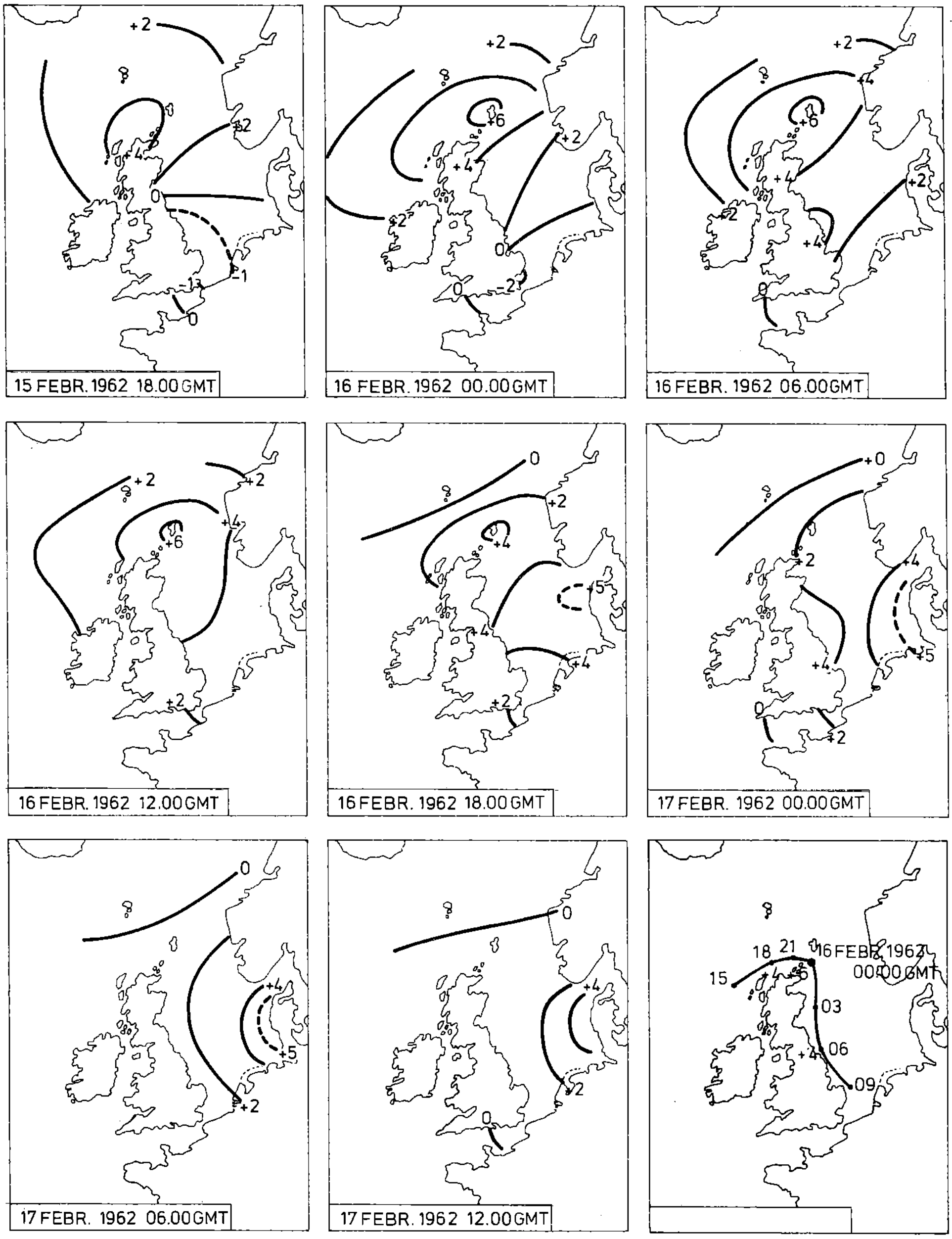

Fig. 9.4.3.2 Distribution of the air pressure effect in dm over the North Sea and adjacent areas in the period 15 to 17 February 1962.

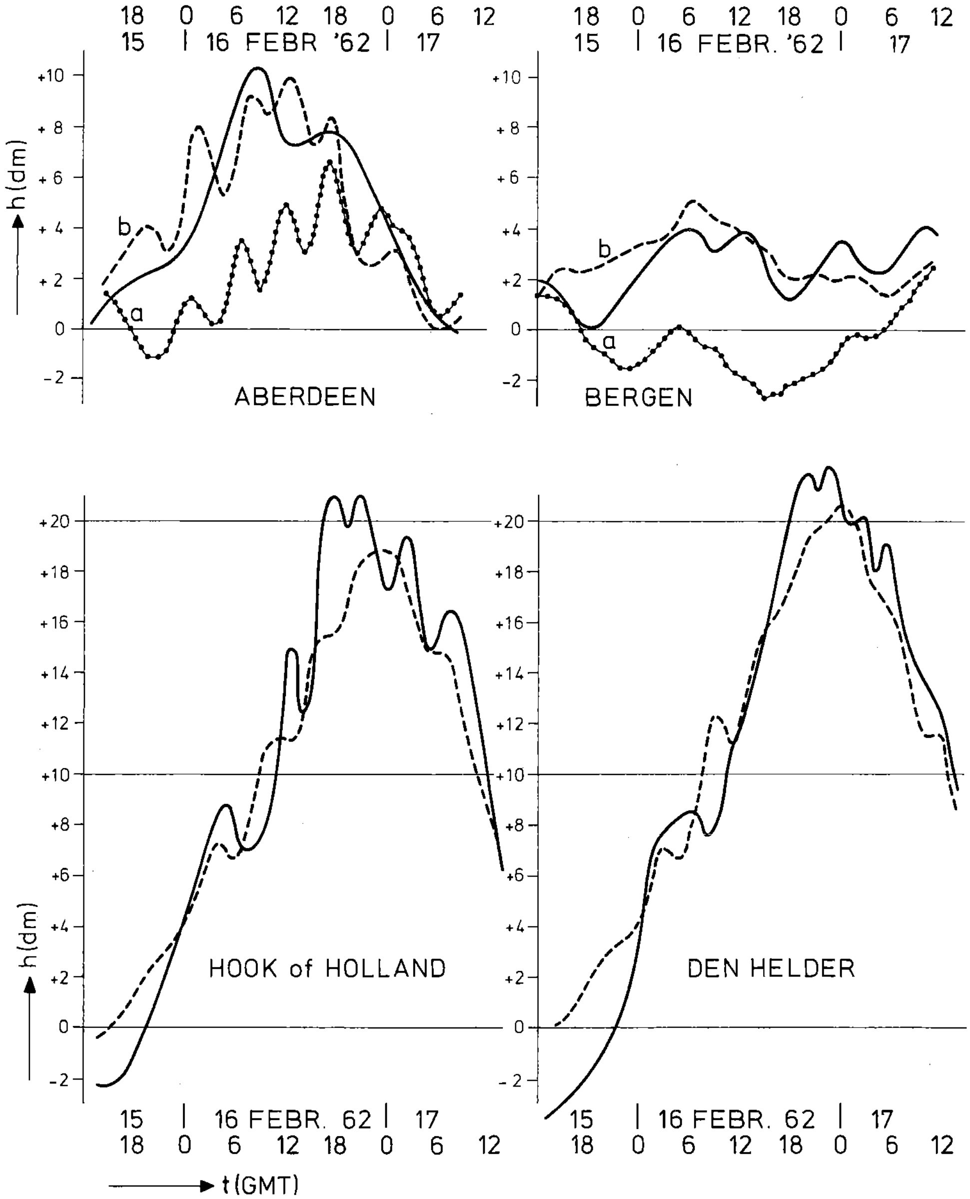

Fig. 9.4.3.3 Surge of 15 to 17 February 1962 at Aberdeen, Hook of Holland, Bergen, Den Helder, Delfzijl and Cuxhaven, respectively.
—— residuals after removal of astronomical tide;
– – – surge, computed with extended model, including air pressure term;
– • – • – • – surge, computed with restricted model, without air pressure term.

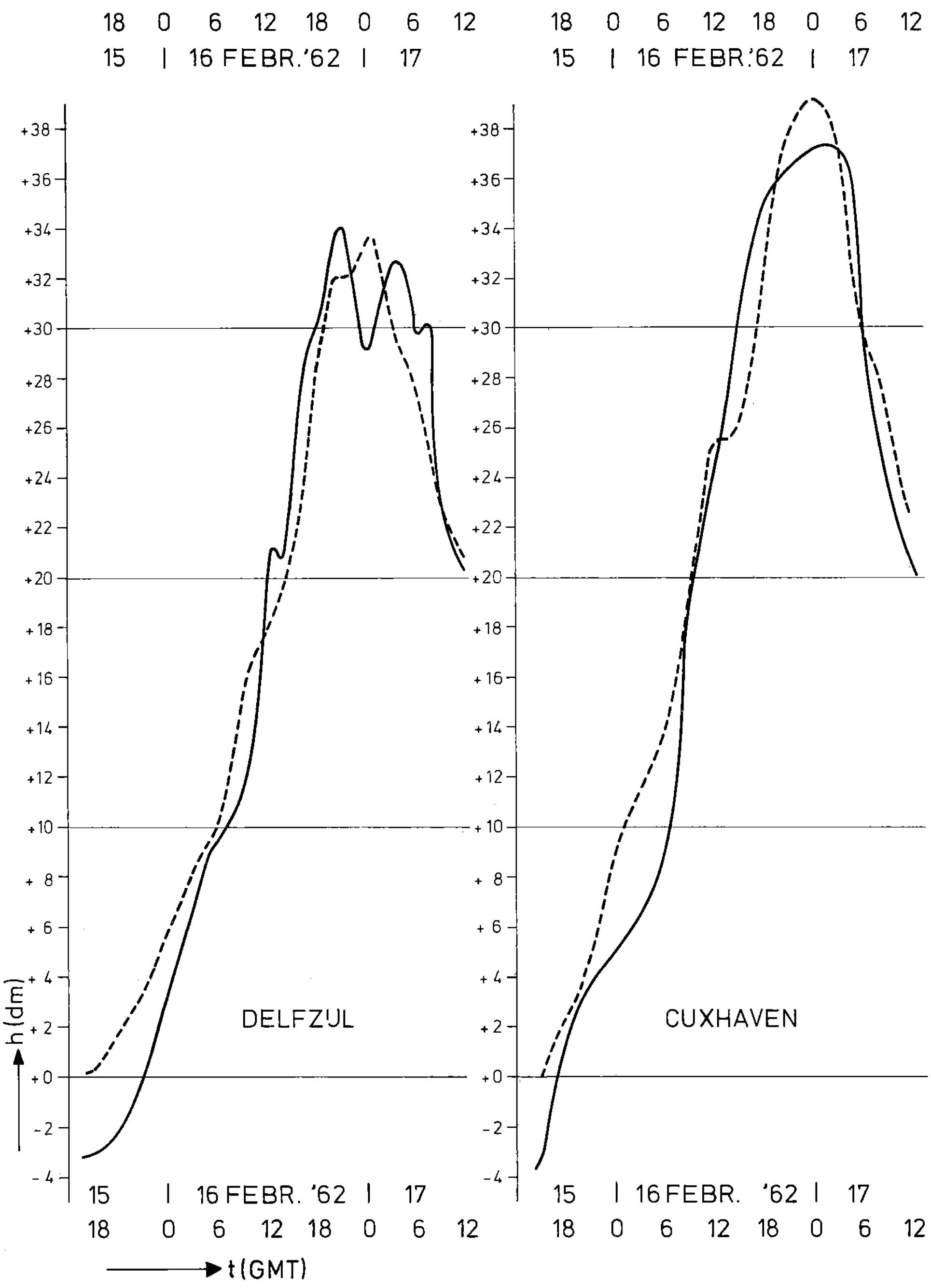
18 0 6 12 18 0 6 12
15 | 16 FEBR.'62 | 17
DELFZIJL
CUXHAVEN
h (dm)
+38
+36
+34
+32
+30
+28
+26
+24
+22
+20
+18
+16
+14
+12
+10
+8
+6
+4
+2
+0
-2
-4
15 | 16 FEBR. '62 | 17
18 0 6 12 18 0 6 12
t (GMT)

9.5 The surge of 1 February 1953.

The surge of 1 February 1953 is described in detail in the report of the Deltacommissie [1960]. The disaster was caused by a depression moving via the sea area between Iceland and Scotland over the North Sea in a southeasterly direction towards the German Bight. At the same time an anticyclone was moving east over the Atlantic Ocean towards the sea area west of Ireland. Between these two pressure systems a very severe northwesterly gale developed, which maintained itself for a rather long time. Wind velocities, averaged over 10 minutes, of about 70 knots from directions between NW and N were observed. Fig. 9.5.1 presents a number of weather charts from 31 January to 2 February 1953, while in Table 9.5.1 a survey is given of observed and computed winds in tenths of degrees, and in knots on the lightvessels Goeree, Texel and Terschellingerbank. The computation was carried out along the lines described in Chapter 7.

Table 9.5.1 generally shows a good agreement between the observed and computed winds as far as these stations are concerned. However, there is a tendency to too high observed values for the highest wind speeds, which may be caused by the conversion table of the Beaufortscale. See Chapter 7.

Table 9.5.1 Comparison between observed and computed winds (wind direction in tenths of degrees and wind speed in knots) on the lightvessels Goeree, Texel and Terschellingerbank.

		Goeree		Texel		Terschellingerb.	
		O	C	O	C	O	C
31 January	15h GMT	29/36	29/40	27/40	26/40	28/40	25/42
1953	18h GMT	29/48	28/48	28/56	28/43	27/56	28/36
	21h GMT	29/63	30/55	29/56	31/51	32/49	32/45
1 February	00h GMT	33/58	30/58	30/60	32/58	34/63	33/56
1953	03h GMT	32/55	31/59	30/62	32/59	34/63	33/57
	06h GMT	32/60	32/56	30/58	33/56	34/63	34/52
	09h GMT	34/57	34/49	—	—	35/55	35/47
	12h GMT	34/53	34/46	—	—	36/49	34/39
	15h GMT	34/44	34/44	—	—	36/40	35/40
	18h GMT	36/41	36/41	36/44	35/36	01/42	35/34
	21h GMT	35/40	34/38	36/24	35/35	02/29	36/32
2 February	00h GMT	36/40	35/36	36/21	35/37	02/25	34/36
1953	03h GMT	35/40	35/31	36/24	35/33	03/25	35/31
	06h GMT	02/39	34/24	01/27	35/25	02/25	35/25
	09h GMT	36/33	34/25	01/23	35/29	02/32	35/29

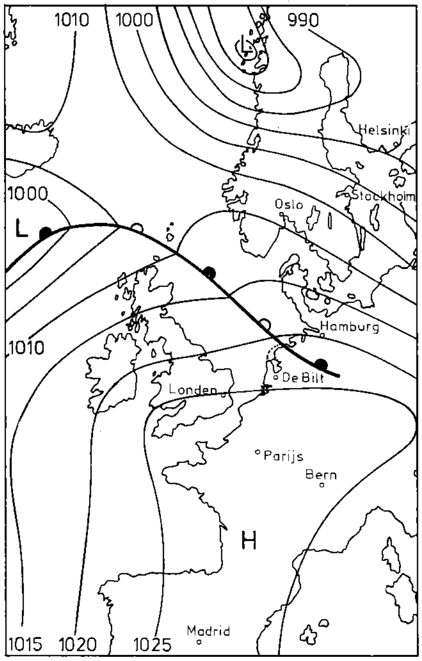

30 JAN. 1953 00.00 GMT

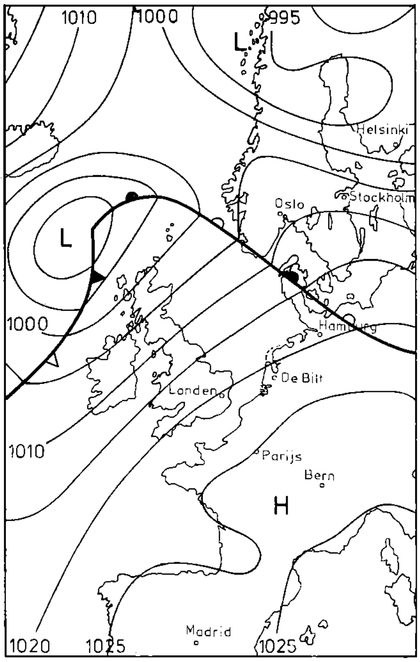

30 JAN. 1953 12.00 GMT

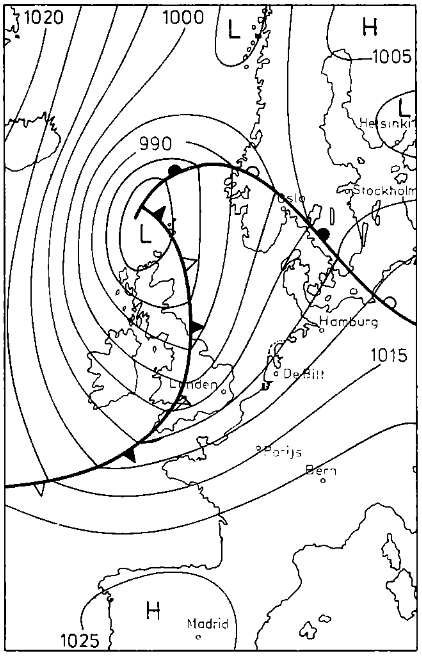

31 JAN. 1953 00.00 GMT

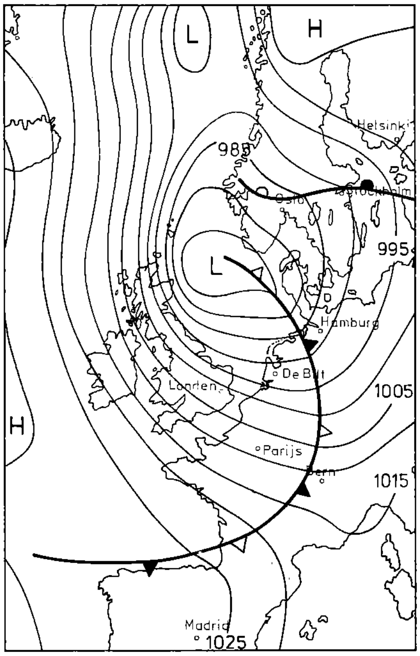

31 JAN. 1953 12.00 GMT

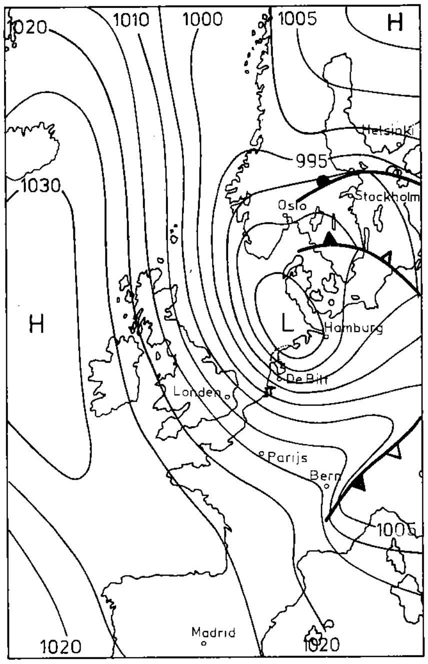

1 FEBR. 1953 00.00 GMT

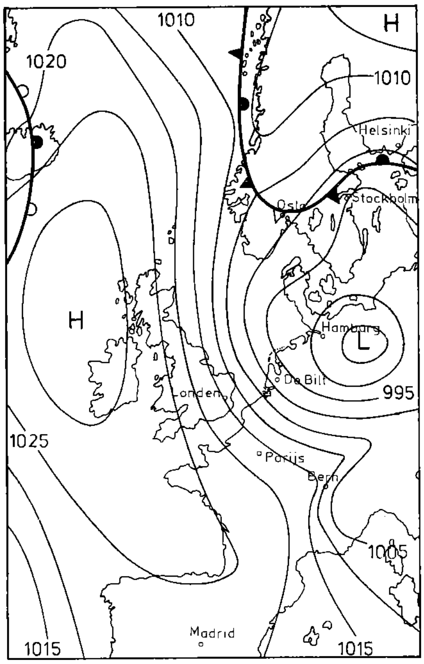

1 FEBR. 1953 12.00 GMT

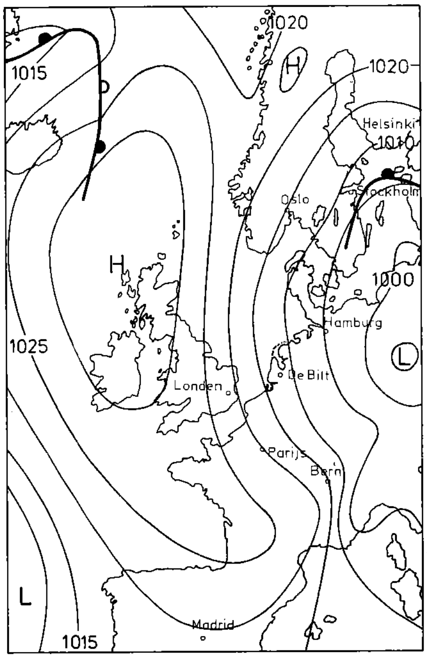

2 FEBR. 1953 00.00 GMT

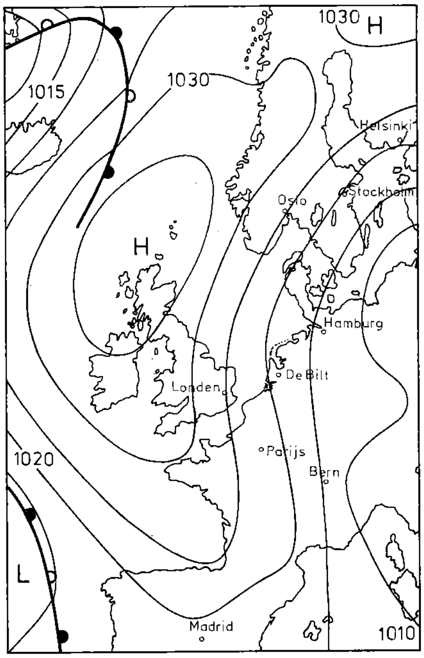

2 FEBR. 1953 12.00 GMT

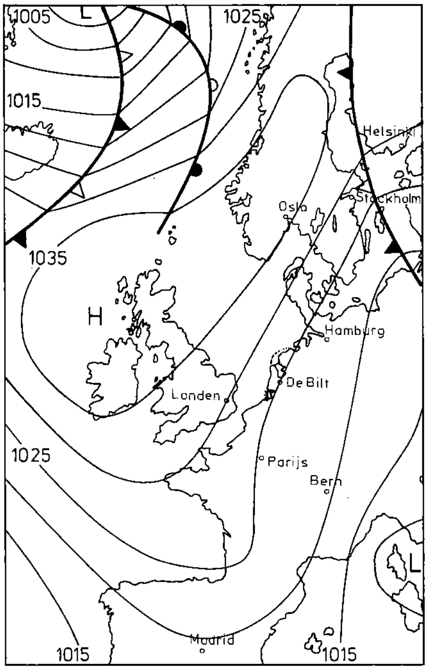

Fig. 9.5.1 Weather charts of 30 January to 3 February 1953.

The field of the water-levels over the North Sea is analyzed with the aid of observed values of the meteorological effect of several stations around the North Sea. See Fig. 9.5.2. This means that the 'observed' pattern, indicated by the solid lines, has to be considered with some caution, as the analysis is based on observations of coastal stations only. Fig. 9.5.2 also shows an analysis of the water-levels computed with the extended model II. The observed and the computed values both clearly demonstrate that the surge is generated within the North Sea area.

Fig. 9.5.3 gives the observed and computed water-levels of Flushing, Hook of Holland and Delfzijl. The observed maximum set-up at Flushing and Hook of Holland amounted to 31 and 33 dm respectively. The computed maximum set-up was 33 dm at both stations. At Delfzijl the observed and computed maximum values were 30 dm and 26 dm respectively. Considering Fig. 9.5.3, the observed maximum set-up at Delfzijl, which occurred during low tide, seems to be too high. Furthermore, the increasing branch of the surge is computed more accurately than the decreasing branch. From Fig. 9.5.2 it appears that during the afternoon of 1 February 1953 the computed set-up is about 5 dm higher than the observed one. Along the coast the agreement between the computed and observed values is in general fairly satisfactory.

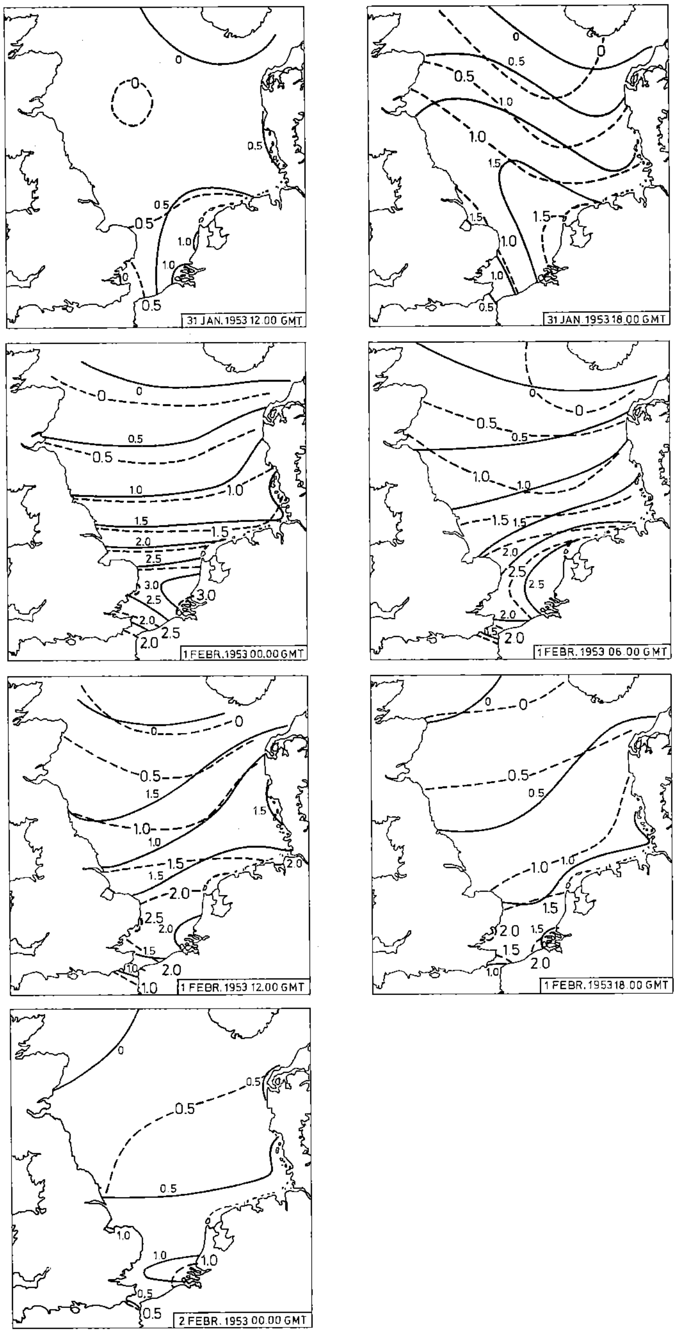

Fig. 9.5.2 Distribution of analyzed (——) and computed (– – –) meteorological effect in m over the North Sea in the period 31 January to 2 February 1953.

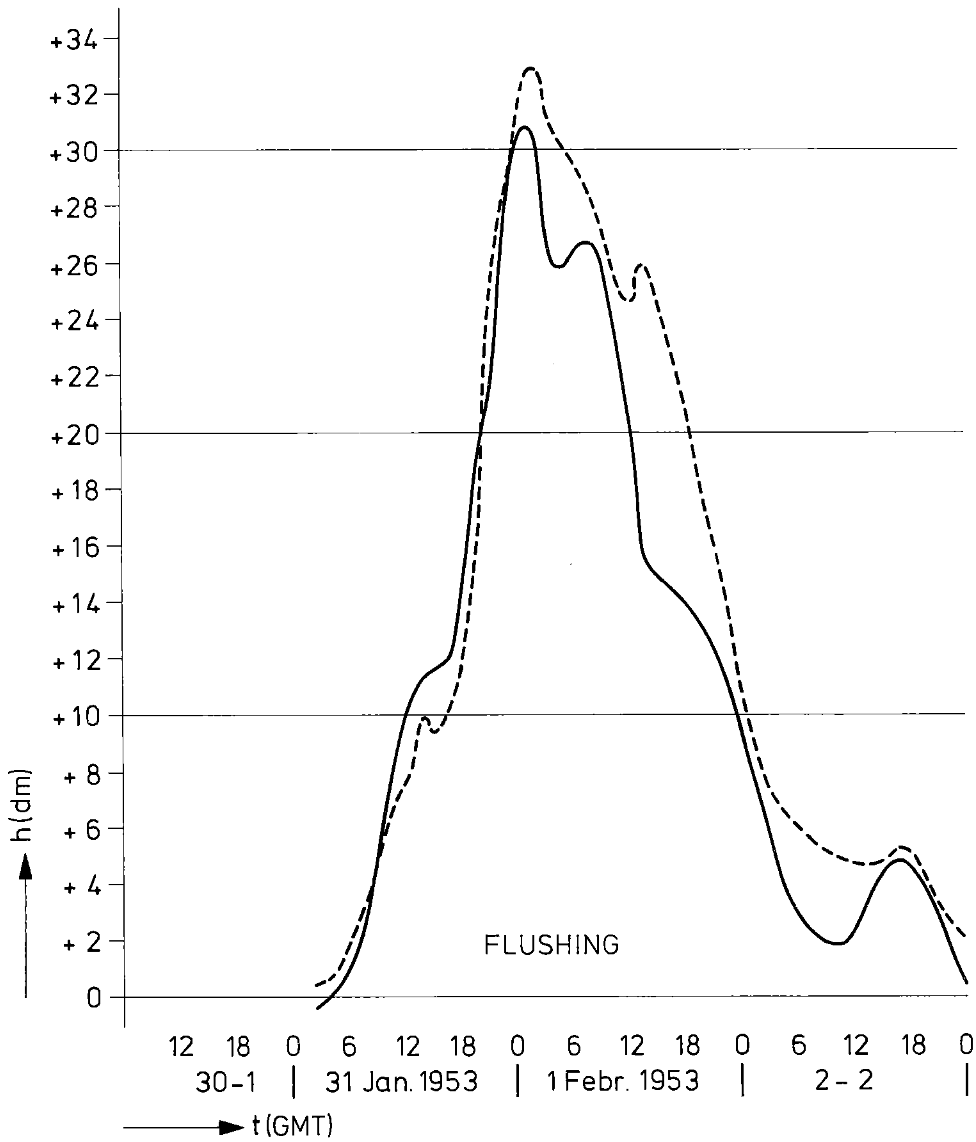

For legend see page 83

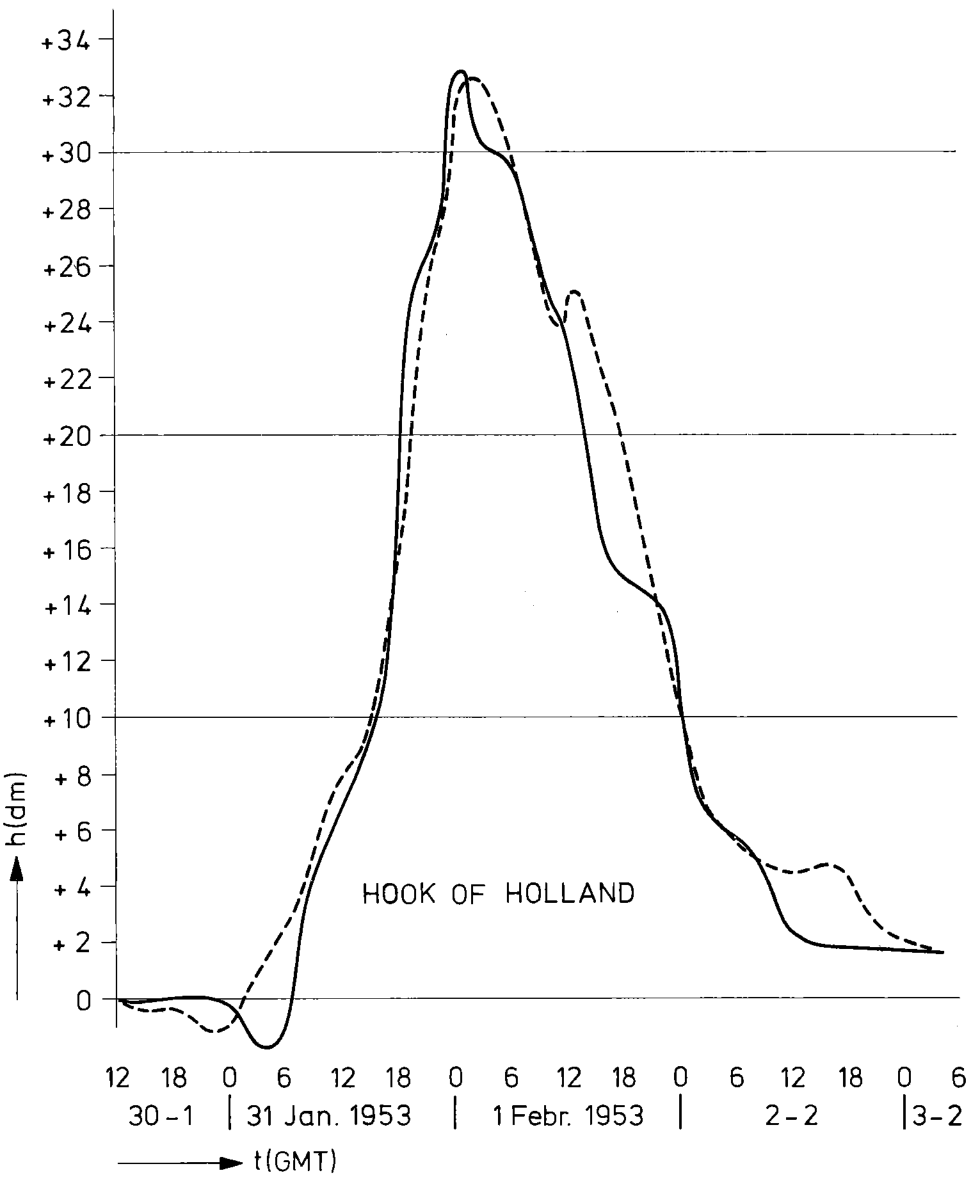
+34
+32
+30
+28
+26
+24
+22
+20
+18
+16
+14
+12
+10
+8
+6
+4
+2
0
h(dm)
HOOK OF HOLLAND
12 18 0 6 12 18 0 6 12 18 0 6 12 18 0 6
30-1
31 Jan. 1953
1 Febr. 1953
2-2
3-2
t(GMT)

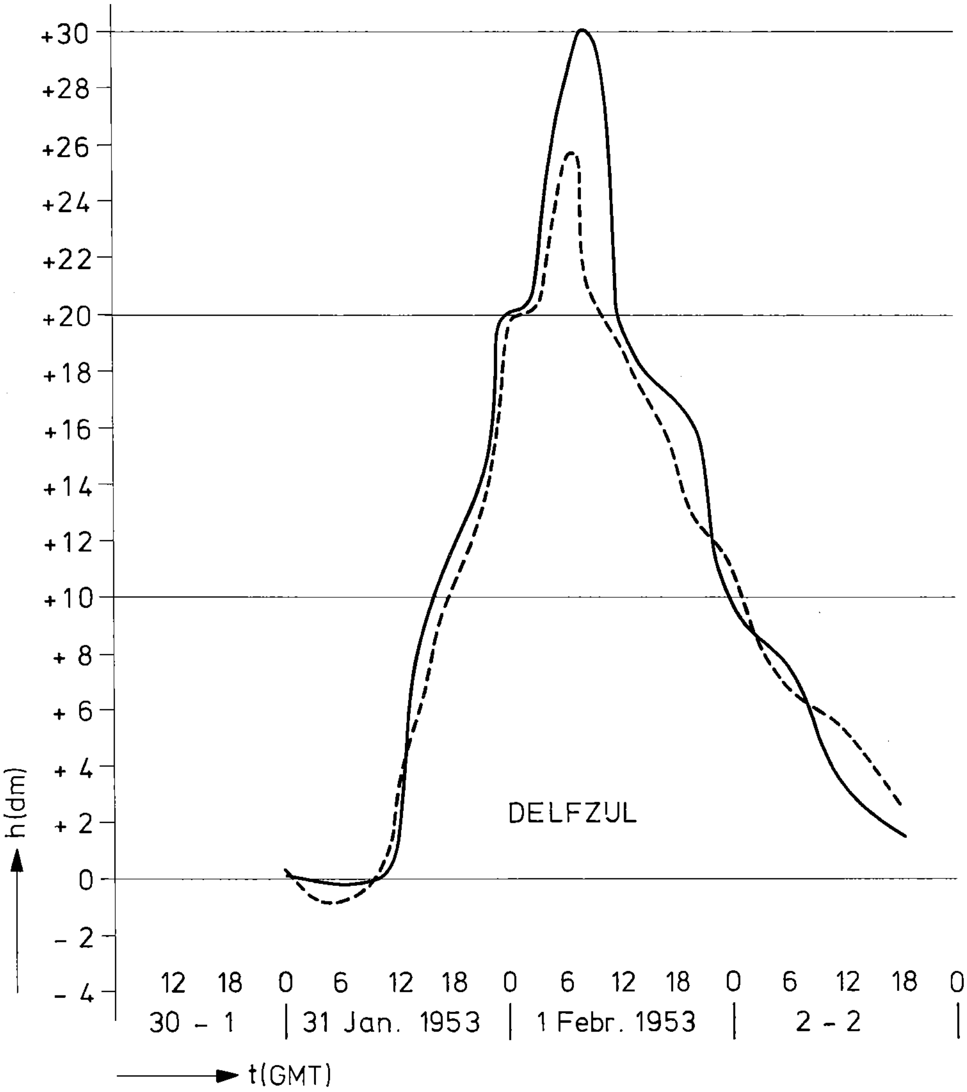

Fig. 9.5.3 Surge of 30 January to 2 February 1953 at Flushing, Hook of Holland and Delfzijl, respectively.
—— residuals after removal of astronomical tide;
– – – surge, computed with extended model, including air pressure term.

9.6 The meteorological effect in the period of 17-22 January 1960.

The period of 17 January to 22 January 1960 was a period favourable for testing a hydrodynamical model under rapidly changing meteorological conditions.

On 17 January the winds on the North Sea were weak at first, but a small depression moving over southern Scandinavia in a southeasterly direction caused a northwesterly windfield of 7-8 Beaufort later on. On 18 January a second depression moved via Scotland and the northern part of the North Sea to the east. The wind on the southern part of the North Sea freshened again to wind force 7-8 from the west. Afterwards the winds weakened again, but on 19 and 20 January a very deep storm depression developed over the North Sea, moving southeastwards towards northern Germany. The northwesterly gale increased to wind force 10-12. On 21 January the winds were weak again, but on 22 January the winds increased from a southerly direction to wind force 8-10. See Fig. 9.6.1. So during this period the winds over the North Sea were very variable in direction as well as in force. Table 9.6.1 gives a survey of the observed and computed winds, respectively O and C, on the lightvessels Noord-Hinder, Goeree, Texel and Terschellingerbank.

Table 9.6.1 shows that on 22 January 1960 the computed southerly winds are too high compared with the observed values. However, bearing in mind the standard deviation of the differences between observed and computed winds mentioned in Table 7.2.1, it can be stated that there is a good agreement between observation and computation.

The observed and computed deviations of the water-levels for the five main stations throughout the period 17-22 January 1960 can be compared in Fig. 9.6.2. The magnitude of the differences between the two types of values could be expected, since in Table 9.1.1.2 the standard deviation of these differences is given. The agreement between observed and computed set-up is fairly good, particularly during the surge of 20 January 1960 caused by the deep storm depression over the North Sea. This depression gave rise to an inhomogeneous and non-stationary wind field. Owing to these circumstances the results of the operational tables indicated in Fig. 9.6.2 is a little less satisfying. The wind fields were taken from Timmerman [1965, Annex to Verslagen V-174]. The positive surge is immediately followed by a negative surge, which is reproduced in a reasonable way.

Furthermore, it can be remarked that the computations remained stable throughout the whole period.

Table 9.6.1 Verification of the wind computation in the period 17-22 January 1960.
O = observed wind; C = computed wind; direction in tenths of degrees, wind speed in knots.

	Noord-Hinder		Goeree		Texel		Terschellingerb.	
	O	C	O	C	O	C	O	C
17 January '60								
03 GMT	02/11	01/12	09/19	01/09	08/08	36/11	04/07	36/09
06 GMT	04/11	35/10	11/13	33/06	14/13	22/05	21/08	19/10
09 GMT	16/01	30/06	23/12	27/07	21/10	24/17	20/12	22/25
12 GMT	29/09	28/15	22/18	25/16	24/22	25/24	22/20	24/27
15 GMT	29/10	27/18	28/19	27/19	27/22	28/25	27/20	27/28
18 GMT	29/15	28/15	29/20	27/15	30/19	28/18	33/20	28/22
21 GMT	29/17	27/16	27/18	27/19	30/14	28/19	33/15	29/22
18 January '60								
00 GMT	30/18	27/16	30/18	27/16	29/14	28/18	30/13	28/19
03 GMT	29/15	26/18	29/18	26/18	29/16	28/17	28/15	28/16
06 GMT	27/16	26/20	27/20	26/18	28/18	25/15	27/18	24/14
09 GMT	26/17	24/21	24/22	24/22	24/19	24/23	24/19	23/24
12 GMT	27/23	25/24	25/25	24/25	24/23	24/27	25/20	24/30
15 GMT	25/24	24/25	25/25	24/27	25/28	24/32	25/29	24/36
18 GMT	25/28	25/22	25/28	25/23	26/35	24/31	26/29	25/38
21 GMT	25/30	24/31	25/30	23/34	26/33	24/38	26/32	25/38
19 January '60								
00 GMT	25/32	24/26	26/33	25/29	26/34	25/31	26/32	26/31
03 GMT	24/27	24/25	25/22	24/28	26/30	25/26	26/25	26/23
06 GMT	24/21	23/25	23/25	24/25	26/26	25/18	26/25	25/14
09 GMT	22/20	22/24	24/23	23/23	23/17	22/20	23/13	21/17
12 GMT	24/29	22/28	23/33	22/28	22/20	22/22	21/15	22/19
15 GMT	22/29	22/28	21/28	21/27	—	—	21/26	20/28
18 GMT	22/35	22/36	21/36	21/37	20/39	20/42	21/33	20/40
21 GMT	22/40	25/27	20/40	23/29	20/46	21/34	21/40	20/40
20 January '60								
00 GMT	28/40	28/36	28/40	27/38	27/46	25/47	27/30	23/48
03 GMT	28/40	27/43	27/46	26/47	—	—	27/52	26/49
06 GMT	29/47	28/55	28/55	28/55	27/56	29/47	27/55	28/39
09 GMT	29/50	29/52	30/55	29/57	31/58	31/58	32/54	31/53
12 GMT	29/52	30/37	31/55	31/48	31/56	32/52	33/54	33/51
15 GMT	28/38	31/25	31/44	32/36	—	—	34/47	34/47
18 GMT	29/19	29/15	32/32	31/24	34/40	33/28	34/35	34/32
21 GMT	28/10	28/10	32/15	30/18	34/32	31/19	34/30	32/20
21 January '60								
00 GMT	25/01	07/02	34/02	31/08	01/08	29/13	34/19	29/13
03 GMT	18/08	14/12	13/06	16/04	36/05	30/08	36/08	30/11
06 GMT	18/17	16/15	18/08	14/08	15/06	11/01	09/06	02/01
09 GMT	16/19	16/17	15/14	15/13	15/12	14/11	14/09	14/10
12 GMT	16/19	18/14	16/18	16/14	17/17	14/15	14/10	14/14
15 GMT	16/17	18/16	16/18	16/17	16/18	15/21	16/12	15/21
18 GMT	21/09	20/20	16/18	18/20	16/21	16/24	16/16	16/26
21 GMT	19/07	21/20	20/16	20/18	17/20	17/23	16/19	16/26
22 January '60								
00 GMT	20/12	21/24	18/14	20/23	17/19	19/26	16/19	18/27
03 GMT	20/13	21/23	20/16	20/25	20/18	20/18	18/19	20/28
06 GMT	20/09	21/24	20/18	21/23	20/22	20/23	18/17	20/24
09 GMT	21/09	21/26	20/18	21/24	20/19	21/24	20/16	21/24
12 GMT	21/08	21/22	20/18	21/20	20/19	20/20	19/15	20/21
15 GMT	16/13	20/24	17/18	20/24	20/18	20/23	20/16	20/25
18 GMT	20/15	20/24	18/18	20/24	20/23	20/23	20/16	20/23

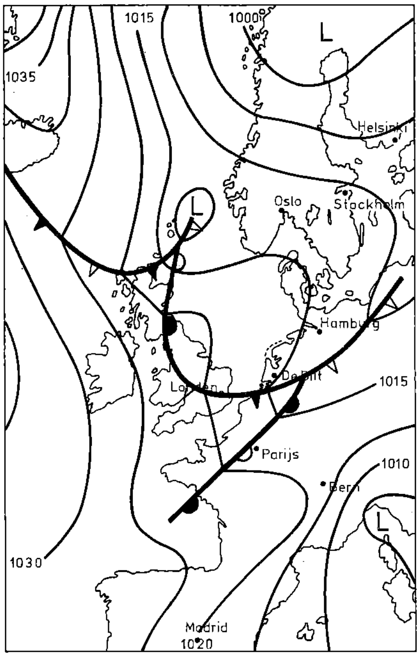

17 JAN. 1960 00.00 GMT

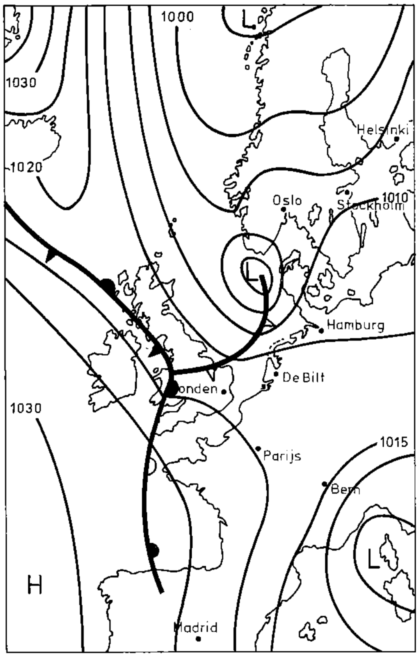

17 JAN. 1960 12.00 GMT

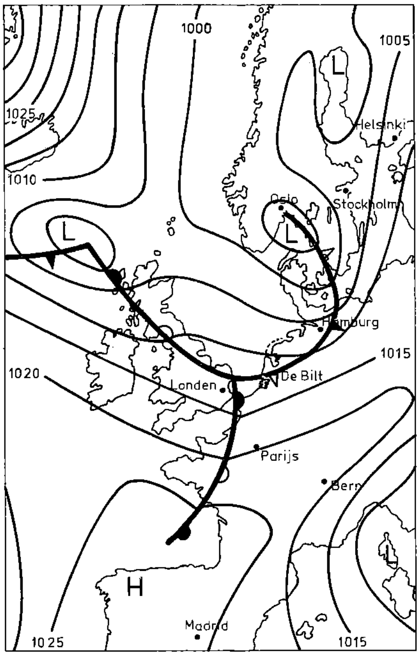

18 JAN. 1960 00.00 GMT

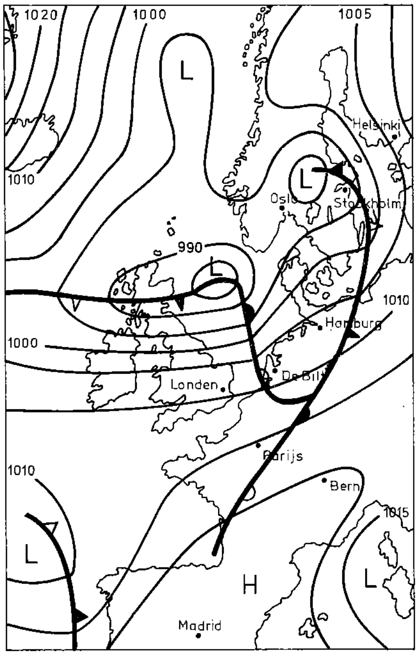

18 JAN. 1960 12.00 GMT

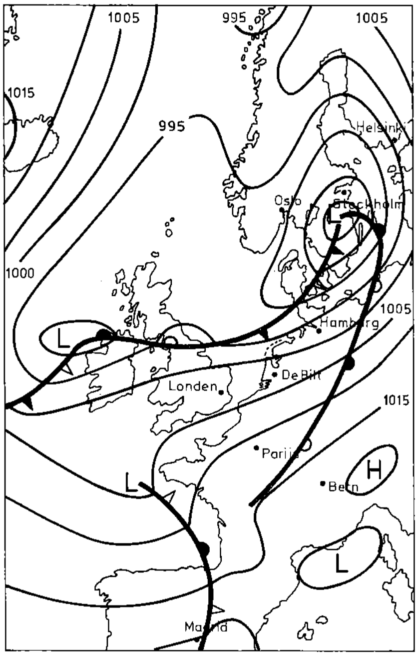

19 JAN. 1960 00.00 GMT

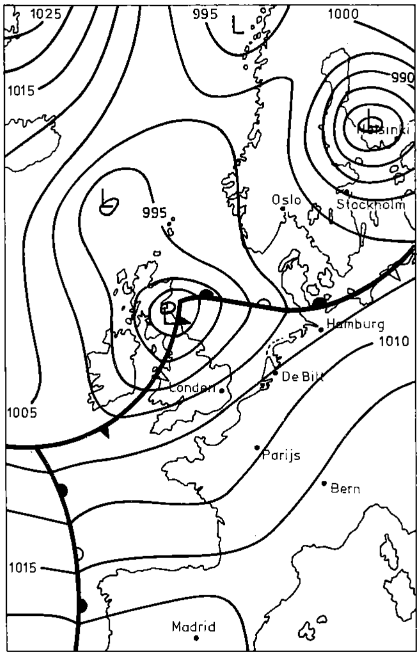

19 JAN. 1960 12.00 GMT

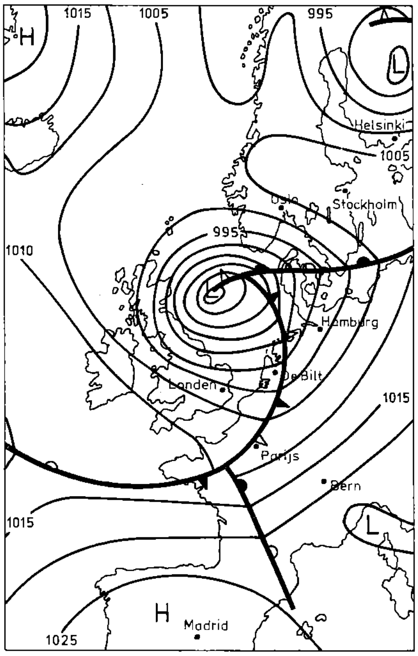

20 JAN. 1960 00.00 GMT

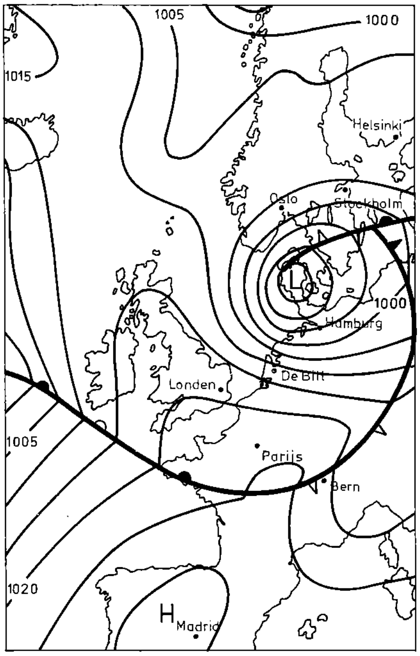

20 JAN. 1960 12.00 GMT

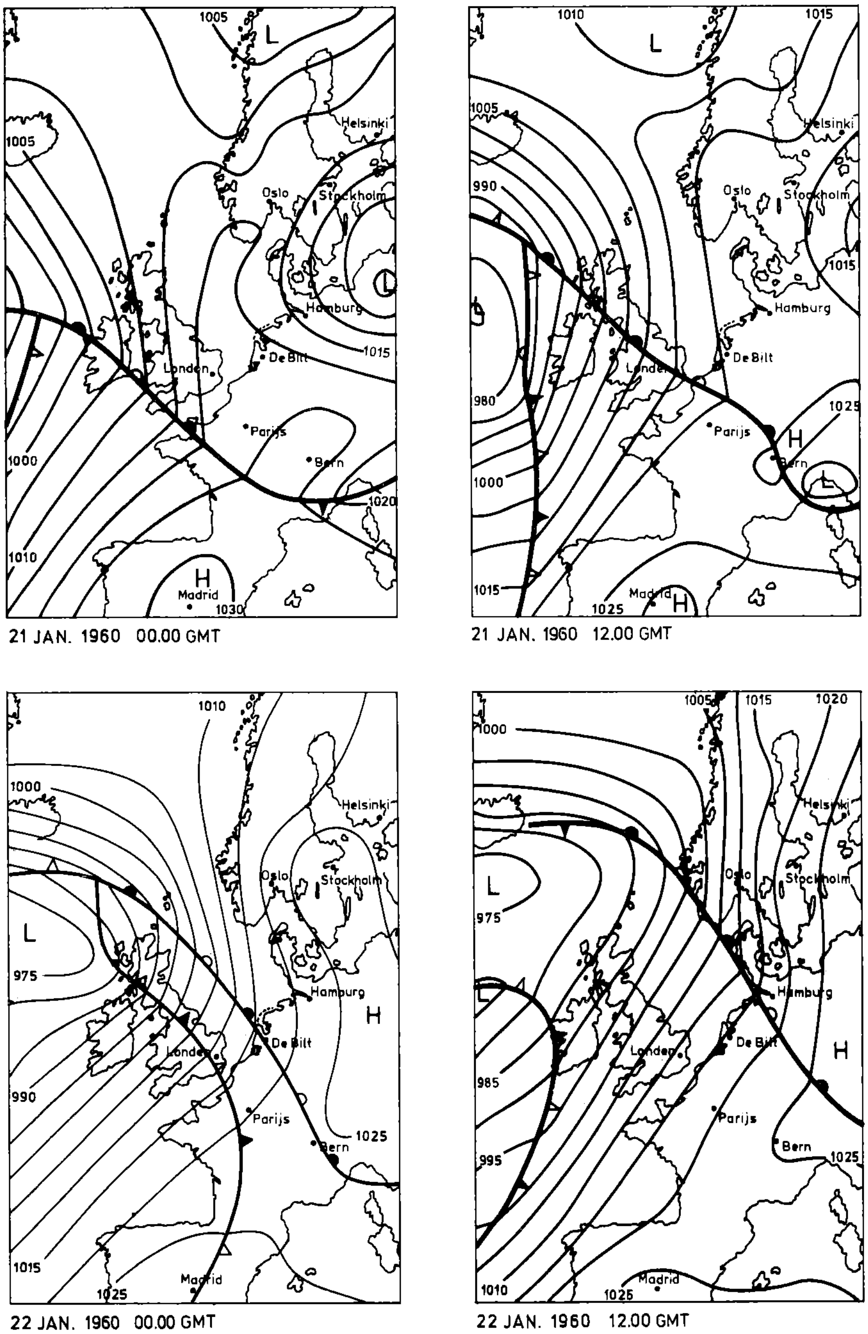

Fig. 9.6.1 Weather charts of 17 to 22 January 1960.

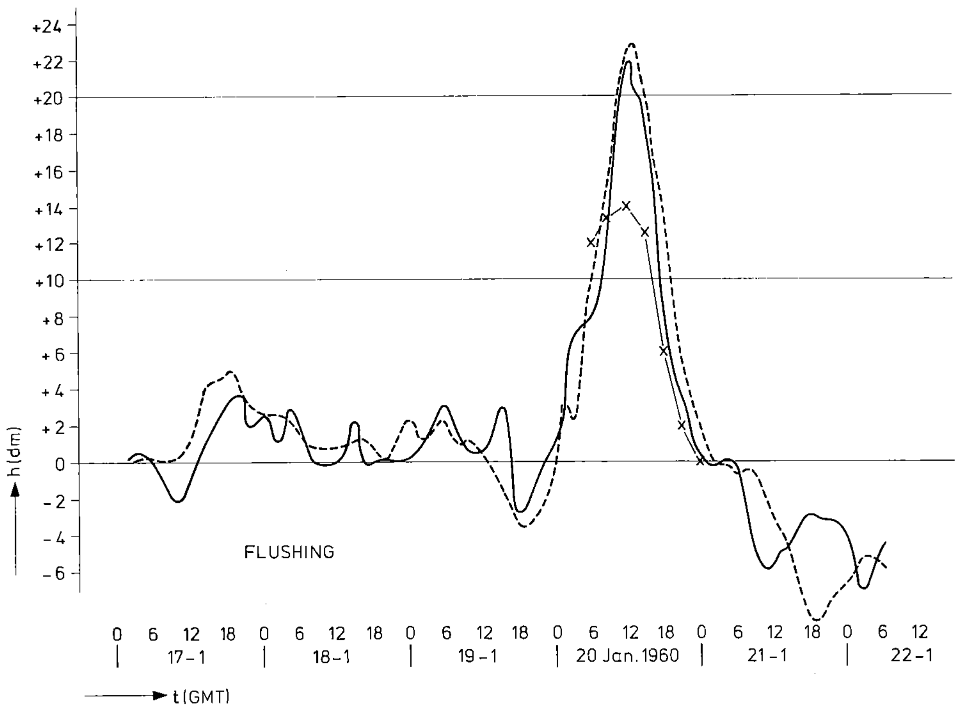

For legend see page 93

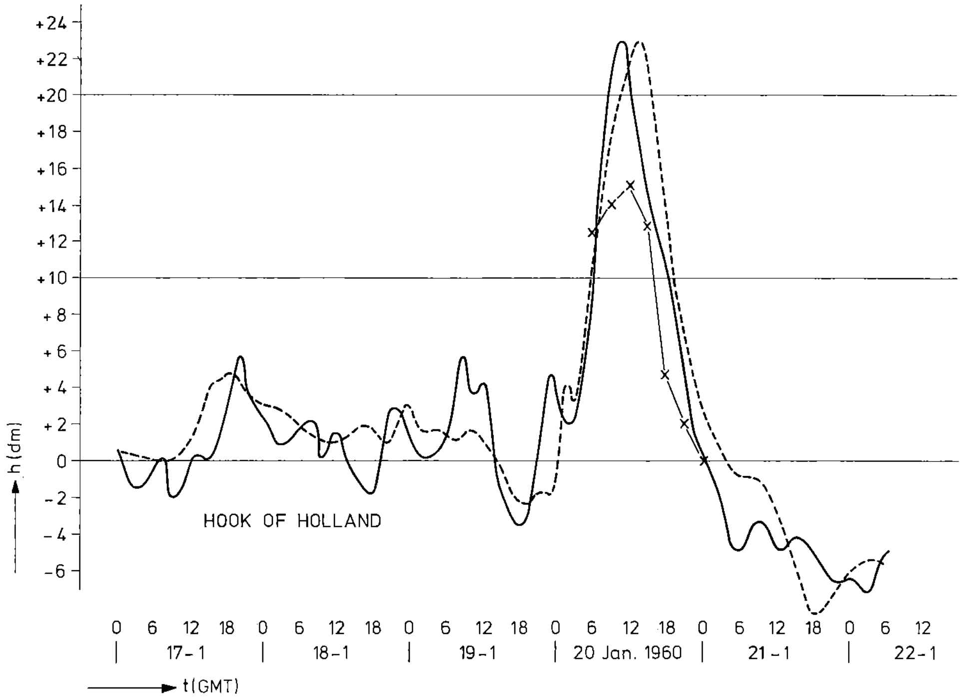

For legend see page 93

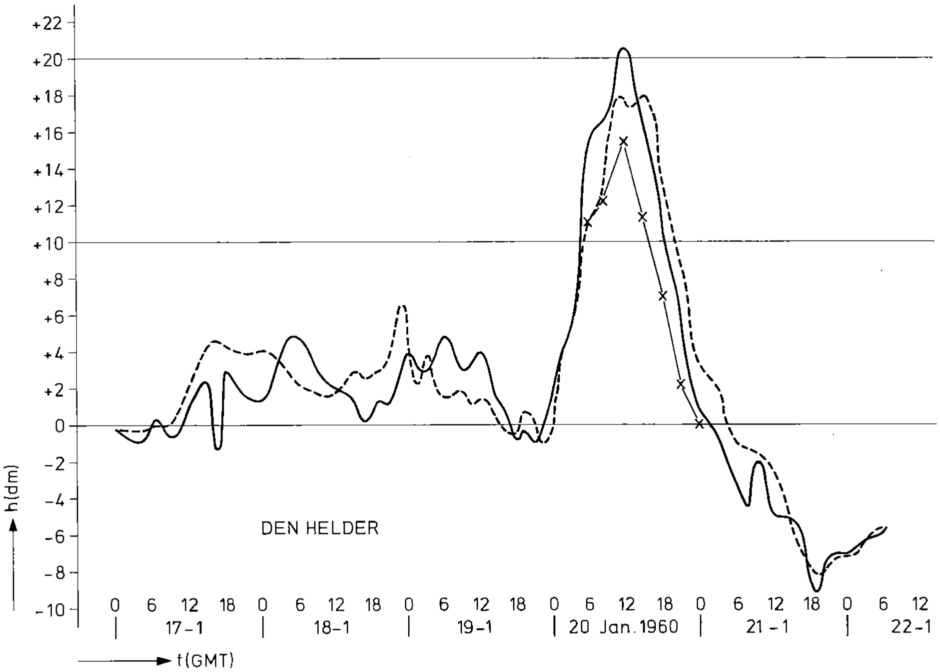

For legend see page 93

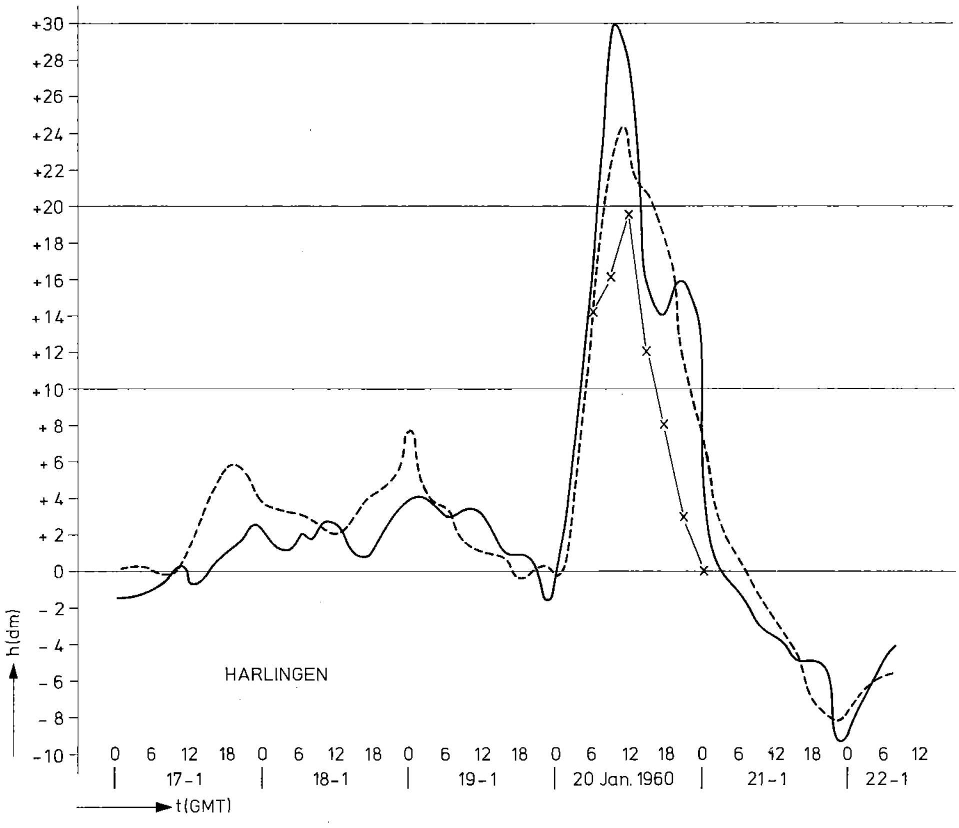

+30
+28
+26
+24
+22
+20
+18
+16
+14
+12
+10
+ 8
+ 6
+ 4
+ 2
0
- 2
- 4
- 6
- 8
-10
h(dm)
HARLINGEN
0 6 12 18 0 6 12 18 0 6 12 18 0 6 12 18 0 6 12 18 0 6 12
17-1
18-1
19-1
20 Jan. 1960
21-1
22-1
t(GMT)

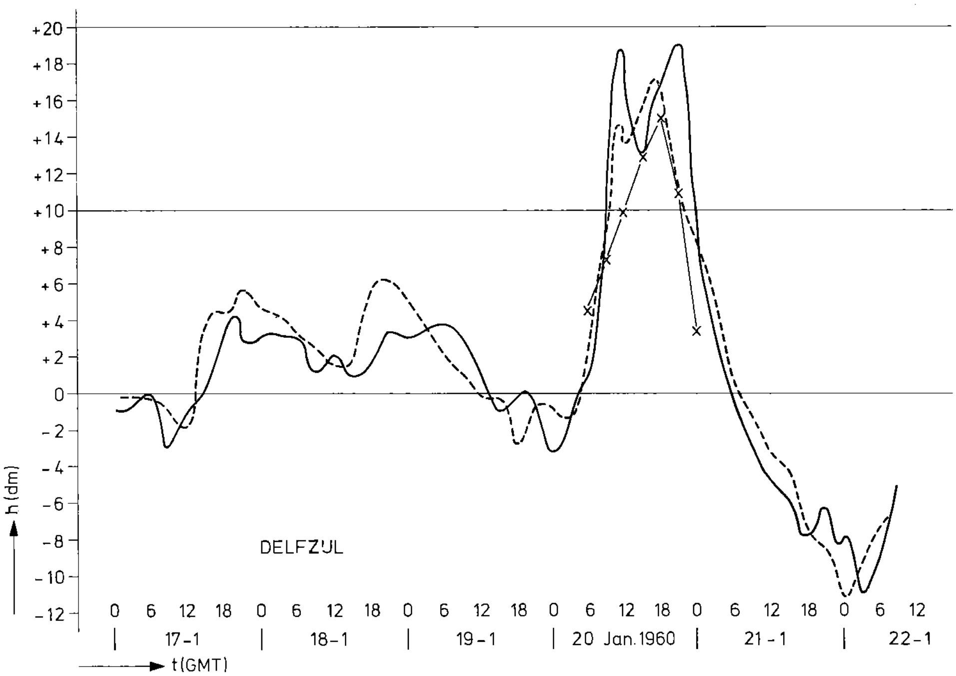

Fig. 9.6.2 Meteorological effects on water-levels in the period 17 to 22 January 1960 at Flushing, Hook of Holland, Den Helder, Harlingen and Delfzijl, respectively.

10 Extreme surges generated by displaced depressions

10.1 From a practical point of view it is necessary to investigate problems about the height to which the water-level may rise under extreme conditions, or about the maximum rise of the water-level in a fixed period of time. Generally these questions are answered by using statistical techniques, based on an extrapolation of a curve derived from observations. See for instance Rapport Deltacommissie [1960], part 3 and 4. However, the problem can also be approached by applying the numerical model, described in Chapter 5, to depressions characterized by very severe gales and displaced in such a way that the conditions in the southern part of the North Sea are as unfavourable as possible. Two depressions were selected for that purpose, viz. the depression of 6 December 1959 near weathership K on 45 °N, 16 °W, and the depression of 31 January-1 February 1953, which caused the catastrophic flood in the southwestern part of the Netherlands. Of course, the extent to which a displacement of a depression is admissible, is open to question. In particular this is the case when the depression is displaced from a position near weathership K to the North Sea, since the temperature of the sea water as well as the homogeneity of the surface of the earth are quite different for these two positions. So the exchange of energy between the surface of the earth and the atmosphere, which is an important factor with respect to the velocity of the wind, is not the same in both situations. Nevertheless, for estimating an upper limit of the wind effect on the North Sea these displacements may be regarded as not unreasonable.

10.2 The depression of 6 December 1959 was described by Timmerman [1960]. On 6 December 1959, 1200 GMT, the weathership K observed a wind velocity of 90 kts. This means that the gale was very severe. Position and track of this depression were changed in such a way that a maximum wind effect along the coast of the southwestern part of the Netherlands could be expected. See Fig. 10.2.1. On the basis of these constructed weather maps the wind field over the North Sea was computed. The computed maximum wind velocity amounted to 100 kts. This means a maximum velocity on 45° latitude of $\frac{\sin 55}{\sin 45} * 100 = 115$ kts. In 7.2 it was already pointed out that computed wind velocities exceeding 56 kts must be reduced. According to formula 7.2.1 a wind velocity of 100 kts will be reduced to 74 kts, which seems to be somewhat too low. Therefore, for dealing with these extreme situations formula 7.2.1 has been slightly changed and replaced by:

$$C_{\text{corrected}} = 56 + 0.55 * (C_{\text{computed}} - 56) \qquad (10.2.1)$$

Fig. 10.2.2 shows the computed wind direction and wind speed near the entrance of the Eastern Scheldt after applying the reduction given in formula 10.2.1. The curve demonstrates that a wind speed exceeding 60 kts should have blown during a period of about 9 hours, first W, veering to NW later, with a maximum value of 78 kts.

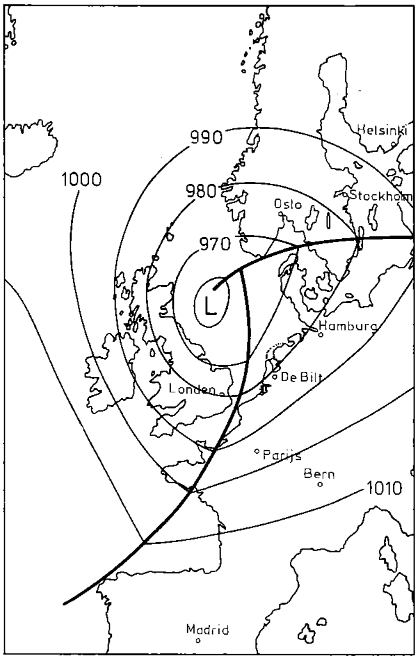

6-12-'59 06.00 GMT DISPLACED

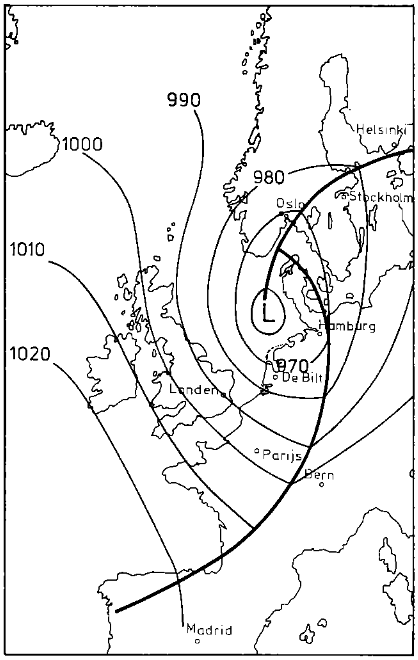

6-12-'59 12.00 GMT DISPLACED

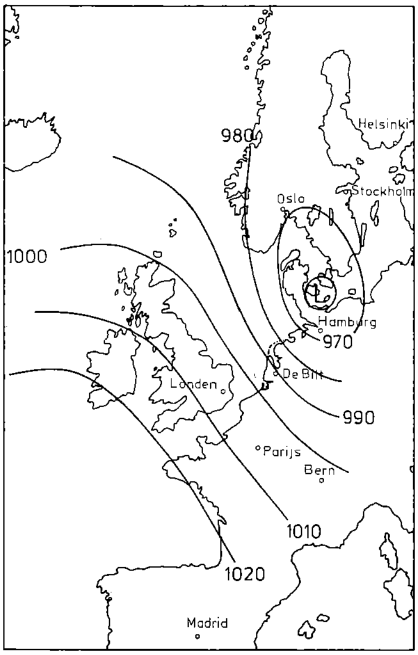

6-12-'59 1800 GMT DISPLACED

Fig. 10.2.1
Displaced depression of 6 December 1959.

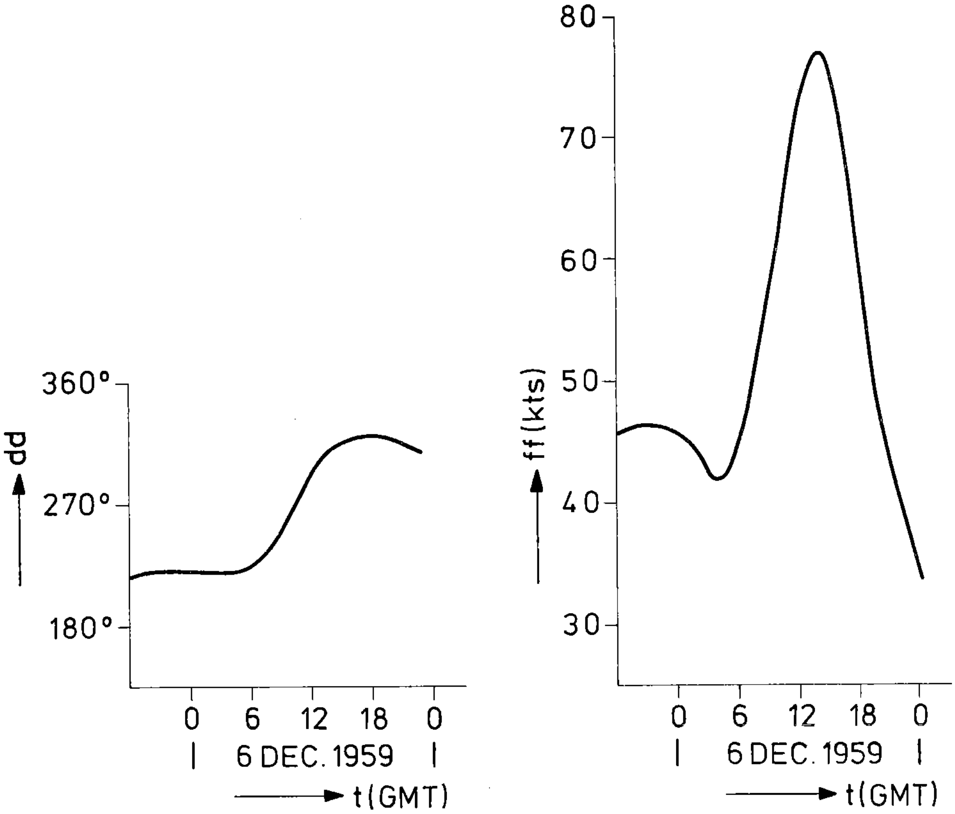

Fig. 10.2.2 Computed wind (direction and speed) near the entrance of the Eastern Scheldt of 6 December 1959 (displaced depression.)

The effect on the North Sea of this displaced gale was computed with the numerical model, using the drag coefficient given by Miller (see 4.1.). Fig. 10.2.3 gives the computed meteorological effect for Flushing and Hook of Holland. The computed maximum values for these stations were 40 dm and 38 dm respectively.

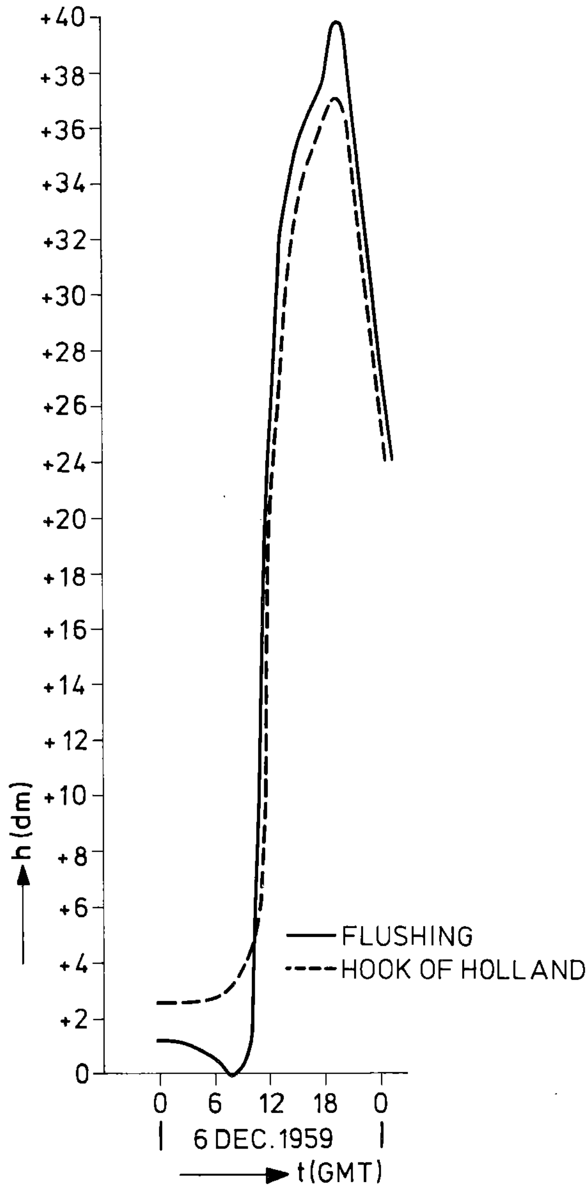

Fig. 10.2.3 Computed meteorological effect on the water-levels at Flushing and Hook of Holland on 6 December 1959 (displaced depression).

10.3 The second experiment refers to the depression of 31 January-1 February 1953, which was displaced and rotated according to the Deltarapport, part 1, p. 196, Fig. 3.4.1. The displaced positions of 31 January 1953, 06, 12 and 18 GMT are shown in Fig. 10.3.1. The wind field has been computed with application of formula 7.2.1. The computed wind near the entrance of the Eastern Scheldt is given in Fig. 10.3.2. From the curve it appears that the wind should have blown with a speed exceeding 60 kts during a period of about 11 hours WNW at first, and NW later, with a maximum value of 67 kts.

The computation of the effect on the North Sea was carried out with the drag coefficient of Miller (see 4.1). The computed set-up at Flushing and Hook of Holland is given in Fig. 10.3.3.

10.4 With respect to the maximum values of the computed water-levels the two experiments only show slight differences. However, the first experiment, based on the situation of 6 December 1959, is characterized by a very rapid increase of the meteorological effect, whereas the second experiment of January-February 1953 demonstrates a much slower increase of the set-up. Under springtide conditions the astronomical tidal height at Hook of Holland may amount to about 12 dm above N.A.P. (Amsterdam ordnance datum). This means, assuming linearity between the astronomical and meteorological tide, absolute heights of the water-level at Hook of Holland for the two surges of $38+12=50$ dm and $37+12=49$ dm, respectively. According to the Deltarapport, part 4, p. 93, a water-level of 50 dm will be exceeded once in 10000 years. This result can be interpreted as an indication that a surge generated by a depression like the displaced ones of 6 December 1959 and of 31 January 1953 will be very exceptional. A comparison of the two constructed surges is given in Table 10.4.1.

Table 10.4.1 Comparison between Flushing and Hook of Holland.

		wind near entrance of Eastern Scheldt exceeding indicated value during 6 hours	maximum increase in a period of 3 hours	maximum increase in a period of 1 hour	maximum value of computed set-up.
Flushing	6 Dec. '59	67 kts	23 dm	9 dm	40 dm
	31 Jan. '53	63 kts	11 dm	4 dm	39 dm
Hook of Holland	6 Dec. '59	67 kts	17 dm	6 dm	38 dm
	31 Jan. '53	63 kts	11 dm	5 dm	37 dm

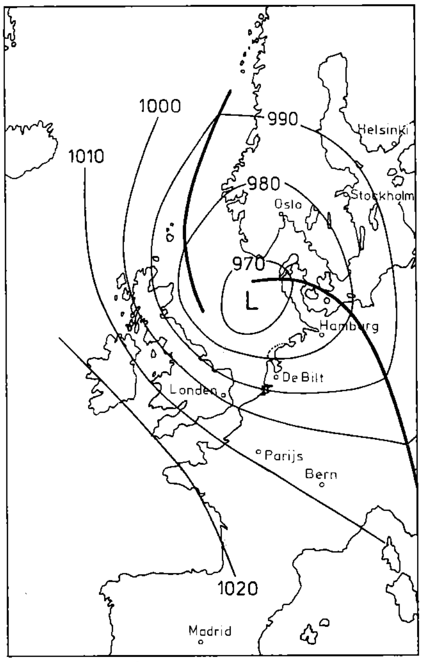

31-1-'53 06.00 GMT DISPLACED

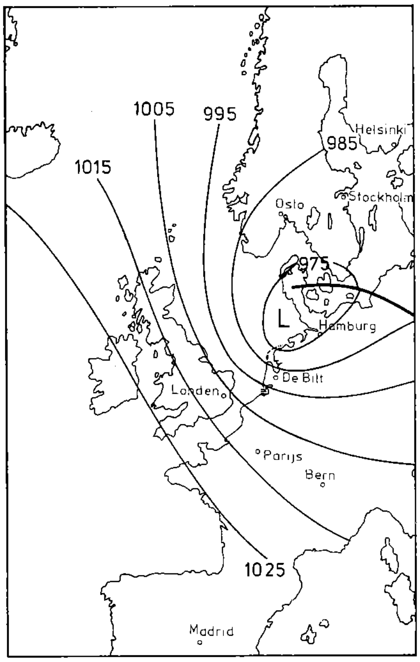

31-1-'53 12.00 G.M.T DISPLACED

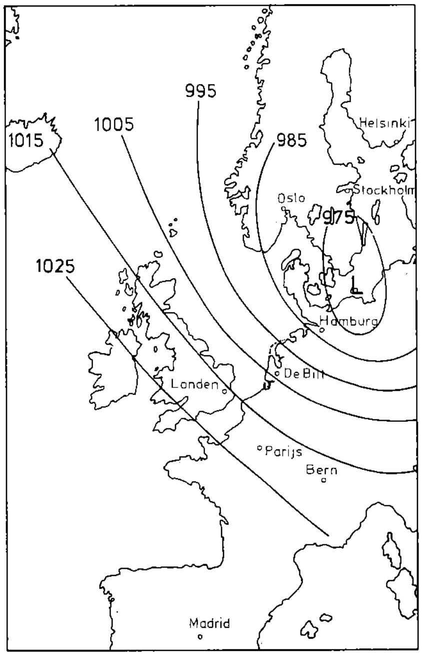

31-1-'53 1800 GMT DISPLACED

Fig. 10.3.1 Displaced depression of 31 January 1953.

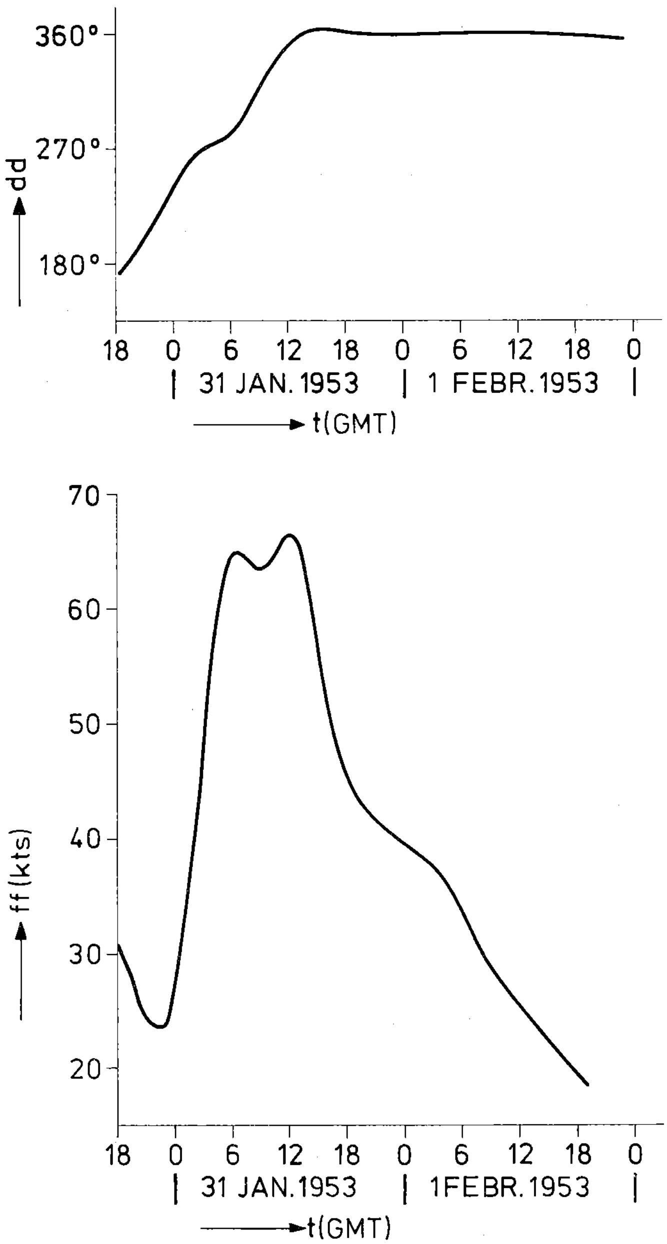

Fig. 10.3.2 Computed wind (direction and speed) near the entrance of the Eastern Scheldt of 31 January 1953 to 1 February 1953 (displaced depression).

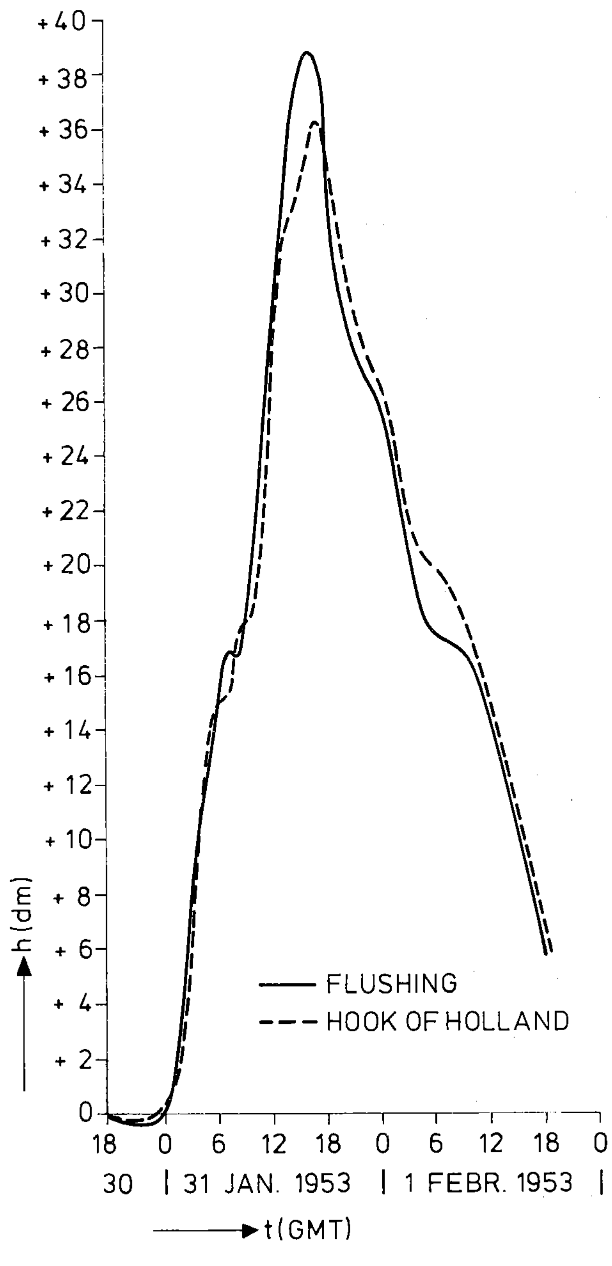

Fig. 10.3.3 Computed meteorological effects on the water-levels at Flushing and Hook of Holland on 31 January to 1 February 1953 (displaced depression).

List of symbols

a_N, a_K	constants.
$a_z(\psi)$	describing the distribution of the wind effect as a function of the wind direction ψ.
C_b	friction-coefficient at the sea bottom.
C_d	drag-coefficient.
f	$2\omega \sin \varphi$.
g	acceleration of gravity.
$\vec{G}$	$\rho^{-1}\, grad_H\, p$
G_x, G_y	x- and y-component of G.
h	height of the sea surface with respect to a mean, undisturbed sea surface.
H	depth of the sea.
k	constant of Von Kármán.
L	stability parameter of Monin-Obukow.
p(h)	air pressure at the sea surface.
r	friction-factor at the sea bottom.
Ri_v	Richardson-number based on the vertical virtual temperature lapse rate.
s, c	x- and y-component of unity vector parallel to the coast.
t	time in s.
T_a	air temperature.
T_S	seawater temperature.
u, v	x- and y-component of the velocity of a water particle.
$\bar{u}_{10}$	mean wind velocity at a height of 10 m.
U	$\int_{-H}^{h} u\, dz$
V	$\int_{-H}^{h} v\, dz$
V_N, V_Z, V_K	wind velocities in the districts North, South and Channel (See Fig. 3.0.1).
v_x, v_y	x- and y-components of the surface wind.
x, y	horizontal Cartesian coordinates, rotated 22 degrees in a positive sense with respect to the East- and North-direction.
z	vertical Cartesian coordinate.
z_0	measure for the roughness of the sea surface.
ε_N, ε_K	direction of maximum wind-effect in the districts North and Channel.
ψ_N, ψ_Z, ψ_K	wind direction in the districts North, South and Channel.
ρ	density of the air.
ρ_s	density of the sea water.
τ_b	shearing stress along the sea bottom.
τ_0	shearing stress along the sea surface.
τ^{xx}, τ^{xy}; τ^{yx}, τ^{yy}; τ^{zx}, τ^{zv}	x- and y-components of the stress on a plane perpendicular to respectively the x-, y- and z-axis.
θ_v	potential virtual temperature.

References

1. BAKKER, A. C., 1967, Een poging tot eliminatie van onnauwkeurigheden in de getijtafels voor Vlissingen en Hoek van Holland ten behoeve van de waterstandsverwachtingen. KNMI Verslagen V-204-II.
2. BAKKER, A. C., 1969, De invloed van de wind boven de westelijke Waddenzee op de hoog- en laagwaterstanden te Harlingen. KNMI Verslagen V-218.
3. BROCKS, K. and KRUGERMEYER, L., 1970, The hydrodynamic roughness of the sea surface. Ber. Inst. für Radiometeor. und Maritime Meteor. Nr. 14, Hamburg.
4. BIJVOET, H. C., 1957, A new overlay for the determination of the surface wind over sea from surface weather charts. KNMI Med. en Verh. Nr. 71.
5. CORKAN, R. H., 1948, Storm surges in the North Sea, Vol. 1 and 2, U.S. Hydrographic Off. Misc. 15702, Washington D.C.
6. DEACON, E. L., 1973, Geostrophic drag coefficients. Boundary Layer Meteor. 5, 321.
7. 1960, Rapport Deltacommissie. Bijdragen van KNMI, Mathematisch Centrum en Rijkswaterstaat.
8. DUUN CHRISTENSEN, J. T., 1975, The representation of the surface pressure field in a two-dimensional Hydrodynamic Numerical Model for the North Sea, the Skagerrak and the Kattegat. Deutsche Hydr. Z. Bd 28, H. 3.
9. EMCK, P. J., 1973, Verband tussen de wind op het lichtschip Goeree en de gelijktijdige wind op de meetpaal Roggenplaat. KNMI Verslagen V-250.
10. 1920, Rapport Staatscommissie Rotterdamse Waterweg.
11. HANSEN, W., 1966, The reproduction of the motion in the sea by means of hydrodynamical-numerical methods. Mitt. des Inst. für Meereskunde der Universität Hamburg Nr. V, 43.
12. HAWKINS, H. F. and RUBSAM, D. T., 1968, Hurricane Hilda, 1964. II Structure and Budgets of the Hurricane on October 1. Mon. Weath. Rev. 96, 617-636, Washington D.C.
13. HEAPS, N. S., 1969, A two-dimensional numerical sea model. Philos. Trans. A, 265, 93, London.
14. HESSELBERG, TH., 1915, Über eine Beziehung zwischen Druckgradient, Wind und Gradientänderungen. Veröff. d. Geophysischen Inst. Serie 2, Bd 1, 207-210, Leipzig.
15. HOUWEN, P. J. VAN DER, 1966, On the stability of a difference scheme for the North Sea problem. Rep. TW 100, Mathematisch Centrum, Amsterdam.
16. ISOZAKI, I., 1970, Variations of the sea level due to meteorological disturbances. Papers in meteor. and geophysics, Vol. XXI, Nr. 1, April, Japan.
17. KOOPMANN, G., 1963, Schwallerscheinungen am 16/17. Oktober 1963 in der Deutschen Bucht. Deutsche Hydr. Z., Bd. 16, H. 5.
18. KONDO, J., 1975, Air-sea bulk transfer coefficients in diabatic conditions. Boundary Layer Meteor. Vol. 9, Nr. 1, 91-112.
19. KRAUS, E. B., 1972, Atmosphere-ocean Interaction. Oxford Monographs on meteor.
20. KUNISHI, H. and IMASATO, N., 1966, On the growth of wind waves by high-speed wind flume. Ann. Disaster Prevention. Research Inst. Kyoto University 9, 667-676.
21. LAUWERIER, H. A. and DAMSTE, B. R., 1963, The North Sea problem VIII. A numerical treatment. Proc. Kon. Nederlandse Akad. v. Wetenschappen A 66, 167-184.
22. LEENDERTSE, J. J., 1967, Aspects of a computational model for long-period water-wave propagation. Memorandum RM-5294-PR Rand Corporation, Santa Monica, California.
23. MILLER, B. I., 1966, Energy exchanges between the atmosphere and the oceans. Amer. Soc. for Oceanogr. Publ. Nr. 1, Hurricane Symposium, October 10-11, Houston, Texas.
24. MUNCH, W. H., 1955, Windstress over water: an hypothesis. Quart. J. Roy. Met. Soc. 81, 320-332, London.
25. PANOFSKY, H. A. 1963, Determination of stress from wind and temperature measurementr. Quart. J. Roy. Met. Soc. 89, 85-94, London.
26. PEECK, H. H., 1974, Bepaling van de windschuifspanningscoefficient boven water met een numeriek model. KNMI Wetenschappelijk Rapport 74-8.
27. PHILLIPS, O. M., 1966, The dynamics of the upper ocean. 46-56, Cambridge Univ. Press.
28. ROLL, H. U., 1965, Physics of the marine atmosphere. Acad. Press. New York.
29. ROSSITER, J. R., 1959, Research on methods of forecasting storm surges on the east and south coasts of Great Britain. Quart. J. Roy. Met. Soc. 85, 262.
30. SCHALKWIJK, W. F., 1947, A contribution to the study of storm surges on the Dutch coast. Dissertatie, Algemene Landsdrukkerij, Den Haag.
31. SCHMITZ, H. P., 1956, Modellberechnungen zur deep-water-surge Entwicklung — das external surge problem. Deutsche Hydr. Z., Bd 18, 49-70.
32. SCHMITZ, H. P., 1962, On external surges and special meteorohydrographical problems in computing storm surges in adjacent seas and lakes by physical methods. Proceedings of the Symposium on Mathematical Hydrodynamical Methods of Physical Oceanography. Inst. für Meereskunde der Universität Hamburg.
33. TIMMERMAN, H., 1960, De zware stormen van begin december 1959. De Zee, Nr. 2.

34. TIMMERMAN, H., 1965, Waterstanden langs de Nederlandse kust. KNMI Verslagen V-174.
35. TIMMERMAN, H., 1969, Numerieke berekening van waterstanden langs de Nederlandse kust. KNMI Wetenschappelijk Rapport 69-3, 91-112.
36. TIMMERMAN, H., 1971, On the connection between cold fronts and gust bumps. Deutsche Hydr. Z., Bd 24, H. 4.
37. TIMMERMAN, H., 1975, On the importance of atmospheric pressure gradients for the generation of external surges in the North Sea. Deutsche Hydr. Z., Bd 28, H. 2.
38. VERPLOEGH, G. and GROEN, P., 1955, De uitwerking van de wind over de Groningse Waddenzee op de hoogwaterstanden van Delfzijl. KNMI Wetenschappelijk Rapport 55-009.
39. VERPLOEGH, G., 1956, The equivalent velocities for the Beaufort estimates of the wind force at sea. KNMI Med. en Verh. Nr. 66.
40. WEBB, E. K., 1970, Profile relationships: on the log-linear range, and extension to strong stability. Quart. J. Roy. Met. Soc. 96, 67-90, London.
41. WEENINK, M. P. H., 1958, A theory and method of calculation of wind effects on sea levels in a partly enclosed sea, with special application to the southern coast of the North Sea. KNMI, Med. en Verh. Nr. 73.
42. WEMELSFELDER, P. J., 1960, Rapport Deltacommissie, Deel III, 89-108.
43. WIERINGA, J., 1973, Applications of turbulence measurements over Lake Flevo. Drukkerij Elinkwijk, Utrecht.
44. WILSON, B. W., 1960, Note on surface wind stress over water at low and high wind speeds. J. of Geoph. Research 65, 3377-3381.

Summary

In the previous chapters it has been shown that numerical computations of water levels can be carried out with reasonable results. Besides, they may be applied to situations constructed by displacing very severe gales to a position favourable for extreme increases of the height of the water level along the Dutch coast.

The computations may serve on the one hand as a basis for the construction of operational tables valid for stationary situations, and on the other as a link in an automatic system consisting of data extraction, objective pressure analysis, wind analysis. The second application has a wider scope than the first, because it may deal not only with non-stationary effects but also with wind- and pressure effects outside the North Sea area.

Besides water levels, a pattern of an average stream in the North Sea caused by meteorological forces is obtained as well. Further investigation is needed to determine to what extent this pattern agrees with measurements of the residue-current.

Some improvement may be expected from computations on a finer grid, giving a better adjustment to the topography of the sea bottom and the shallow coastal areas. Replacing the linear two-dimensional model by a non-linear and/or a three-dimensional model may also be given consideration. There are indications that the analysis of the pressure field, the relationship between pressure gradient and wind, especially at high wind speeds, and the relationship between wind and wind stress are susceptible to some improvement as well. Inaccuracies in the astronomical tide can probably be removed, which leads to a better agreement between observed and computed meteorological effects on the water level.

However, the skill of both approaches with respect to the practical forecasting of deviations of the water level is not so much determined by the factors just mentioned as by the accuracy with which the pressure field 6, 12 or eventually 24 hours in advance may be forecast. The present publication does not deal with this important aspect of the problem.

Acknowledgement

The author wishes to thank Prof. Dr. R. Dorrestein for his critical remarks.

Van de reeks MEDEDELINGEN EN VERHANDELINGEN *zijn bij het Staatsdrukkerij- en Uitgeverij-bedrijf nog verkrijgbaar de volgende nummers:*

23, 25, 27, 29*b*, 30, 31, 34*b*, 35, 36, 37, 38, 39, 40, 42, 43, 44, 45, 46, 47, 48, 50, 51, 52, 53, 54, 55, 56, 57, 59.

alsmede

60. C. Kramer, J. J. Post en J. P. M. Woudenberg. Nauwkeurigheid en betrouwbaarheid van temperatuur- en vochtigheidsbepalingen in buitenlucht met behulp van kwikthermometers, 1954. (60 blz. met 11 fig.) 3,60

62. C. Levert. Regens. Een statistische studie. 1954. (246 blz. met 67 fig. en 143 tab.) 10,30

63. P. Groen. On the behaviour of gravity waves in a turbulent medium, with application to the decay and apparent period increase of swell. 1954. (23 blz.) . . . 1,55

64. H. M. de Jong. Theoretical aspects of aeronavigation and its application in aviation meteorology. 1956. (124 blz. met 80 fig., 9 krt. en 3 tab.) 4,60

65. J. G. J. Scholte. On seismic waves in a spherical earth. 1956. (55 blz. met 24 fig.) 5,15

66. G. Verploegh. The equivalent velocities for the Beaufort estimates of the wind force at sea. 1956. (38 blz. met 17 tab.) 1,80

67. G. Verploegh. Klimatologische gegevens van de Nederlandse lichtschepen over de periode 1910—1940.

Deel I: Stormstatistieken. — Climatological data of the Netherlands light-vessels over the period 1910—1940. P. I: Statistics of gales. 1956. (68 blz. met tabellen) 3,60

Deel II: Luchtdruk en wind; zeegang. — Climatological data of the Netherlands light-vessels over the period 1910—1940. P. II: Air pressure and wind: state of the sea. 1958. (91 blz. met tabellen.) 7,70

Deel III: Temperaturen en hydrometeoren; onweer. — Climatological data of the Netherlands light-vessels over the period 1910—1940. P. III: temperatures and hydrometeors; thunderstorms. 1953. (146 blz. met tabellen.) 8,25

68. F. H. Schmidt. On the diffusion of stack gases in the atmosphere. 1957. (60 blz., 12 fig. en tab.) 5,15

69. H. P. Berlage. Fluctuations of the general atmospheric circulation of more than one year; their nature and prognostic values. 1957 7,70

70. C. Kramer. Berekening van de gemiddelde grootte van de verdamping voor verschillende delen van Nederland volgens de methode van Penman. 1957. (85 blz., fig. en tab.) 7,20

71. H. C. Bijvoet. A new overlay for the determination of the surface wind over sea from surface weather charts. 1957. (35 blz., fig. en tab.) 2,60

72. J. G. J. Scholte. Rayleigh waves in isotropic and anisotropic elastic media. 1958. (43 blz., fig. en tab.) 3,10

73. M. P. H. Weenink. A theory and method of calculation of wind effects on sea levels in a partly-enclosed sea, with special application to the southern coast of the North Sea. 1958. (111 blz. met 28 fig. en tab.) 8,25

74. H. M. de Jong. Geostrophic flow. Geostrophic approximation in the upper air flow with application to aeronavigation and air trajectories. 1959. (100 blz. met 17 fig., 14 krt. en 2 tab.) 5,15

75. S. W. Visser. A new analysis of some features of the 11-year and 27-day cycles in solar activity and their reflection in geophysical phenomena. 1959. (65 blz. met 16 fig. en 12 tab.) 3,60

76. A. R. Ritsema and J. Veldkamp. Fault plane mechanisms of South East Asian earthquakes. 1960. (63 blz. met 26 fig. en 11 tab.) 4,10

77. G. Verploegh. On the annual variation of climatic elements of the Indian Ocean. P. I: text. P. II: charts. 1960. (64 blz., 15 fig., 28 krt.) 6,15

78. J. A. As. Instruments and measuring methods in paleomagnetic research. 1960. (56 blz., 20 fig.) 2,55

79. D. J. Bouman. Consistency of approximations in discontinuous fields of motion in the atmosphere with an introduction to the use of generalized functions or distributions in meteorology. 1961. (94 blz., 6 fig.) 6,70

80. H. Timmerman. The influence of topography and orography on the precipitation patterns in the Netherlands. 1963. (49 blz., 37 fig. en 5 tab.) 6,70

81. A. W. Hanssen & W. J. A. Kuipers: On the relationship between the frequency of rain and various meteorological parameters (with reference to the problem of objective forecasting). 1965. (77 blz., 18 fig. en 12 tab.) 10,25

82. G. A. de Weille: Forecasting crop infection by the potato blight fungus. A fundamental approach to the ecology of a parasite — host relationship. 1964. (144 blz., 37 fig. en 37 tab.) 14,90

83. H. J. de Fluiter, P. H. van de Pol, J. P. M. Woudenberg (redactie) e.a. Fenologisch en faunistisch onderzoek over boomgaardinsekten. Phenological and faunistic investigations on orchard insects. 1964. (226 blz., 84 fig. en 59 tab.) 9,50

84. D. J. Bouman & H. M. de Jong: Generalized theory of adjustment of observations with applications in meteorology. 1964. (89 blz., 8 fig. en 1 tab.) 11,30

85. L. Otto: Results of current observations at the Netherlands lightvessels over the period 1910—1939. P. I: Tidal analysis and the mean residual currents. 1964. (56 blz. en 8 tab.) 6,40

86. F. H. Schmidt: An analysis of dust measurements in three cities in the Netherlands. 1964. (68 blz., 14 fig. en 22 tab.) 5,65

87. Commissie Meteorologische Voorlichting van Straalvliegtuigen: Climatology of Amsterdam Airport (Schiphol). 1966. (145 blz., 6 fig., 10 tab.) 17,00

88. H. P. Berlage: The southern oscillation and world weather. 1966. (152 blz.) 46 fig., 34 tab.) 15,95

89. G. Verploegh: Observation and analysis of the surface wind over the ocean. 1967. (67 blz., 14 tab., 4 krt.) 6,70

90. R. Dorrestein: Wind and wave data of Netherlands lightvessels since 1949. 1967. (123 blz., 22 tab.) 15,95

91. P. J. Rijkoort: The increase of mean wind speed with height in the surface friction layer. 1968. (115 blz., 31 fig., 16 tab.) 15,95

92. C. J. E. Schuurmans: The influence of solar flares on the tropospheric circulation. Statistical indications, tentative explanation and related anomalies of weather and climate in Western Europe. 1969. (123 blz., 40 fig., 19 tab.) 19,00

93. H. M. de Jong: Optimal track selection and 3-dimensional flight planning Theory and practice of the optimization problem in air navigation under space-time varying meteorological conditions. 1974. (140 blz., 41 fig., 14 tabl., 4 fig. in annex) . 55,00

94. S. J. Bijlsma: On minimal-time ship routing. 40,00

95. L. Csikós: On the theory of the electromagnetic seismograph. . . . . 22,[illegible]

96. L. Otto: Oceanography of the Ria de Arosa (N.W. Spain). 1975. (210 blz., [illegible] fig., 19 tab., 3 fig. in annex, 5 tab. in annex) 60,00

97. G. A. de Weille: An approach to the possibilities of forecasting downy m[illegible] infection in onion crops. (83 blz., 19 fig., 6 tab.) 17,50

98. L. C. Heijboer: Design of a baroclinic three-level quasi-geostrophic mode[illegible] with special emphasis on developing short frontal waves. 49,00

725603 F - 316